

DAVII22.001APC

PATENT

IN THE UNITED STATES PATENT AND TRADEMARK OFFICE

Applicant : Thomas M. Cocks et al.  
Appl. No. : 09/787,356  
Filed : June 25, 2001  
For : METHODS OF TREATING  
AIRWAY DISEASES BY  
ACTIVATING PAR  
Examiner : Robert S. Landman  
Group Art Unit : 1647

DECLARATION UNDER 37 C.F.R. § 1.132

Commissioner for Patents  
P.O. Box 1450  
Alexandria, VA 22313-1450

Dear Sir:

I, Thomas M. Cocks, hereby declare that

1. I am currently a National Health and Medical Research Council (NHMRC) Principal Research Fellow at The University of Melbourne of Gratton Street, Parkville, in the State of Victoria in Australia.

2. I am considered to be an expert in the field of peptide signaling physiology. I have published extensively in this field and a list of my publications is attached in my Curriculum Vitae attached hereto as Exhibit TC-1.

3. I am familiar with the above-identified patent application, an Amendment accompanying this Declaration, and the Office Action mailed April 1, 2004, and hereby make the following comments.

4. The claims currently pending in the application define subject matter directed *inter alia* to a method of treating inflammation of the airways by administering an agent capable of activating airway epithelium protease activated receptor-2 (PAR<sub>2</sub>).

5. Airway inflammation with conditions, such as asthma, bronchitis, emphysema and the like, causes the smooth muscle airway bronchioles and bronchi to become unnaturally hypersensitive to numerous substances and to over-contract. Since the airway muscle is arranged

Appl. No. : 09/787,356  
Filed : June 25, 2001

in a cylindrical fashion around the air conducting tubes, over-contraction can result in increased resistance to airflow and difficulty breathing. In a severe asthma attack this narrowing, together with hypersecretion of mucus, obliterates the lumen of the airway tubes and no air exchange at all is possible and the patient will die unless they can be quickly re-opened. One way to rapidly achieve this outcome is to apply a drug that acts on the contracted muscle to make the muscle relax. A common example of one such drug is Ventolin, a  $\beta_2$  adrenoreceptor agonist. For most asthmatic patients, these drugs, inhaled *via* a nebuliser, make up the first line of defense against such inflammation-triggered, over-contraction of the airways.

6. The pending claims in the above-referenced application are directed to embodiments which provide an alternative to treating airway inflammation. I discovered using a number of different models and markers that PAR<sub>2</sub> agonists are useful in the treatment of airway inflammation.

7. Example 5 of the Application describes experiments in which the PAR<sub>2</sub> agonist peptide, SLIGRL, was used on mouse bronchi which had been subjected to treatment with acetylcholine, a substance known to induce contractions. These experiments demonstrate that the addition of PAR<sub>2</sub> agonists, when added to the bronchi, resulted in powerful concentration dependent relaxation.

8. The above-referenced patent application also describes other models of inflammation and the therapeutic effects of PAR<sub>2</sub> agonists. In these studies, as shown in Example 14, mice were challenged intranasally with lipopolysaccharide (LPS). The intranasal LPS model mimics a severe acute inflammation of the lungs, the severity of which is often characterized by bleeding into the airways. Prior to challenge, the mice were treated either with saline or SLIGRL.

9. Three hours following challenge, the mice were sacrificed and the total number of cells retrieved from the lungs determined. Neutrophils, a type of inflammatory cell, numbers were ascertained and found to be significantly reduced (See Figure 36) in mice pre-treated with SLIGRL.

10. These experiments have since been repeated and in addition to neutrophil numbers being decreased, it was also found that macrophage numbers were decreased in the animals pretreated with the PAR<sub>2</sub> agonist, SLIGRL (Moffat *et al.* 2002; attached as Exhibit TC-2).

Appl. No. : 09/787,356  
Filed : June 25, 2001

11. In addition to inflammatory cells being measured bronchial alveolar lavage samples were also screened 24 hours post-challenge for the presence of red blood cells. As can be seen in TC-3, pre-treatment with SLIGRL significantly reduced the presence of red blood cells in the bronchial alveolar lavage.

12. In additional studies, LPS was administered to mice *via* an aerosol. This type of model mimics an acute inflammation, characterized by decreased neutrophil trafficking into the airway and an absence of airway bleeding. As with the studies described in Paragraph 8, neutrophil numbers were also significantly decreased in mice that were pre-treated with SLIGRL (see TC-4).

13. In another mouse model of inflammation, mice were challenged with Ovalbumin, which mimics an antigen-specific immune response in humans. Briefly, Albumin, chicken egg, Grade V: Minimum 98% (Sigma A5503) is dissolved in sterile saline at a concentration of 250 µg/ml. Aluminium hydroxide (Al(OH)<sub>3</sub>) is then added to a concentration of 10 mg/ml. The aluminium hydroxide will not dissolve and therefore must be agitated to keep it in suspension before drawing it up into a syringe.

14. Administration of OVA in Al(OH)<sub>3</sub>

On day 0, male BALB/c mice, 8 weeks of age, are injected with 0.2 ml of OVA in Al(OH)<sub>3</sub> intraperitoneally (ie. A dose of 50 µg OVA per animal). Due to the colloidal nature of Al(OH)<sub>3</sub> in aqueous solution, a 21G needle has to be used to prevent the suspension clogging the end of the needle. On day 12, mice are given a booster i.p. injection of the same solution. On day 21 mice begin their OVA aerosol challenges.

15. Aerosoled OVA challenges

Starting on day 21 of the experiment, mice begin receiving daily aerosol challenges of OVA. Mice from each group are placed in a nebulising chamber and OVA (1% w/v in sterile saline) is introduced to the chamber at a rate of 5 ml/10 min. Mice receive 2 x 10 min OVA exposures each day for 7 days. Mice that are treated with PAR<sub>2</sub> activators by aerosol receive a 10 min exposure immediately prior to receiving OVA. (The control/untreated group receives saline via the nebuliser). 24 h after the final aerosol challenge mice are killed with an overdose of Nembutal (i.p.) and bronchial alveolar lavage is performed as previously described for the LPS-induced airways inflammatory model.

Appl. No. : 09/787,356  
Filed : June 25, 2001

16. TC-5 shows that mice pre-treated with SLIGRL have decreased levels of eosinophil in their bronchial alveolar lavage fluid.

17. Such mouse models are well accepted models for the treatment of airway inflammation in humans.

18. The data presented here details the development of a pharmacological assay for screening for derivatives of the PAR<sub>2</sub> agonist SLIGRL using the human PAR<sub>2</sub> receptor expressed endogenously in a human epithelial cell line (A549 cells). The assay utilizes FURA 2 and A549 cells in suspension to measure intracellular increases in calcium upon receptor activation.

19. Development of a PAR<sub>2</sub> bioassay

A549 cells

A549 cells represent a human cell line of epithelial morphology derived from lung carcinoma and express PAR<sub>1</sub>, PAR<sub>2</sub>, PAR<sub>3</sub> and PAR<sub>4</sub>. The use of a human derived non-transfected cell line that endogenously expresses the receptor of interest circumvents a number of complications that can arise in drug discovery programs that utilise transfected cellular systems. First, the receptor PAR<sub>2</sub> is stably expressed at physiologically relevant levels. Transfection of surrogate cell lines with a G-Protein Coupled Receptor (GPCR) can often lead to over or under expression compared to physiological levels with differences in receptor density affecting the perceived efficacy of drugs. Secondly, transfection of a GPCR into a surrogate cell line can alter the signalling profile of the receptor due to differences in the identity or expression levels of intracellular signalling molecules.

20. While PAR<sub>1</sub> is present in A549 cells, the potential for false positives (ie. responses to novel peptides mediated by PAR<sub>1</sub> and not PAR<sub>2</sub>) can be minimised by selectively desensitising the PAR<sub>1</sub> receptor. My colleagues and I have developed a protocol that involves pretreatment of the A549 cells with a PAR<sub>1</sub> maximally activating concentration of thrombin to selectively desensitise PAR<sub>1</sub> while not affecting PAR<sub>2</sub> mediated responses. This protocol is employed in all tests of novel peptides. PAR<sub>3</sub> and PAR<sub>4</sub> present less of a problem in the design of assays since human PAR<sub>3</sub> cannot be stimulated with activating peptides, and the tethered ligand sequence of PAR<sub>4</sub> (GYPGQV) is so different to that of PAR<sub>2</sub> that cross-reactivity does not occur.

21. The technique of intracellular Ca<sup>2+</sup> measurement using the Ca<sup>2+</sup> sensitive fluorescent dye, FURA 2AM is considered to be a sensitive and physiologically relevant means of detecting agonist activity at the PAR<sub>2</sub> receptor. In regard to the relevance of intracellular Ca<sup>2+</sup>

Appl. No. : 09/787,356  
Filed : June 25, 2001

measurement as an index of biological response, a rise in cytosolic calcium is generally the immediate precursor to a "functional" response and as such is a more faithful measure of drug biological activity than the measuring the accumulation of second messengers closer to the initial receptor activation step. High-throughput measurement of intracellular  $\text{Ca}^{2+}$  accumulation is a widely used and highly regarded assay in most drug discovery programs. Moreover, the fluorimetry assay employed in this program ensures that cells are only exposed to a single concentration of drug thus removing phenomena such as tachyphylaxis that can affect GPCRs after prolonged or repeated exposure to agonists and interfere with data analysis.

22. Due to the unique mode of activation of PARs compared to other GPCRs, the use of the human form of the  $\text{PAR}_2$  receptor is of additional importance to this drug discovery program in order to minimise the potential for false negative and false positive results. For the vast majority of GPCRs that are activated by freely diffusible ligands, amino acid sequence homology between species of the extracellular or transmembrane domains comprising the orthosteric site of the receptor means that rank orders of agonist potency are generally comparable across a variety of mammalian species. This generalisation does not necessarily apply to the PARs since the amino acid sequence of the tethered ligand responsible for receptor activation differs across species. An awareness of this phenomenon is paramount in the selection of bioassay systems in which to develop candidate molecules and will most likely necessitate the use of human derived cells lines and tissues wherever possible.

23. Care and Passaging of A549 cells

A549 cells were grown in 75  $\text{cm}^2$  tissue culture flasks in Dulbeccos Modified Eagle Medium (DMEM) containing 5% (v/v) heat inactivated foetal bovine serum (FBS), and 50 mg/ml penicillin-streptomycin and maintained in a humidified incubator at 37°C and 95% (v/v)  $\text{O}_2$ . Upon reaching ~80% confluence cells were harvested with trypsin/versine solution and passaged at approximately  $10^6$  cells/flask.

24. Measurement of intracellular  $\text{Ca}^{2+}$  fluorescence in A549 cells

A549 cells were grown to ~ 80% confluence. On the day of each experiment cells were harvested using 8 ml of Cell Dissociation Solution (Non-enzymatic) and washed with 12 ml of DMEM before centrifugation (500 g, 5 min). The supernatant was discarded and the pellet resuspended by titration in 5 ml of assay buffer (Krebs-HEPES buffer, in mM; 118 NaCl, 4.6 KCl, 10 HEPES, 1.8  $\text{CaCl}_2$ , 1.2  $\text{MgCl}_2 \cdot 6\text{H}_2\text{O}$ , 24.9  $\text{NaHCO}_3$ , 1.0  $\text{KH}_2\text{PO}_4$ , 11.1 dextrose, pH 7.4)

Appl. No. : 09/787,356  
Filed : June 25, 2001

containing 1 mM probenecid and 0.1% (v/v) bovine serum albumin (BSA). Cells were centrifuged as before and the pellet resuspended in 4 ml of the same buffer.

25. FURA 2AM and 10  $\mu$ l of Pluronic F 127 (0.02%) dissolved in 1 ml of assay buffer was added to the light protected cells to give a final concentration of 2  $\mu$ M FURA 2AM. The cells were swirled gently for 15 sec and then incubated for 30 min at 37°C. Following incubation, the cells were pelleted by centrifugation (400 g, 3 min), washed twice with 5 ml of assay buffer to remove excess/unloaded dye before resuspension in 5 ml of assay buffer.

26. Cells were allowed to sit for 20 min at room temperature prior to the measurement of intracellular  $\text{Ca}^{2+}$  accumulation. Cells used for the determination of  $\text{PAR}_2$  activation by novel peptides underwent  $\text{PAR}_1$  desensitisation by 10 min pretreatment with 1 U/ml thrombin followed by centrifugation (400 g, 3 min) and resuspension in 5 ml of assay buffer immediately prior to assaying. Cells were stored on ice for up to 45 min prior to measurement of intracellular  $\text{Ca}^{2+}$  fluorescence.

27. Experiments were performed using a fluorometer (FluoSTAR OPTIMA). For each determination, 180  $\mu$ l of cells ( $2 - 4 \times 10^6$  cells/ml) were added to the well of a 96 well plate maintained at a constant temperature (37°C). Each sample was exposed to only one concentration of agonist and all concentrations of drug were conducted in triplicate. Thus repetitive estimations were not made using the same cell suspension to avoid possible receptor desensitisation. After cells were allowed to stabilise for a period of 2 min, the cells were subjected to excitation at two wavelengths of 340 and 380 nm, and emitted light was collected at the photomultiplier through a 500 nm filter. The ratio of the fluorescence due to excitation at 340 nm to that at 380 nm ( $R_{340/380}$ ) was calculated by the FluoSTAR software. Baseline fluorescence measurements were taken for 30 sec prior to automated injection of  $\text{PAR}_2$  activating peptides with the resultant  $\text{Ca}^{2+}$  response being measured for a further 90 sec.

28. The results show the significantly higher potency of the rat  $\text{PAR}_2$  activating peptide (SLIGRL;  $\text{pEC}_{50} = 4.84 \pm 0.09$ ,  $n = 4$ ) compared to the human sequence (SLIGKV;  $\text{pEC}_{50} = 4.37 \pm 0.14$ ;  $p < 0.05$ ) at the human  $\text{PAR}_2$  receptor (Figure 1 of Exhibit TC-6). A549 cells also express the human  $\text{PAR}_1$  receptor however the response to the selective  $\text{PAR}_1$  agonist, TFLLR, is less robust than for  $\text{PAR}_2$ . In addition, the scramble peptide LSLIGRL is inactive in this cell line. Figure 1 in Exhibit TC-6 shows the comparison of the activities of these peptides in A549 cells.


Appl. No. : 09/787,356  
Filed : June 25, 2001

29. Exhibit TC-7 shows results from a pharmacological screen of protease-activated receptor peptide library. Initial pharmacological screening of the library was conducted at a single concentration (10 $\mu$ M) in triplicate A549 cells that has undergone PAR1 receptor desensitization using thrombin. In addition, SLIGRL was assayed at a concentration of 10 $\mu$ M along with derivatives of SLIGRL in order to obtain a reference response. Data for the novel library of peptides has been normalized to the reference response to 10 $\mu$ M SLIGRL, shown in Exhibit TC-7. Exhibit TC-7 shows relative activity of 60 different peptides that were tested according to the procedure in Paragraphs 24-27 of the Declaration

30. I declare that all statements made herein of my knowledge are true and that all statements made on information and belief are believed to be true; and further that these statements were made with the knowledge that willful, false statements and the like so made are punishable by fine or imprisonment, or both, under Section 1001 of Title 18 of the United States Code and that such willful, false statements may jeopardize the validity of the application or patent issuing therefrom.

Respectfully submitted,

Dated: 1/10/2004

By:   
Signature

\_\_\_\_\_  
Thomas M. Cocks

H:\DOCS\CCT\CCT-6440.DOC  
082604  
H:\DOCS\CCT\CCT-6581.DOC  
092904

# Curriculum Vitae

Thomas M Cocks



**1.1 Name** Thomas M Cocks

**Address** Department of Pharmacology,  
The University of Melbourne,  
Victoria, 3010

**Courier:** Level 8  
Triradiate Medical Building  
The University of Melbourne,  
Grattan St,  
Parkville,  
Victoria. 3010

**Work Telephone** 03-83445678

**Work Facsimile** 03-83448328

**email** thomasmc@unimelb.edu.au

**1.2 Citizenship** Australian

**DOB** 17/7/49

**Gender** Male

**1.3 Academic Qualifications**

**B.Sc. (Hons) 1973 First Class**

*Enzyme adaptation in mammalian tissues.*

Department of Biochemistry, University of New South Wales,  
Australia. (Dr George Zalitis)

**Ph.D. (1979)**

*Purinergic innervation of smooth muscle.*

Departments of Zoology (University of Melbourne), and  
Anatomy and Embryology (UCL London University)  
(Professor Geoff Burnstock).

**1.4 Current Appointment** NHMRC PRF1

**1.5 Current Source of Salary** NHMRC (five years  
from 2001)

**1.6 Previous Appointments**

June 1978 - Sept 1979: Postdoctoral Fellow (Department of  
Anatomy and Embryology, University College London).

Sept 1979 - Oct 1981: Postdoctoral Fellow (Department of Pharmacology, University College London).

Jan 1982 - Oct 1990: Senior Research Officer, Baker Medical Research Institute.

Oct 1990 - Dec 1993: Senior Research Fellow (NHMRC) Baker Medical Research Institute.

Jan 1994 - Dec 2000: Senior Research Fellow (NHMRC)  
Department of Pharmacology  
University of Melbourne

## 1.7 Publications

### Refereed Journal Article (best 10 in bold)

1. PhD Thesis (1979) University of London, Purinergic innervation of smooth muscle.
2. Burnstock G, Cocks T, Paddle BM & Staszewska-Barczak J. Evidence that prostaglandin is responsible for the rebound contraction following stimulation of non-adrenergic, non-cholinergic ("purinergic") inhibitory nerves. *Eur. J. Pharmacol.* **31**:360-362 (1975).
3. Burnstock G, Cocks T & Crowe R. Evidence for purinergic innervation of the anococcygeus muscle. *Br. J. Pharmacol.* **64**:13-20 (1978).
4. Burnstock G, Cocks T, Crowe R & Kasakov L. Purinergic innervation of the guinea-pig urinary bladder. *Br. J. Pharmacol.* **63**:125-138 (1978).
5. Burnstock G, Cocks T, Kasakov K & Wong HK. Direct evidence for ATP release from non-adrenergic, non-cholinergic ("purinergic") nerves in the guinea-pig taenia and bladder. *Eur. J. Pharmacol.* **49**:145-149 (1978).
6. Banks, BEC, Brown C, Burgess GM, Burnstock G, Claret M, Cocks T & Jenkinson, DH. Apamin blocks certain neurotransmitter-induced increases in potassium permeability. *Nature.* **282**:415-417 (1979).
7. Brown C, Burnstock G & Cocks T. Effects of adenosine 5'-triphosphate (ATP) and  $\beta$ ,  $\delta$ -methylene ATP on the rat urinary bladder. *Br. J. Pharmacol.* **65**: 97-102 (1979).
8. Burnstock G, Cocks T & Crowe R. Non-adrenergic, non-cholinergic (purinergic) inhibitory innervation of the rabbit retococcygeus muscle. *Eur. J. Pharmacol.* **54**:261-271 (1979).
9. Cocks T & Burnstock G. Effects of neuronal polypeptides on intestinal smooth muscle: A comparison with non-adrenergic, non-cholinergic nerve stimulation and ATP. *Eur. J. Pharmacol.* **54**:251-259 (1979).

10. Ferrero JD, Cocks TM & Burnstock G. A comparison between ATP and bradykinin as possible mediators of the responses of smooth muscle to non-adrenergic, non-cholinergic nerves. *Eur. J. Pharmacol.* **63**:295-302 (1980).
11. Burgess GM, Cocks TM & Jenkinson DH. The use of K<sup>+</sup>- sensitive electrodes to study drug-induced release of K<sup>+</sup> from suspensions of isolated hepatocytes. *Br. J. Pharmacol.* **73**:319(1981).
12. Cocks TM, Dilger P & Jenkinson DH. The mechanism of the blockade by trifluoperazine of some actions of phenylephrine on liver and smooth muscle. *Biochem. Pharmacol.* **30**:2873-2875 (1981).
13. Cocks TM & Angus JA. Antagonists of endothelial cell mediated relaxation of coronary arterial smooth muscle. *Blood Vessels.* **20**:188 (1983).
14. Angus JA, Campbell GR, Cocks TM & Manderson JA. Vasodilatation by acetylcholine is endothelium-dependent. A study by sonomicrometry in canine femoral artery *in vivo*. *J. Physiol (London)*. **344**:2098-222 (1983).
15. Cocks TM & Angus JA. **Endothelium-dependent relaxation of coronary arteries by noradrenaline and serotonin.** *Nature.* **305**:627-630 (1983).
16. Cocks TM, Jenkinson DH & Koller K. Interactions between receptors that increase cytosolic calcium and cyclic AMP in guinea-pig liver cells. *Br. J. Pharmacol.* **83**:281-291 (1984).
17. Cocks TM & Angus JA. Endothelium-dependent modulation of blood vessel reactivity. In: *The Peripheral Circulation*, pp 9-21, 1984. Eds., Hunyor S, Ludbrook J, Shaw J & McGrath M, Elsevier, Amsterdam.
18. Angus JA & Cocks TM. Role of endothelium in vascular responses to norepinephrine, serotonin and acetylcholine. *Bibl. Cardiol.* **38**:43-52 (1984).
19. Angus JA & Cocks TM. Endothelium-derived relaxing factor (EDRF) - progress with its isolation and properties. *Proc. Aust. Physiol. Pharmacol. Soc.* **15**:59-65 (1984).
20. Cocks TM & Angus JA. Bioassay of the release of endothelium-derived relaxing factor (EDRF) from isolated endothelial cells *in vitro*. In: *Vascular Neuroeffector Mechanisms*, pp 131-136. Eds., Bevan JA, Godfraind T, Maxwell RA, Stoclet JC & Worcel M, Elsevier, Amsterdam.
21. Cocks TM, Angus JA, Campbell JH & Campbell GR. **Release and properties of endothelium-derived relaxing factor (EDRF) from endothelial cells in culture.** *J. Cell. Physiol.* **123**:310-320 (1985).
22. Angus JA, Cocks TM, Campbell JH, Wright CE & Satoh K. The endothelium as an endocrine organ. *Proc. Endocrine Soc. Aust.* Suppl. 1:1-4 (1985).

23. Angus JA, Cocks TM & Satoh K. Alpha-adrenoceptors on endothelial cells. *Fed Proc.* **45**:2355-2350 (1986).
24. Angus JA, Cocks TM & Satoh K. Alpha<sub>2</sub>-adrenoceptors and endothelium-dependent relaxation in canine large arteries. *Br. J. Pharmacol.* **88**:767-777 (1986).
25. Angus JA, Satoh K & Cocks TM. Selectivity of calcium antagonists on canine large and small coronary arteries. In: *II Asian Pacific Adalat Symposium*, pp 12-27, Eds., Kelly DT, ADIS Press, Auckland, NZ (1986).
26. Angus JA, Wright CE, Cocks TM, Satoh K & Campbell G. Endothelium-dependent relaxation is unaltered by hypertension, cholesterol or intimal thickening. *Clin. Exp. Pharmacol. Physiol.* **13**:289-293 (1986).
27. Angus JA & Cocks TM. Vasodilatation and the discovery of endothelium-derived relaxing factor. *Med. J. Aust.* **146**:250-253 (1987).
28. Angus JA & Cocks TM. The half-life of endothelium-derived relaxing factor released from bovine aortic endothelial cells in culture. *J. Physiol. (London)*. **388**:71-81 (1987).
29. Cocks TM, Angus JA & Grego B. Properties of endothelium-derived relaxing factor (EDRF) released from cultured endothelial cell. In: *Proc. Xth. Int Cong. Pharmacol., Sydney*, p S72, Elsevier, Amsterdam (1987).
30. Cocks TM, Manderson JA, Mosse PRL, Campbell GR & Angus JA. Development of a large fibromuscular intimal thickening does not impair endothelium-dependent relaxation in the rabbit carotid artery. *Blood Vessels*. **24**:192-200 (1987).
31. Cocks TM, Angus JA, Little PJ & Cragoe EJ Jr. Amiloride analogues cause endothelium-dependent relaxation in the canine coronary artery in vitro; possible role of Na<sup>+</sup>/Ca<sup>+</sup> exchange. *Br. J. Pharmacol.* **95**:67-76 (1988).
32. Angus JA, Cocks TM, Wright CE, Satoh K & Campbell GR. Endothelium-dependent responses in large arteries and in the microvasculature. In: *Relaxing and Contracting Factors*, pp 361-387, Ed., Vanhoutte PM, Humana Press, New Jersey (1988).
33. Angus JA, Cocks TM, Satoh K & White TD. Receptor heterogeneity and EDRF release. In: *Sixth International Symposium on Vascular Neuroeffector Mechanisms*, pp 85-91, Eds., Bevan JA, Majewski HM, Maxwell RA & Story DF, IRL Press, Oxford (1988).
34. Cocks TM, Angus JA, Campbell JH & Campbell GR. Endothelial cells in culture and production of endothelium-derived relaxing factor. In: *Relaxing and Contracting Factors*, pp 107-135, Ed., Vanhoutte PM, Humana Press, New Jersey, USA (1988).
35. Angus JA & Cocks TM. Endothelium-derived relaxing factor. *Pharmacol. Ther.* **41**:303-351 (1989).

36. Angus JA & Cocks TM. Endothelial cell function and blood vessel reactivity. *New Ethicals*. 26:45-56 (1989).
37. Cocks TM, Broughton A, Dib M, Sudhir K & Angus JA. Endothelin is blood vessel selective: studies on a variety of human and dog vessels *in vitro* and on regional blood flow in the conscious rabbit. *Clin. Exp. Pharmacol. Physiol.* 16:243-246 (1989).
38. Manderson JA, Cocks TM & Campbell GR. Balloon catheter injury to rabbit carotid artery II. Selective increase in reactivity to some vasoconstrictor drugs. *Atherosclerosis*. 9:299-307 (1989).
39. Cocks TM, Faulkner NL, Sudhir K & Angus JA. Reactivity of endothelin-1 on human and canine large veins compared with large arteries *in vitro*. *Euro. J. Pharmacol.* 171:17-24 (1989).
40. Cocks TM, Angus JA & Broughton A. Endothelin-1 as a selective vasoconstrictor: Studies on human, dog and rabbit blood vessels *in vitro* and *in vivo*. In: *Endothelium-derived vasoactive factors*, pp 73-79, Eds., Rubanyi GM & Vanhoutte PM, Karger, Basel (1990).
41. Cocks TM, King SJ & Angus JA. Glibenclamide is a competitive antagonist of the thromboxane A<sub>2</sub> receptor in dog coronary artery *in vitro*. *Br. J. Pharmacol.* 100:375-378 (1990).
42. Cocks TM & Angus JA. Comparison of relaxation responses of vascular and non-vascular smooth muscle to endothelium-derived relaxing factor (EDRF), acidified sodium nitrite (NO) and sodium nitroprusside. *Naunyn-Schmiedeberg's Arch. Pharmacol.* 341:364-372 (1990).
43. Cocks TM, Malta E, King SJ, Woods RL & Angus JA. Oxyhaemoglobin increases the production of endothelin-1 (ET-1) by endothelial cells in culture. *Eur. J. Pharmacol.* 196:177-182 (1991).
44. Cocks TM & Angus JA. Are the contractions to the EDRF blocking drugs, L-NMMA and NOLA in isolated arteries due to removal of basal EDRF release? *J. Cardiovascular Pharmacol.* 17(Suppl.3):S159-164 (1991).
45. Angus JA, Broughton A, Cocks TM & McPherson GA. The acetylcholine paradox - a constrictor of human small coronary arteries even in the presence of endothelium. *Clin. Exp. Pharmacol. Physiol.* 18:33-36 (1991).
46. Cocks TM & Arnold PJ. 5-Hydroxytryptamine (5-HT) mediates potent relaxation in the sheep isolated pulmonary vein via activation of 5-HT<sub>4</sub> receptors. *Br. J. Pharmacol.* 107:591-596 (1992).
47. Crack P & Cocks T. The effect of thimerosal on relaxation responses to EDRF agonists in the canine, isolated coronary artery. Possible role of arachidonic acid. *Br. J. Pharmacol.* 107:566-572 (1992).

48. Cocks TM, Kemp BK, Pruneau D & Angus JA. Comparison of contractile responses to 5-hydroxytryptamine (5-HT) and sumatriptan in human isolated coronary artery: Synergy with the thromboxane A<sub>2</sub>-receptor agonist, U46619. *Br. J. Pharmacol.* 110:360-368 (1993).
49. Angus JA, Cocks TM & Ross-Smith M. Pharmacological analysis of 5-HT-receptors in human coronary arteries. In: *Serotonin- From cell biology to pharmacology and therapeutics*, pp 297-305, Eds., Vanhoutte PM et al., Kluwer Academic Publishers, The Netherlands (1993).
50. Cocks TM. Changes in vascular reactivity in atherogenesis; markers of endothelial cell dysfunction associated with initiation of the disease. In: *Airways and vascular remodelling in asthma and cardiovascular disease: implications for therapeutic intervention*, pp 21-26, Eds., Page C & Black J, Academic Press, London, San Diego (1994).
51. Kilpatrick N & Cocks TM. Evidence for differential roles of nitric oxide and hyperpolarization in endothelium-dependent relaxation of pig isolated coronary artery. *Br. J. Pharmacol.* 112:557-565 (1994).
52. Stork AP & Cocks TM. Pharmacological reactivity of human coronary arteries: phasic and tonic contractions to vasoconstrictor compounds differentiated by nifedipine. *Br. J. Pharmacol.* 113:1093-1098 (1994).
53. Stork AP & Cocks TM. Pharmacological reactivity of human epicardial coronary arteries: characterization of relaxation responses to endothelium-derived relaxing factor (EDRF). *Br. J. Pharmacol.* 113:1099-1105 (1994).
54. Garland CJ, Plane F, Kemp BK & Cocks TM. Endothelium-dependent hyperpolarization: a role in the control of vascular tone. *Trends in Pharmacol. Sci.* 16:23-30 (1995).
55. Drummond GR & Cocks TM. Endothelium-dependent relaxations mediated by inducible B<sub>1</sub> and constitutive B<sub>2</sub> kinin receptors in the bovine isolated coronary artery. *Br. J. Pharmacol.* 116:2473-2481 (1995).
56. Drummond GR & Cocks TM. Endothelium-dependent relaxation to the kinin B<sub>1</sub> receptor agonist des-Arg<sup>9</sup>-bradykinin in human coronary arteries. *Br. J. Pharmacol.* 116:3083-3085 (1995).
57. Kemp BK & Cocks TM. Effects of the thromboxane A<sub>2</sub> mimetic U46619, on contractions to 5-hydroxytryptamine (5-HT) sumatriptan and methysergide in canine coronary artery and saphenous vein *in vitro*. *Br. J. Pharmacol.* 116:2183-2190 (1995).
58. Kemp BK, Smolich JJ, Ritchie BC & Cocks TM. Endothelium-dependent relaxations in sheep pulmonary arteries and veins: resistance to block by N<sup>G</sup>-nitro-L-arginine (L-NNA) in pulmonary hypertension. *Br. J. Pharmacol.* 116:2457-2467 (1995).
59. Cocks TM. Endothelium-dependent vasodilator mechanisms. In: *Pharmacology of Vascular Smooth Muscle*, pp 231-251, Eds., Garland CJ & Angus JA, Oxford University Press, Oxford (1996).

60. Angus JA & Cocks TM. Pharmacology of human isolated large and small coronary arteries. In: *Pharmacology of Vascular Smooth Muscle*, pp 276-305, Eds., Garland CJ & Angus JA, Oxford University Press, Oxford (1996).

61. Drummond GR & Cocks, TM. Evidence that endothelium-dependent hyperpolarization can mediate relaxation to bradykinin in the bovine isolated coronary artery independently of voltage-operated  $Ca^{2+}$  channels. *Br. J. Pharmacol.* **117**:1035-1040 (1996).

62. Kemp, BK, Smolich, JJ & Cocks, TM. Evidence for specific regional patterns of responses to different vasoconstrictors and vasodilators in sheep isolated pulmonary arteries and veins. *Br. J. Pharmacol.* **121**, 441-450, 1997.

63. Kemp, BK & Cocks, TM. Evidence that mechanisms dependent and independent of nitric oxide mediate endothelium-dependent relaxation to bradykinin in human small resistance-like coronary arteries. *Br. J. Pharmacol.* **120**: 757-762, 1997.

64. Selemidis, S & Cocks, TM. Evidence that nitric-oxide (NO) and a non-NO factor elicit non-adrenergic, non cholinergic (NANC) nerve inhibitory responses in the rat isolated anococcygeus. *Br. J. Pharmacol.* **120**, 662-666, 1997.

65. Selemidis, S, Satchell, DG & Cocks, TM. Evidence that NO acts as a redundant NANC inhibitory neurotransmitter in the guinea-pig isolated taenia coli. *Br. J. Pharmacol.* **121**, 604-611, 1997.

**66. Hamilton, JR, Nguyen, PB & Cocks. Atypical protease-activated receptor mediates endothelium-dependent relaxation of human coronary arteries. *Circ. Res.* **82**, 1306-1311, 1998.**

67. Sobey, CG & Cocks, TM. Activation of protease-activated receptor-2 (PAR-2) elicits nitric oxide-dependent dilatation of the basilar artery in vivo. *Stroke*, **29**, 1439-1444, 1998.

68. Cocks, TM & Moffatt JD. International Patent Application. "A method of treatment and agents useful for the same". N° PCT/AU99/00775

69. Selemidis, S, Ziogas, J & Cocks, TM. Apamin- and nitric oxide-sensitive biphasic non-adrenergic non-cholinergic inhibitory junction potentials in the rat anococcygeus muscle. *J. Physiol.* **513**, 835-844, 1998.

70. Moffat, JD & Cocks, TM. Endothelium-dependent and -independent responses to protease-activated receptor-2 (PAR-2) activation in mouse isolated renal arteries. *Br. J. Pharmacol.* **125**, 591-594, 1998.

71. Cocks, TM, Sozzi, V, Moffatt, JD & Selemidis, S. Protease-activated receptors mediate apamin-sensitive relaxation of mouse and guinea-pig gastrointestinal smooth muscle. *Gastroenterology* **116**, 586-592, 1999.

72. Cocks, TM, Fong, B, Chow, JM, Anderson, GP, Frauman, AG, Goldie, RG, Henry, PJ, Carr, MJ, Hamilton, JR & Moffatt, JD. A protective role for protease-activated receptors in the airways. *Nature*, 398, 156-160, 1999.
73. Kemp, BK & Cocks, TM. Adenosine mediates relaxation of human small resistance-like coronary arteries via A<sub>2B</sub> receptors. *Br. J. Pharmacol.* 126, 1796-1800, 1999.
74. Sobey, CG, Moffatt, JD & Cocks, TM. Evidence for selective effects of chronic hypertension on cerebral artery vasodilatation to protease-activated receptor-2 (PAR-2) activation. *Stroke*, 30, 1933-1941, 1999.
75. Moffatt, JD & Cocks, TM. The role of protease-activated receptor-2 (PAR-2) in the modulation of beating of the mouse isolated ureter: lack of involvement of mast cells or sensory nerves. *Br. J. Pharmacol.*, 128: 860-864, 1999.
76. Tatoulis, J, Jiang, G-C, Moffatt, JD & Cocks, TM. Storage of radial artery grafts in blood increase vessel reactivity to vasoconstrictors *in vitro*. *Ann. Thoracic Surg.*, 68: 2191-2196, 1999.
77. Hamilton, JR., Chow, JM & Cocks, TM. Protease-activated receptor-2 turnover stimulated independently of receptor activation in porcine coronary endothelial cells. *Br. J. Pharmacol.*, 127:617-622, 1999.
78. Hamilton, JR, Chow, JM & Cocks, TM. Protease-activated receptor-2 turnover stimulated independently of receptor activation in porcine coronary endothelial cells. *Br. J. Pharmacol.*, 127: 617-622, 1999.
79. Drummond, GR., Selemidis, S & Cocks, TM. Apamin-sensitive, non-nitric oxide (NO) endothelium-dependent relaxations to bradykinin in the bovine isolated coronary artery: no role for cytochrome P<sub>450</sub> and K<sup>+</sup>. *Br. J. Pharmacol.*, 129: 811-819, 2000.
80. Cocks, TM & Moffatt, JD (2000) Protease-activated receptors: sentries for inflammation? *Trends in Pharmacol. Sci.*, 23 : 103-108,2000.
81. Cocks, TM & Selemidis, S. Interactions between nitric oxide and other NANC inhibitory neurotransmitters in the periphery: clues from the endothelium. In: *Nitric oxide and Free Radicals in Peripheral Neurotransmission*. Ed. S. Kalsner, Birkhauser, New York, pp 57-77, 2000.
82. Selemidis S & Cocks, TM. Nitroregic relaxations of the mouse gastric fundus is mediated by cGMP-dependent and ryanodine-sensitive mechanisms. *Br. J. Pharmacol.*, 129: 1315-1322, 2000.
83. Chow JM, Moffatt JD & Cocks TM. Protease-activated receptors (PARs) in rat airways: activation of PAR1, PAR2 and PAR4 *in vitro* by synthetic peptides but not by thrombin and trypsin. *Br. J. Pharmacol.*, 131, 1584-159, 2000.
84. Hamilton JR, Moffatt JD, Frauman AG & Cocks TM. Protease-activated receptor-1 (PAR1) but not PAR2 or PAR4 mediates



endothelium-dependent relaxation to thrombin and trypsin in human pulmonary arteries. *J Cardiovasc. Pharmacol.*, **38**, 108-119, 2001.

**85 Hamilton JR, Frauman AG & Cocks TM. Increased expression of protease-activated receptor-2 (PAR2) and PAR4 in human coronary artery by inflammatory stimuli unveils endothelium-dependent relaxations to PAR2 and PAR4 agonists. *Circ Res.*, **89**, 92-98, 2001.**

86. Cocks, TM & Moffatt, JD. Protease-activated receptor-2 (PAR2) in the airways. *Pulmonary Pharmacol and Therap.* **14**, 183-191, 2001.

**87. Cocks, TM & Selemedis, S. Endothelium-dependent hyperpolarization as a remote, anti-atherogenic signalling mechanism. *Trends in Pharmacol. Sci.*, **23**, 213-220, 2002.**

88. Selemedis, S & Cocks T.M. Myoendothelial and circumferential spread of endothelium-dependent hyperpolarization in coronary arteries. In: *EDHF 2000*, ed. PM Vanhoutte, Harwood Academic Publishers, UK. pp 75-86, 2001.

**89. Moffatt, JD, Jeffrey, KL & Cocks, TM. Protease-activated receptor-2 (PAR2) activating peptide SLIGRL inhibits bacterial lipopolysaccharide (LPS)-induced recruitment of polymorphonuclear leucocytes into the airways of mice. *Am J Resp Cell & Mol Biol*, **26**, 680-684, 2002.**

90. Hamilton, JR, Moffatt, JD, Tatuolis, J & Cocks, TM. Enzymatic activation of endothelial protease-activated receptors is dependent on artery diameter in human and porcine isolated coronary arteries *Br. J. Pharmacol*, **136**, 492-501, 2002.

91. Moffatt, JD & Cocks, TM. Pharmacologically distinct intracellular calcium pools regulate tonic and oscillatory responses in porcine thoracic duct. *J. Cardiovasc. Pharm.*, **43**, 83-92, 2004.

92. Moffatt, JD, Cocks, TM & Page, CP. Role of the epithelium and acetylcholine in mediating the contraction to 5-hydroxytryptamine in the mouse isolated trachea. *Br J Pharmacol*. 2004 Mar 15 [Epub ahead of print].

93. Cocks, TM & Koulis, C. Role of protease-activated receptor-2 in keratinocyte growth. *J. Invest. Dermatol.* (submitted for publication).

94. Selemedis, S & Cocks, TM. Endothelium-independent relaxation to angiotensin-11 in the sheep coronary artery is mediated by AT1 receptors, prostanoids and Ca<sup>2+</sup>-activated K<sup>+</sup> channels. *Br. J. Pharmacol.* (submitted for publication).

## **Invited Reviews**

### ***1 Trends in Pharmacological Sciences***

One review on EDHF published in 1995 (Ref 54), one on protease-activated receptors (PARs) as sensors of inflammation (Ref 80) and another on our novel finding that EDHF acts as a remote electrical signalling mechanism in blood vessels (ref 87).

## **2 Pharmacology and Therapeutics**

A major review on EDRF (Ref 35)

## **3 Medical Journal of Australia**

A review on EDRF (Ref 27)

### **Invited book chapters**

**1** *Endothelium-dependent modulation of blood vessel reactivity* In: The Peripheral Circulation: Eds S Hunyor, J Ludbrook, J Shaw & M McGrath. Elsevier, Amsterdam, (Ref 17).

**2** *Bioassay of the release of endothelium-derived relaxing factor (EDRF) from isolated endothelial cells in vitro.* In: Vascular Neuroeffector Mechanisms. Eds JA Bevan, T Godfraind, RA Maxwell, JC Stoclet & M Woerzel, Elsevier, Amsterdam, (Ref 20).

**3** *Endothelium-dependent responses in large arteries and in the microvasculature* In: Relaxing and Contracting Factors. Ed. PM Vanhoutte, Humana Press, New Jersey, Ref (32).

**4** *Endothelial cells in culture and production of endothelium-derived relaxing factor.* In Relaxing and Contracting Factors. Ed. PM Vanhoutte, Humana Press, New Jersey, (34).

**5** *Receptor heterogeneity and EDRF release.* In: Sixth International Symposium on Vascular Neuroeffector Mechanisms. Eds JA Bevan, HM Majewski, RA Maxwell & DF Story, IRL Press, Oxford, (Ref 33).

**6** *Endothelin-1 as a selective vasoconstrictor: Studies on human, dog and rabbit blood vessels in vitro and in vivo.* In: Endothelium- (Ref 40).

**7** *Pharmacological analysis of 5-HT receptors in human coronary arteries.* In: Serotonin -From cell biology to pharmacology and therapeutic. Ed. PM Vanhoutte, Kluwer, The Netherlands, (Ref 49).

**8** *Changes in vascular reactivity in atherogenesis; markers of endothelial cell dysfunction associated with initiation of the disease.* In: Airway and vascular remodelling in asthma and cardiovascular disease. Eds C Page & J Black. Academic Press, London, (Ref 50).

**9** *Endothelium-dependent vasodilator mechanisms.* In: The Pharmacology of Vascular Smooth Muscle. Eds, CJ Garland & JA Angus. Oxford University Press, Oxford, (Ref 59).

**10** *Pharmacology of the coronary circulation.* In: The Pharmacology of Vascular Smooth Muscle. Eds, CJ Garland & JA Angus. Oxford University Press, Oxford, (Ref 60).

**11** *Interactions between nitric oxide and other NANC inhibitory neurotransmitters in the periphery: clues from the endothelium.* In: Nitric oxide and Free Radicals in Peripheral Neurotransmission. Ed. S Kalsner, Birkhauser. New York, Ref (81).

**12** *Myoendothelial and circumferential spread of endothelium-dependent hyperpolarization in coronary arteries.* In: EDHF 2000. ed. PM Vanhoutte, Harwood Academic Publishers, UK. (Ref 88)

## **Conference papers and published abstracts**

These are numerous and I never use them as calibrators of my track record.

### **1.8 Other research Outcomes**

#### **Patents**

1. International Patent Application. "A method of treatment and agents useful for the same" N° PCT/AU99/00775
2. Australian Provisional Patent "A method of treatment and /or prophylaxis and agents useful for same"
3. **Set up Spin-off Biotechnology Company:- Pargenex Pharmaceuticals Pty Ltd funded by Uniseed Pty Ltd and a competitive BIF Grant from the Commonwealth Government.**

### **1.9 Teaching**

I have a strong commitment to postgraduate (7 PhDs, 1 Masters and 8 Honours students) and other teaching include advanced study units to third year medical students, practicals to science students and supervision of work experience and summer vacation students.

### **1.10 Research Grant Support (last 7 years)**

#### **1994-1996 NHMRC Project Grant 940157**

"Regulation and roles of nitric oxide in cardiovascular function".

Publications: TC5 - TC15

Funding: 1994 \$146,135.39; 1995 \$152,940.58; 1996 \$143,590.82

#### **1997 NHMRC Equipment Grant 971441**

Funding: \$30,000

#### **1997-2001 NHMRC Project Grant 970327**

"Mechanisms of endothelium- and NANC nerve-mediated relaxation of smooth muscle". Publications: TC-16 - TC36

Funding: 1997 153,351.53 1998 \$158,128.10 1999 \$160,144.34 2000 \$161,782.33 2001 \$163,418.91

#### **2000-2002 NHMRC Project Grant 114256**

"Mechanisms of protease-activated receptor-2 mediated broncho-protection"

Funding: 2000 \$109,591 2001 \$111,705 2002 \$113,819

#### **2001-2006 NHMRC Fellowship Grant 145828**

"Characterisation of PAR2 knockout and transgenic mice: towards gene therapy for epithelia based inflammatory diseases"

Funding: 2001-2006; \$180,000 per year

## **2003-2005 NHMRC Project Grant 252811**

“Design and development of potent and selective PAR-2 antagonists”

Funding: 2003 –2005; \$140,000 per year

### **1.11 Editorial Boards of Scientific Journals**

British Journal of Pharmacology 1995 -1998

Endothelium 1990 - 1996

### **1.12 Journal Referee**

American Journal of Physiology

Blood

British Journal of Pharmacology

Circulation Research

Gastroenterology

Journal of Pharmacology and Experimental Therapeutics

Journal of Cardiovascular Pharmacology

### **1.13 Societies and duties**

*ASCEPT* - The Australasian Society of Clinical and Experimental Pharmacologists and Toxicologists.

*ISHR* -International Society of Heart Research, Secretary, Australian Branch 1997.

### **1.14 Referee for Societies, Institutes and funding bodies**

*The Wellcome Trust, UK*

I have reviewed two major five year Grant applications for this funding body and another this year for a two year grant.

*John Curtin School of Medical Research*

Performance reviewer for a member of this Institute as requested by its Head for internal auditing

*NHMRC, NHF and MRC Grant reviewer*

Approximately fifteen years service for the NHMRC and three for the NHF.

NHMRC Grants Review Panel – Pharmacology. 2002 and 2004

### **1.15 Theses Examiner**

External PhD (four over the last three years) and internal and external (Department of Anatomy) Honours examiner.

# Protease-Activated Receptor-2 Activating Peptide SLIGRL Inhibits Bacterial Lipopolysaccharide-Induced Recruitment of Polymorphonuclear Leukocytes into the Airways of Mice

James D. Moffatt, Kate L. Jeffrey, and Thomas M. Cocks

Department of Pharmacology, The University of Melbourne, Parkville, Victoria, Australia

Protease-activated receptor-2 (PAR2) acts as a receptor for trypsin and trypsin-like enzymes. The role of this receptor in airway inflammation is uncertain. In this study we assessed the effect of activation of PAR2 following intranasal administration of the peptide activator of PAR2, SLIGRL, over 72 h in mice. The extent of immune cell infiltration into the airways and activities of matrix metalloproteinase-2 (MMP-2) and MMP-9 were assessed in bronchoalveolar lavage (BAL) by differential cell counts and gelatin zymography, respectively. SLIGRL did not cause a change in the number or types of cells retrieved in BAL at any time point and did not alter the levels of MMP-2 and MMP-9 present in BAL. In contrast, similar intranasal administration of bacterial lipopolysaccharide (LPS) caused a large influx of neutrophilic polymorphonuclear leukocytes, which was associated with increased MMP-2 at 3 h only and MMP-9 activity from 3–72 h. Simultaneous administration of SLIGRL and LPS transiently potentiated increased MMP-9 activity at 3 h but markedly inhibited neutrophil influx and elevated MMP-2 activity at 3 h. These findings suggest that PAR2 agonists may be useful therapeutic molecules in pulmonary inflammatory diseases.

Protease-activated receptor-2 (PAR2) is a member of a family of four receptors that are activated by serine proteases (1). All members of this receptor family are activated by an extracellular amino acid sequence that is able to bind intramolecularly only after proteolytic removal of a blocking upstream sequence. As such, these receptors act as "sensors" of serine proteases (1). PAR2 is a unique member of this receptor family because it is activated by trypsin and similar enzymes rather than by thrombin, which activates PAR1, PAR3, and PAR4 (1). It is widely held that PAR2 is a receptor for the mast cell-derived serine protease tryptase and that PAR2 may therefore participate in the progression of inflammatory diseases (2). Indeed, intraplantar injection of the hexapeptide SLIGRL (single amino acid code), which mimics the "tethered ligand" region of PAR2 and causes receptor activation, causes an inflammatory response associated with an influx of polymorphonuclear leukocytes (3). However, we have suggested that in some organs, including the lung, PAR2 serves as a detector of inflammatory responses and is coupled to protective rather than destructive pathways (1, 4). Support

for this hypothesis includes the observations that SLIGRL protects against coronary ischemia-reperfusion injury (5) and inhibits the development of gastric ulcers (6).

Activation of PAR2 using the peptide SLIGRL causes relaxation of isolated airway preparations (7–9) and protects against bronchoconstrictor challenges *in vivo* in guinea pigs (10) and rats (7). Whether PAR2 activation has any inflammatory effect after administration to the lungs has not been explored in depth, although Cicala and coworkers (10) showed that intravenous SLIGRL had a modest inhibitory effect on histamine-induced pulmonary microvascular leakage in guinea pigs. PAR2 activation has been shown to initiate the release of matrix metalloproteinases (MMPs) (11), particularly MMP-9 and eosinophil survival factors (12) from a human alveolar epithelial cell line, suggesting a possible proinflammatory role for PAR2 over a longer time scale. In preliminary studies we have found that SLIGRL modestly inhibits lipopolysaccharide (LPS)-induced pulmonary neutrophilia (4) over a short (3 h) time frame. In the present study we have examined the possible inflammatory effect of SLIGRL delivered intranasally to the airways alone, and during a bacterial LPS-induced inflammatory response over a 72-h time course by examining cell populations obtained from bronchoalveolar lavage (BAL). We have also analyzed BAL fluid using zymographic techniques that can detect both changes in MMP-9 (13) and trypsin levels (14) to determine if either enzyme is regulated by inflammation or PAR2 activation. The results clearly demonstrate that SLIGRL does not cause pulmonary inflammation but can markedly inhibit the accumulation of neutrophils in response to an inflammatory stimulus.

## Materials and Methods

### Animals

Specific-pathogen free Balb/C mice (18–22 g) were obtained from the Animal Resource Centre (Perth, WA, Australia) and housed locally for less than 2 wk on a standard diet and constant light cycle. Animals received SLIGRL (50  $\mu$ l, 10 mg/ml; custom synthesis of amidated peptide by Auspep, Melbourne, Vic., Australia), LPS (50  $\mu$ l, 0.2 mg/ml; *Escherichia coli* serotype 0127:B8; Sigma, St. Louis, MO), or both in combination (25  $\mu$ l SLIGRL, 20 mg/ml; 25  $\mu$ l LPS, 0.4 mg/ml) intranasally under light halothane anesthesia as previously described (15). LPS and SLIGRL were dissolved in sterile phosphate-buffered saline (PBS). In preliminary studies, we found the dose of SLIGRL used had a modest anti-inflammatory effect against LPS-induced pulmonary neutrophilia, whereas lower doses had minimal effect (4). In the present study we also determined that the inactive peptide LSIGRL (16; amidated peptide a gift of Dr. P. Henry, University of Western Australia) had no effect in this model (see RESULTS). Animals were allowed to recover and were killed at 1, 3, 6, 24, 48, and 72 h and bronchoal-

(Received in original form November 26, 2001 and in revised form January 28, 2002)

Address correspondence to: James D. Moffatt, Ph.D., Department of Pharmacology, The University of Melbourne, Parkville, Victoria 3010, Australia. E-mail: jdm@unimelb.edu.au

Abbreviations: analysis of variance, ANOVA; bronchoalveolar lavage, BAL; BAL fluid, BALF; ethylenediaminetetraacetic acid, EDTA; lipopolysaccharide, LPS; matrix metalloproteinase, MMP; protease-activated receptor-2, PAR2; phosphate-buffered saline, PBS; prostaglandin  $E_2$ , PGE<sub>2</sub>; sodium dodecyl sulfate, SDS; SDS-polyacrylamide gel electrophoresis, SDS-PAGE.

Am. J. Respir. Cell Mol. Biol. Vol. 26, pp. 680–684, 2002  
Internet address: www.atsjournals.org

veolar lavage performed. Because we have previously established that saline alone has no significant effect on BAL cell populations (data not shown), we did not perform time-matched saline controls, but used untreated animals as controls to establish that the baseline inflammatory status of each group was similar.

## BAL

Mice were killed with an overdose of sodium pentobarbitone (80 mg/kg, intraperitoneally; Rhone Merieux, Pinkenba, QLD, Australia). The trachea was exposed and cannulated with a polyethylene tube held in place with a small artery clamp and BAL performed with three 0.5-ml aliquots of PBS. A total of 1.2–1.4 ml of BAL fluid (BALF) was consistently recovered by this technique.

## BALF Cell Counts

The total number of cells retrieved in BALF was determined using a hemocytometer and differential cell counts were performed on cytopsin (Shandon Scientific, Pittsburgh, PA) preparations of BALF stained with May-Grünwald and Geimsa stains (Sigma). At least 200 cells were counted in each sample.

## Gelatin Zymography

Supernatants of centrifuged BALF samples were mixed 1:1 with nonreducing sample buffer (125 mM Tris [pH 6.8], 20% glycerol, 4% sodium dodecylsulfate [SDS], and 0.002% bromophenol blue) and separated by SDS-polyacrylamide gel electrophoresis (PAGE) in 10% polyacrylamide gels (Mini-Protein 3; Bio-Rad, Hercules, CA) which had been copolymerized with gelatin (5 mg/ml; type B, porcine skin, Sigma). The gels were then washed for 30 min in 2% Triton X-100 to refold proteins and then incubated at 37°C for 18 h in 50 mM Tris buffer (pH 7.3) containing 10 mM  $\text{CaCl}_2$  and 200 mM NaCl. In some experiments 20 mM ethylenediaminetetraacetic acid (EDTA) was added to the incubation buffer to inhibit metalloproteinases by chelating  $\text{Zn}^{2+}$  ions required for proteolytic activity (17). After incubation the gels were stained with Coomassie Blue (Brilliant Blue R250 [Sigma] in 40% methanol/10% acetic acid) and destained by boiling in distilled water for 10 min in a microwave oven (500 W). This destaining procedure produced reproducible background staining between individual gels. Areas of gelatinolytic activity appear as clear bands against a dark blue background. Images of the gels were captured with an external linear gray-scale calibration standard using a CCD camera coupled to a personal computer. The density of individual bands of gelatinolytic activity was estimated on a Macintosh computer using the public domain software NIH Image (available at <http://rsb.info.nih.gov/nih-image>) and is expressed in arbitrary units.

## Western Blotting

Samples of BALF were mixed with sample buffer (*see above*) and proteins separated by SDS-PAGE on 10% polyacrylamide gels and electrophoretically transferred to nitrocellulose membranes (Bio-Rad) using the Bio-Rad mini transblot apparatus (100 V, 1 h). The membranes were blocked for 1 h in PBS containing 1% bovine serum albumin, 0.05% Tween 20, and 5% skim milk powder at 37°C (PBST-BSA), briefly rinsed and incubated overnight at 4°C in a rabbit primary antisera raised against MMP-9 (AB19047, diluted 1:5,000; Chemicon, Temecula, CA). After washing the membranes with PBST-BSA, an anti-rabbit secondary antibody conjugated to horseradish peroxidase (diluted 1:1,000; Silenus, Melbourne, Vic., Australia) was applied for 1 h at room temperature. Enhanced chemiluminescence (NEN, Boston, MA) was used to detect labeled antigen.

## Statistics

Data are expressed as the mean  $\pm$  standard error (SE) of the mean. Differences between groups of mice at different time points were

assessed using a one-way analysis of variance (ANOVA) with a Newman-Keuls *post hoc* test. A *P* value  $< 0.05$  was accepted as statistically significant.

## Results

### BALF Cellularity

As we observed in preliminary experiments (4), SLIGRL at a concentration of 10 mg/ml inhibited LPS-induced neutrophilia at 24 h. We now show that this effect of SLIGRL is due to activation of PAR2, because the reverse peptide LSIGRL was ineffective (Figure 1). In our extended study, SLIGRL alone did not significantly modify the number of neutrophils or macrophages present in BALF at any time point, although there were small, statistically insignificant, increases in neutrophils at 48 h and macrophages at 48 and 72 h (Figure 2). By contrast, LPS administration caused a massive influx of neutrophils, starting at 3 h, peaking at 48 h, and then declining by 72 h (Figure 2). Macrophage numbers in BAL also increased after LPS challenge, but at later (48–72 h) time points, indicating that macrophage recruitment was probably secondary to neutrophil entry (Figure 2). The combination of LPS and SLIGRL also elicited cellular recruitment into the airways (Figure 2). However, the number of neutrophils found in BAL was statistically less than that found in response to LPS alone from 6 h onwards. Co-administration of SLIGRL with LPS also resulted in a significant attenuation of the late (48 and 72 h) influx of macrophages compared with LPS alone (Figure 2).

### MMP and Trypsin Activities in BALF

In all BAL samples only two bands of gelatinolytic activity were observed, one at  $\sim 115$  kD and the other at 70 kD (Figure 3A). Neither band was observed when gels were incubated in EDTA (data not shown), suggesting that both are metalloproteinases (17). Because the 115-kD activity was modified by the experimental treatments and because it was consistently 10 kD heavier than the reported molecular weight of 105 kD (13) of murine MMP-9, we further confirmed the identity of this activity as MMP-9

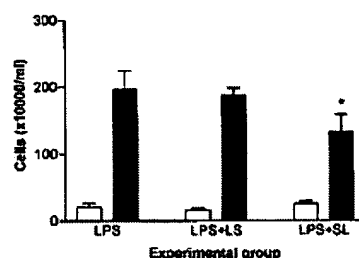


**Figure 1.** Data from studies to test the effectiveness of the reverse peptide LSIGRL, which does not activate PAR2, in abrogating LPS-induced accumulation of neutrophils to the murine lung. BAL fluids were obtained at 24 h after administration of LPS alone or in combination with either the active PAR2-activating peptide SLIGRL (SL) or LSIGRL (LS) as described in the text. Data are expressed as mean  $\pm$  SE from 4–7 animals. \* indicates a significant difference compared with control ( $P < 0.05$ ; ANOVA with Newman-Keuls *post hoc* test). Open bars, macrophages; solid bars, neutrophils.

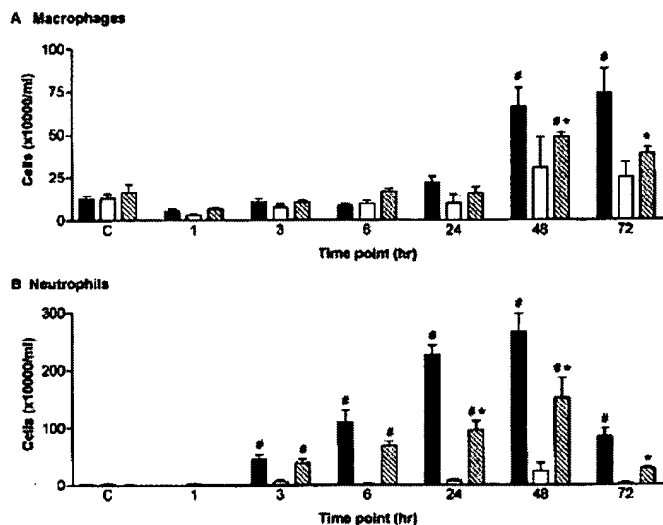


**Figure 2.** Time course of cellular influx into the airways determined by differential cell counts of cytospin preparations of BALF. The time point designated as C indicates cell counts from animals that received no treatment. \* indicates significantly different ( $P < 0.05$ ; ANOVA with Newman-Keuls *post hoc* test) than control (untreated) mice for that group. \* indicates a significant difference ( $P < 0.05$ ; ANOVA with Newman-Keuls *post hoc* test) between the LPS and LPS+SLIGRL groups at that time point. Data are expressed as mean  $\pm$  SE; each group consists of 5–6 animals. Solid bars, LPS; open bars, SLIGRL; striped bars, LPS+SLIGRL.

by Western blot (Figure 3B). MMP-9 was markedly upregulated by LPS or the combination of LPS and SLIGRL, but was unaffected by SLIGRL alone (Figure 3C). There was no significant difference between the amount of MMP-9 activity detected in the LPS and LPS+SLIGRL groups, except at 3 h, at which time SLIGRL significantly potentiated the response to LPS (Figure 3C). The 70-kD activity was unchanged in all groups at all time points with the exception of the LPS-treated group at 3 h (Figure 3D), in which there was a variable but significant increase in activity. This activity almost certainly represents MMP-2 based on its molecular weight, the presence of a slightly heavier pro-form of the protein when higher levels were detected, and its sensitivity to EDTA. Co-administration of LPS and SLIGRL prevented the LPS-induced increase in MMP-2 activity at the 3-h time point (Figure 3D). We did not observe any gelatinolytic activity at 23 kD corresponding to trypsin itself as previously reported using this method (14), although we were able to detect such activity in lung homogenates (data not shown). We were also able to detect trypsin in lung homogenates by Western blotting (data not shown); neither technique revealed a difference in levels of trypsin between control and LPS-treated mice.

## Discussion

The results of this study clearly demonstrate that intranasal delivery of the PAR2-activating peptide SLIGRL did not cause any inflammation in the airways and, importantly, it inhibited the marked immune cell inflammatory response triggered by LPS. Previous studies have demonstrated that intranasally delivered LPS initiates a significant inflammatory response in murine lungs, including infiltration of neutrophils (13). In the present study LPS caused a similar inflammatory response with very high neutrophil numbers in BALF peaking at 48 h after challenge and then declining over the next 24 h. The significant increase the number of macrophages at 48 and 72 h presumably reflects the resolution of inflammation and

phagocytosis of neutrophils by macrophages. This differential cellular response provides both a useful model to compare the effects of different inflammatory stimuli, and an assay for anti-inflammatory drugs. Unlike LPS, SLIGRL did not cause any significant inflammatory cell infiltration in this model. Our additional finding that SLIGRL abrogated the inflammatory cellular response to LPS added further weight to our suggestion that PAR2 agonists may be useful anti-inflammatory drugs in the lungs (1).

Because alterations in MMP levels have been observed in both murine BAL following LPS administration (18), and in conditioned medium from human airway epithelial cells stimulated with PAR2 agonists (11), we performed similar experiments in the present study. Our zymographic analysis of BALF from the same three groups of mice used for the cell infiltration studies revealed two consistent bands of gelatinolytic activity with approximate molecular weights of 115 and 70 kD. The 115-kD band almost certainly corresponds to MMP-9 and we confirmed this using Western blot analysis. The failure of MMP-9 to migrate to its predicted molecular weight of 105 kD (13) may be due to binding of MMP-9 to another protein. For example, human neutrophil-derived MMP-9 is usually bound in an SDS-stable complex to neutrophil gelatinase B-associated lipocalin, giving MMP-9 an apparent molecular weight of 120 kD rather than 92 kD (19). The 70-kD band detected in our studies here presumably represents MMP-2, and because the levels of this enzyme were not dramatically altered in any of the groups, except in the LPS-treated group at 3 h (*see below*), we did not examine the identity of this enzyme further. The marked increase in MMP-9 activity in BALF from LPS-treated mice agrees well with previous reports using this and similar models of lung injury (18, 20–23). Also, using cultured cell populations, Vliagoftis and colleagues (11) demonstrated that PAR2 agonists cause an increase in levels of MMP-9 in culture media. Based on their findings, we had anticipated a similar effect of SLIGRL *in vivo*. Our finding that SLIGRL alone did not alter gelatinolytic activities in BAL may represent a

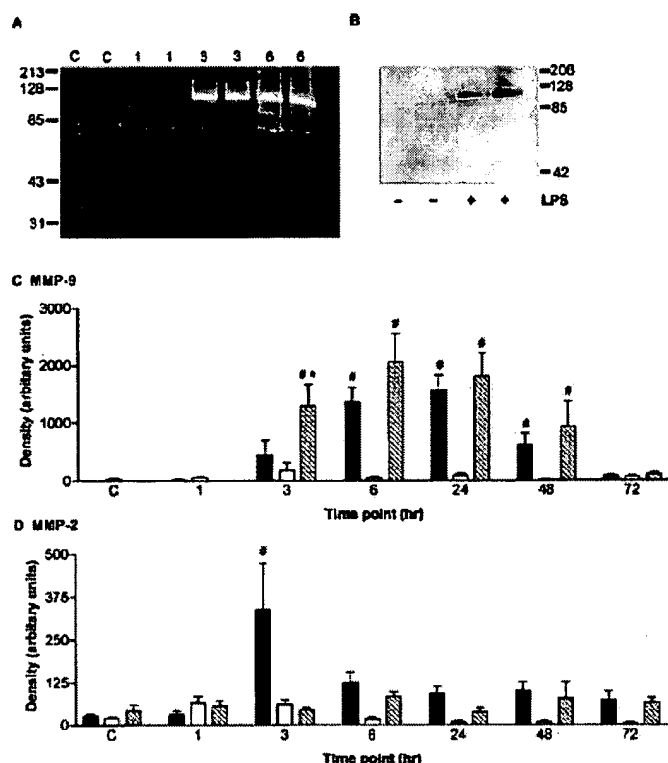


**Figure 3.** Time course of activity of MMP-2 and MMP-9 in BALF. (A) An example of a gelatin zymogram showing the increased gelatinolytic activity at approximately 120 kD and the only minor changes in activity at 70 kD at various time points after LPS challenge. C indicates samples from control (untreated) mice. (B) Western blot demonstrating increased MMP-9 activity at 120 kD 24 h after LPS treatment. The symbols – and + indicate samples from control (untreated) and LPS-treated mice, respectively. (C and D) Time course of changes in estimated density of gelatinolytic bands in zymograms for the three groups of mice. \* indicates significantly different ( $P < 0.05$ ; ANOVA with Newman-Keuls *post hoc* test) than control (untreated) mice. # indicates a significant difference ( $P < 0.05$ ; ANOVA with Newman-Keuls *post hoc* test) between the LPS and LPS+SLIGRL groups at that time point. Data are expressed as mean  $\pm$  SE; each group consists of 5–6 animals. Solid bars, LPS; open bars, SLIGRL; striped bars, LPS+SLIGRL.

species difference, but more likely points to the more complicated *in vivo* environment and the differences between cells *in vitro* and *in vivo*.

Because gelatin zymography has been used to detect 23 kD trypsin in murine lung tissue (14) and trypsin levels have been shown to be elevated in other inflammatory conditions (1, 24), we were surprised that we were unable to detect any such activity in BALF from LPS-treated mice. Trypsin can be detected in lung homogenates using zymography and immunoblotting techniques in these mice, but levels appear unchanged following LPS administration (data not shown). Thus, it appears that in this model of inflammation, release of trypsin does not occur. Because PARs detect serine proteases like trypsin but not MMPs, these receptors are more likely to be involved in serine protease homeostasis, a possibility we are presently exploring using other models of pulmonary disease.

The anti-inflammatory effect of PAR2 activation in the lungs raises the question of how this effect is mediated. PAR2 is expressed by a variety of cell types present in the lung, including epithelial cells (7), endothelial cells (25), and vascular (25) and airway smooth muscle (7). Furthermore, PAR2 is expressed by neutrophils (26) and other inflammatory cells (27). However, little is known about the effects of PAR2 activation on immune cell function, and therefore we can only speculate about which of these cells, or the interactions between them, are important in the anti-inflammatory effect of SLIGRL. For example, activation of PAR2 on these inflammatory cells may directly inhibit their ability to either release chemotactic mediators

or migrate through the submucosal tissues to reach the airway lumen. By contrast, it is established that activation of epithelial PAR2 in murine isolated airway preparations causes release of prostaglandin  $E_2$  ( $PGE_2$ ) by the epithelium (7, 16). Because  $PGE_2$  inhibits a variety of pathways relevant to pulmonary inflammation (1), it is possible that the effects of SLIGRL observed here were mediated via generation of  $PGE_2$ . Notably, in a similar model of murine pulmonary inflammation, inhibitors of prostaglandin synthesis have been shown to amplify, and  $PGE_2$  to inhibit, the cellular infiltration following LPS administration (28). Finally, SLIGRL has been reported in nonmurine tissues to activate unidentified receptors in some tissues (1). Therefore, we cannot exclude the possibility that the anti-inflammatory effects of SLIGRL were in some way unrelated to activation of PAR2. We stress, however, that regardless of possible alternative sites of action of SLIGRL, it is clear that this peptide would have activated airway epithelial PAR2 in our hands and that no proinflammatory effects were observed.

The inhibition of LPS-induced pulmonary neutrophilia by SLIGRL was delayed, suggesting either a long-term effect, or an acute effect that profoundly influences later processes. Because SLIGRL is likely to be metabolized by peptidases in the lung, the latter suggestion is appealing. Co-administration of SLIGRL and LPS had only two effects in the short term that were different from LPS alone in this study and occurred only at the 3-h time point: potentiation of MMP-9 and abolition of the smaller LPS-induced increase in MMP-2. We speculate that these small



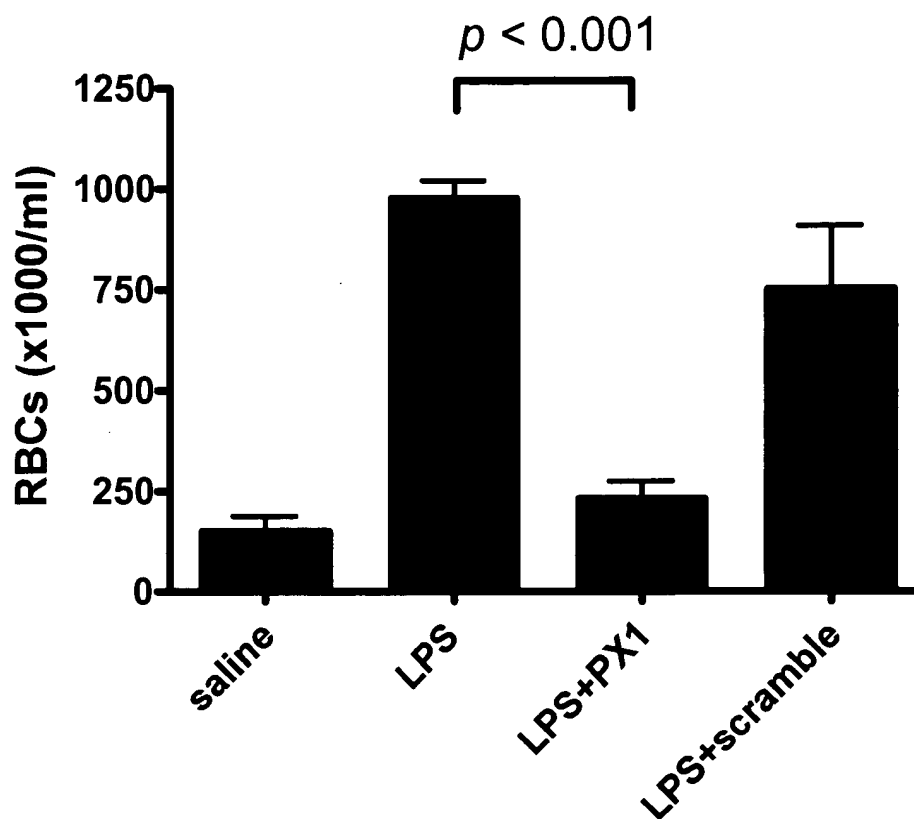
differences at the early part of the inflammatory response may, in some way, be causally related to the subsequent dampening of immune cell influx into the airways. MMP-9 is not thought to be important in LPS-induced neutrophilia because the number of neutrophils found in BAL is similar in wild-type and MMP-9 gene knockout mice (23). This finding agrees with our observation that, although SLIGRL co-administration with LPS increased the level of MMP-9 at the 3-h time point, there was no difference in the numbers of neutrophils retrieved in BALF. Hence, an elevation of the activity of this enzyme at the 3-h time point does not seem a likely cause of the subsequent inhibition of neutrophil influx. However, inhibition of MMPs has been shown to be anti-inflammatory in other models of pulmonary inflammation (28–30). Therefore, it is possible that the abolition of the 3-h increase in LPS-induced MMP-2 by SLIGRL may have reduced the potential for further neutrophil trafficking beyond this time point.

In conclusion, intranasal administration of SLIGRL inhibits LPS-driven recruitment of neutrophils into the airways. Although the precise mechanism underlying this effect is unknown, our findings strongly support our earlier proposal (1) that PAR2 agonists may have therapeutic potential in pulmonary inflammatory diseases.

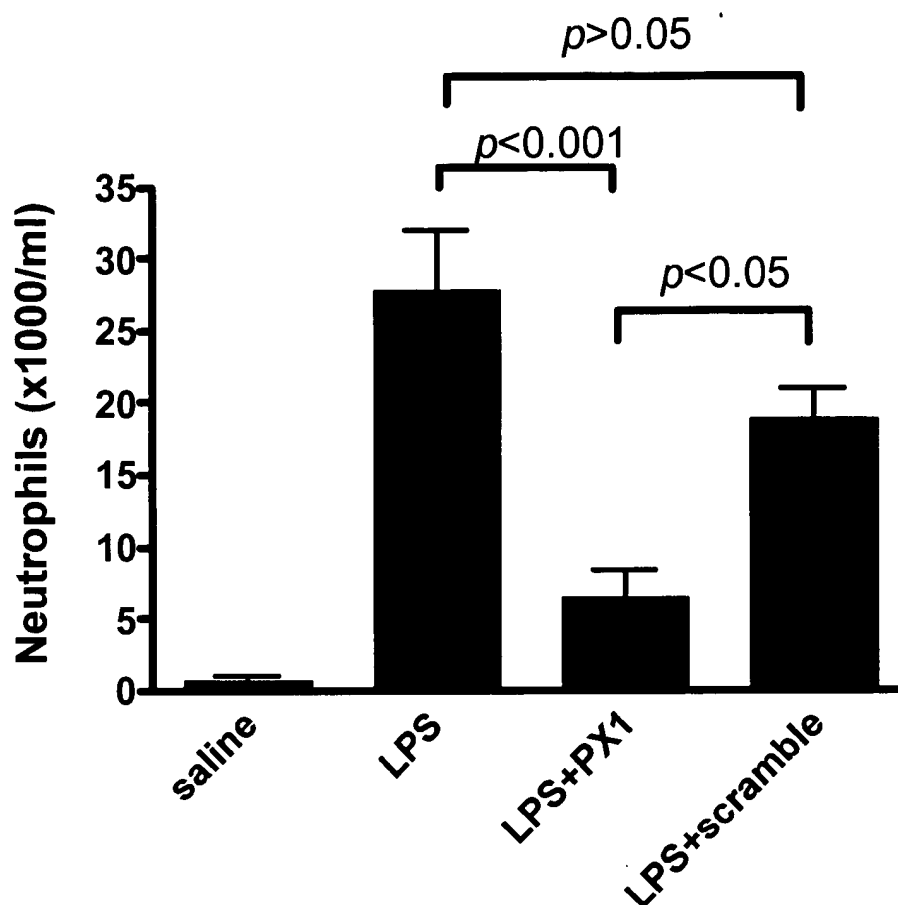
**Acknowledgment:** This project was funded by a grant from the NHRMC of Australia.

## References

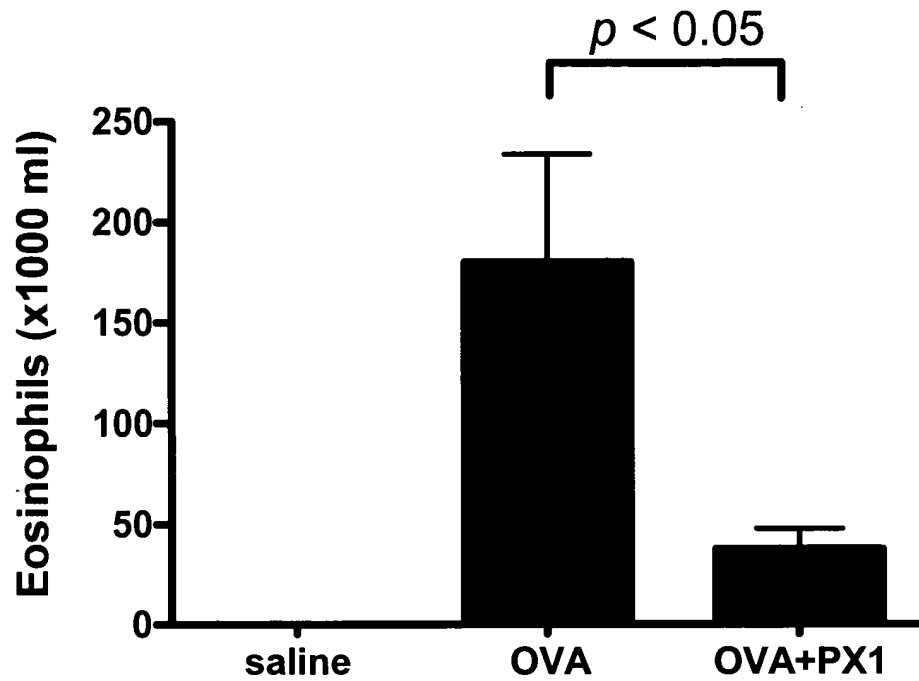
- Cocks, T. M., and J. D. Moffatt. 2000. Protease-activated receptors: sentries for inflammation? *Trends Pharmacol. Sci.* 21:103–108.
- Dery, O., C. U. Corvera, M. Steinhoff, and N. W. Bunnett. 1998. Proteinase-activated receptors: novel mechanisms of signaling by serine proteases. *Am. J. Physiol.* 274:C1429–C1452.
- Vergnolle, N., J. L. Wallace, N. W. Bunnett, and M. D. Hollenberg. 2001. Protease-activated receptors in inflammation, neuronal signaling and pain. *Trends Pharmacol. Sci.* 22:146–152.
- Cocks, T. M., and J. D. Moffatt. 2001. Protease-activated receptor-2 (PAR2) in the airways. *Pulm. Pharmacol. Ther.* 14:183–191.
- Napoli, C., C. Cicala, J. L. Wallace, F. de Nigris, V. Santagada, G. Callendo, F. Franco, L. J. Ignarro, and G. Cirino. 2000. Protease-activated receptor-2 modulates myocardial ischemia-reperfusion injury in the rat heart. *Proc. Natl. Acad. Sci. USA* 97:3678–3683.
- Kawabata, A., M. Kinoshita, H. Nishikawa, R. Kuroda, M. Nishida, H. Arai, N. Arizono, Y. Oda, and K. Kakehi. 2001. The protease-activated receptor-2 agonist induces gastric mucus secretion and mucosal cytoprotection. *J. Clin. Invest.* 107:1443–1450.
- Cocks, T. M., B. Fong, J. M. Chow, G. P. Anderson, A. G. Frauman, R. G. Goldie, P. J. Henry, M. J. Carr, J. R. Hamilton, and J. D. Moffatt. 1999. A protective role for protease-activated receptors in the airways. *Nature* 398:156–160.
- Lan, R. S., D. A. Knight, G. A. Stewart, and P. J. Henry. 2001. Role of PGE(2) in protease-activated receptor-1, -2 and -4 mediated relaxation in the mouse isolated trachea. *Br. J. Pharmacol.* 132:93–100.
- Chow, J. M., J. D. Moffatt, and T. M. Cocks. 2000. Effect of protease-activated receptor (PAR)-1, -2 and -4-activating peptides, thrombin and trypsin in rat isolated airways. *Br. J. Pharmacol.* 131:1584–1591.
- Cicala, C., D. Spina, S. D. Keir, B. Severino, R. Meli, C. P. Page, and G. Cirino. 2001. Protective effect of a PAR2-activating peptide on histamine-induced bronchoconstriction in guinea-pig. *Br. J. Pharmacol.* 132:1229–1234.
- Viliagoffis, H., A. Schwingshackl, C. D. Milne, M. Duszyk, M. D. Hollenberg, J. L. Wallace, A. D. Befus, and R. Moqbel. 2000. Proteinase-activated receptor-2-mediated matrix metalloproteinase-9 release from airway epithelial cells. *J. Allergy Clin. Immunol.* 106:537–545.
- Viliagoffis, H., A. D. Befus, M. D. Hollenberg, and R. Moqbel. 2001. Airway epithelial cells release eosinophil survival-promoting factors (GM-CSF) after stimulation of proteinase-activated receptor 2. *J. Allergy Clin. Immunol.* 107:679–685.
- Tanaka, H., K. Hojo, H. Yoshida, T. Yoshida, and K. Sugita. 1993. Molecular cloning and expression of the mouse 105 kDa gelatinase cDNA. *Biochem. Biophys. Res. Commun.* 190:732–740.
- Koshikawa, N., S. Hasegawa, Y. Nagashima, K. Mitsuhashi, Y. Tsubota, S. Miyata, Y. Miyagi, H. Yasumitsu, and K. Miyazaki. 1998. Expression of trypsin by epithelial cells of various tissues, leukocytes, and neurons in human and mouse. *Am. J. Pathol.* 153:937–944.
- Szarka, R. J., N. Wang, L. Gordon, P. N. Nation, and R. H. Smith. 1997. A murine model of pulmonary damage induced by lipopolysaccharide via intranasal instillation. *J. Immunol. Methods* 202:49–57.
- Lan, R. S., G. A. Stewart, and P. J. Henry. 2000. Modulation of airway smooth muscle tone by protease activated receptor-1, -2, -3 and -4 in trachea isolated from influenza A virus-infected mice. *Br. J. Pharmacol.* 129:63–70.
- Benayon, R. J., and J. S. Bond. 1989. *Proteolytic Enzymes: A Practical Approach*. IRL Press at Oxford University Press, Oxford.
- Corbel, M., E. Boichot, and V. Lagente. 2000. Role of gelatinases MMP-2 and MMP-9 in tissue remodelling following acute lung injury. *Braz. J. Med. Biol. Res.* 33:749–754.
- Opdenakker, G., P. E. Van den Steen, B. Dubois, I. Nelissen, E. Van Coillie, S. Masure, P. Proost, and J. Van Damme. 2001. Gelatinase B functions as a regulator and effector in leukocyte biology. *J. Leukoc. Biol.* 69:851–859.
- Underwood, D. C., R. R. Osborn, S. Bochnowicz, E. F. Webb, D. J. Riemann, J. C. Lee, A. M. Romanic, J. L. Adams, D. W. P. Hay, and D. E. Griswold. 2000. SB 239063, a p38 MAPK inhibitor, reduces neutrophilia, inflammatory cytokines, MMP-9 and fibrosis in lung. *Am. J. Physiol. Lung. Mol. Physiol.* 279:L895–L902.
- Warner, R. L., L. Beltran, E. M. Younkin, C. S. Lewis, S. J. Weiss, J. Varani, and K. J. Johnson. 2000. Role of stromelysin 1 and gelatinase B in experimental acute lung injury. *Am. J. Respir. Cell Mol. Biol.* 24:537–544.
- Wang, Z., T. Zheng, Z. Zhu, R. J. Homer, R. J. Riese, H. A. Chapman, Jr., S. D. Shapiro, and J. A. Elias. 2000. Interferon  $\gamma$  induction of pulmonary emphysema in the adult murine lung. *J. Exp. Med.* 192:1587–1599.
- Betsuyaku, T., J. M. Shipley, Z. Liu, and R. M. Senior. 2000. Neutrophil emigration in the lungs, peritoneum, and skin does not require gelatinase B. *Am. J. Respir. Cell Mol. Biol.* 20:1303–1309.
- Tarleton, J. F., C. V. Whiting, D. Tunmore, S. Bregenholt, J. Reimann, M. H. Claesson, and P. W. Bland. 2000. The role of upregulated serine proteases and matrix metalloproteinases in the pathogenesis of a murine model of colitis. *Am. J. Pathol.* 157:1927–1935.
- D'Andrea, M. R., C. K. Derian, D. Leturcq, S. M. Baker, A. Brunmark, P. Ling, A. L. Darrow, R. J. Santulli, L. F. Brass, and P. Andrade-Gordon. 1998. Characterization of protease-activated receptor-2 immunoreactivity in normal human tissues. *J. Histochem. Cytochem.* 46:157–164.
- Howells, G. L., M. G. Macey, C. Chinnai, L. Hou, M. T. Fox, P. Harriott, and S. R. Stone. 1997. Proteinase-activated receptor-2: expression by human neutrophils. *J. Cell Sci.* 110:881–887.
- D'Andrea, M. R., C. J. Rogahn, and P. Andrade-Gordon. 2000. Localization of protease-activated receptors-1 and -2 in human mast cells: indications for an amplified mast cell degranulation cascade. *Biotech. Histochem.* 75:85–90.
- Morales, V. L. G., B. B. Vargaftig, J. Lefort, A. Meager, and M. Chignard. 1996. Effect of cyclo-oxygenase inhibitors and modulators of cyclic AMP formation on lipopolysaccharide-induced neutrophil infiltration in mouse lung. *Br. J. Pharmacol.* 117:1792–1796.
- Kumagai, K., I. Ohno, S. Okada, Y. Ohtakawa, K. Suzuki, T. Shinya, H. Nagase, K. Iwata, and K. Shirato. 1999. Inhibition of matrix metalloproteinases prevents allergen-induced airway inflammation in a murine model of asthma. *J. Immunol.* 162:4212–4219.
- Zheng, T., Z. Zhu, Z. Wang, R. J. Homer, B. Ma, R. J. Riese, Jr., H. A. Chapman, S. D. Shapiro, and J. A. Elias. 2000. Inducible targeting of IL-13 to the adult lung causes matrix metalloproteinase- and cathepsin-dependent emphysema. *J. Clin. Invest.* 106:1081–1093.



*Red blood cell (RBC) count.* RBC numbers were determined from samples of bronchial alveolar lavage fluid taken 24 h post intranasal administration. Saline,  $n = 6$  (50  $\mu$ l sterile saline); LPS,  $n = 3$  (0.2 mg/ml bacterial lipopolysaccharide in 50  $\mu$ l saline), LPS + PX1,  $n = 3$  (LPS 0.2 mg/ml + SLIGRL 10 mg/ml in 50  $\mu$ l saline); LPS + scramble,  $n = 3$  (LPS 0.2 mg/ml + LRGILS in 50  $\mu$ l sterile saline).



*Neutrophil count.* Neutrophil numbers were determined from samples of bronchial alveolar lavage fluid 24 post aerosol administration. Saline,  $n = 6$  (aerosolisation rate was 10 ml over 20 min). LPS (0.01 mg/ml, 10 ml over 20 min); LPS + PX1,  $n = 6$  (LPS 0.01 mg/ml + SLIGRL 500  $\mu$ M, 10 ml over 20 min); LPS + scramble (LPS 0.01 mg/ml + LRGILS 500  $\mu$ M 10 ml over 20 min).



*Eosinophil count.* Eosinophil numbers were determined from samples of bronchial alveolar lavage fluid taken 24 h after the seventh day of aerosol OVA or saline (control) challenge. Saline,  $n = 6$  (at a rate of 0.5 ml/min); OVA,  $n = 6$  (OVA 1 mg/ml in sterile saline at a rate of 0.5 ml/min), OVA + PX1,  $n = 6$  (OVA 1 mg/ml + SLIGRL 500  $\mu$ M at a rate of 0.5 ml/min).

Figure 1

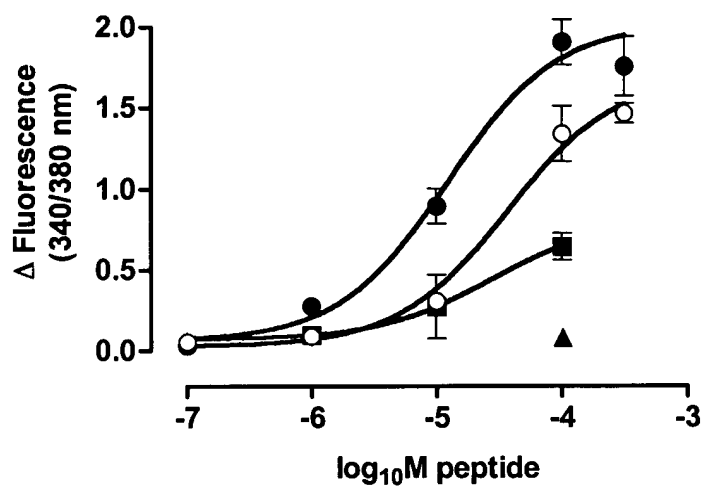


**Figure 1** Response to PAR agonists in an assay of intracellular calcium increase in A549 cells. Rat PAR<sub>2</sub> selective peptide, SLIGRL (●; n = 4), human PAR<sub>2</sub> selective peptide, SLIGKV (○; n = 3), PAR<sub>1</sub> selective peptide TFLLR (■; n = 4) and the scramble peptide LSIGRL (▲; n = 2). All bars represent mean ± S.E.M. of n experiments conducted in triplicate.

# EXHIBIT TC-7

**Table 1, Sequence information and Ca<sup>2+</sup> fluorescence data provide for 60 peptide amides.**

#	Sequence	X-identifier	% SLIGRL 10μM	s.e.m.
1	SLIGR	n/a	64.90	2.92
2	SLIG	n/a	11.61	2.50
3	tLIGRLL	n/a	15.16	2.92
4	SXIGRLL	L-Cha	145.82	6.66
5	SfIGRLL	n/a	5.43	0.32
6	SXIGRLL	L-1Nal	163.36	5.93
7	SXIGRLL	L-Nle	59.40	13.65
8	SXIGRLL	L-MeLeu	31.74	0.93
9	SXIGRLL	L-homoPhe	21.29	7.28
10	SLXGRLL	L-alloIle	45.11	15.09
11	SLIaRLL	n/a	7.41	1.36
12	SLIXRLL	Sar (MeGly)	52.72	4.91
13	SLIXRLL	beta-Ala	14.34	4.23
14	SLIXRLL	gamma-Abu	16.82	3.72
15	SLIGfLL	n/a	19.24	3.96
16	SLIGXLL	L-Phe(NO <sub>2</sub> )	92.32	11.90
17	SLIGXLL	L-homoPhe	46.84	11.65
18	SLIGXLL	D-homoPhe	15.95	1.58
19	SLIGwLL	n/a	15.10	3.98
20	SLIGXLL	L-Ser(Bzl)	37.34	5.65
21	SLIGFRW	n/a	83.17	8.49
22	XLIGRL	L-homoSer	25.65	2.44
23	tLIGRL	n/a	9.24	1.63
24	SXIGRL	L-Cha	90.62	10.15
25	SXIGRL	L-1Nal	30.93	12.42
26	SXIGRL	L-Nva	30.16	2.27
27	SXIGRL	L-MeLeu	6.77	3.09
28	SLIaRL	n/a	9.19	4.03
29	SLIXRL	beta-Ala	8.32	5.07
30	SLIXRL	gamma-Ala	6.82	2.49
31	sliGrIL	n/a	8.19	1.35
32	sliGrLL	n/a	8.13	1.35
33	sliGRIL	n/a	6.84	1.83
34	sliGRLL	n/a	6.37	1.35
35	sliGrIL	n/a	12.15	2.63
36	sliGrLL	n/a	7.08	1.37
37	sliGRIL	n/a	4.87	1.62
38	sliGRLL	n/a	3.23	0.65
39	sLiGrIL	n/a	4.40	1.89
40	sLiGrLL	n/a	2.88	0.78
41	sLiGRIL	n/a	3.95	0.64

42	sLiGRLL	n/a	8.75	1.34
43	sLIGrIL	n/a	9.63	2.82
44	sLIGrLL	n/a	10.10	2.81
45	sLIGRIL	n/a	3.28	1.53
46	sLIGRLL	n/a	9.09	4.36
47	SliGrIL	n/a	7.06	1.89
48	SliGrLL	n/a	13.57	3.16
49	SliGRIL	n/a	11.52	3.47
50	SliGRLL	n/a	7.61	1.27
51	SIIGrIL	n/a	14.84	2.18
52	SIIGrLL	n/a	9.20	2.42
53	SIIGRIL	n/a	9.79	2.54
54	SILGRLL	n/a	9.85	0.54
55	SliGrIL	n/a	8.22	2.03
56	SliGrLL	n/a	11.38	1.19
57	SliGRIL	n/a	4.70	2.69
58	SLiGRLL	n/a	6.51	1.07
59	SLIGrIL	n/a	3.04	1.23
60	SLIGrIL	n/a	6.31	2.25

L-homoSer L-homoserine  
 L-1Nal 3 (1 naphthyl)-L alanine  
 L-Nva L-norvaline (2-aminopentanoicacid)  
 L-Nle L-norleucine (2-aminohexanoicacid)  
 L-MeLeu methyl-L-leucine  
 L-homoPhe L-homophenylalanine  
 L-alloIle L-alloisoleucine  
 Sar (MeGly) methylglycine  
 beta-Ala beta alanine  
 gamma-Abu gamma-amino-butanoic acid  
 L-Phe(NO<sub>2</sub>) nitro-L-phenylalanine  
 L-Ser(Bzl) O-benzyl-L-serine  
 L-Cha cyclohexyl-L-alanine  
 gamma-Ala gamma-alanine

## Permeabilization via the P2X<sub>7</sub> Purinoreceptor Reveals the Presence of a Ca<sup>2+</sup>-activated Cl<sup>-</sup> Conductance in the Apical Membrane of Murine Tracheal Epithelial Cells\*

Received for publication, June 7, 2000, and in revised form, August 8, 2000  
Published, JBC Papers in Press, August 15, 2000, DOI 10.1074/jbc.M004953200

Sherif E. Gabriel†§, Mariya Makhlina†, Elena Martsen†, Emma J. Thomas¶, Mike I. Lethem¶, and Richard C. Boucher†

From the †Cystic Fibrosis/Pulmonary Research and Clinical Treatment Center, University of North Carolina, Chapel Hill, North Carolina 27599 and the ¶School of Pharmacy and Biomolecular Sciences, University of Brighton, Brighton BN2 4GJ, United Kingdom

Calcium-activated Cl<sup>-</sup> secretion is an important modulator of regulated ion transport in murine airway epithelium and is mediated by an unidentified Ca<sup>2+</sup>-stimulated Cl<sup>-</sup> channel. We have transfected immortalized murine tracheal epithelial cells with the cDNA encoding the permeabilizing P2X<sub>7</sub> purinoreceptor (P2X<sub>7</sub>-R) to selectively permeabilize the basolateral membrane and thereby isolate the apical membrane Ca<sup>2+</sup>-activated Cl<sup>-</sup> current. In P2X<sub>7</sub>-R-permeabilized cells, we have demonstrated that UTP stimulates a Cl<sup>-</sup> current across the apical membrane of CF and normal murine tracheal epithelial cells. The magnitude of the UTP-stimulated current was significantly greater in CF than in normal cells. Ion substitution studies demonstrated that the current exhibited a permselectivity sequence of Cl<sup>-</sup> > I<sup>-</sup> > Br<sup>-</sup> > gluconate<sup>-</sup>. We have also determined a rank order of potency for putative Cl<sup>-</sup> channel blockers: niflumic acid ≥ 5-nitro-2-(3-phenylpropylamino)benzoic acid > 4,4'-diisothiocyanostilbene-2,2'-disulfonate > glybenclamide >> diphenylamine-2-carboxylate, tamoxifen, and *p*-tetra-sulfonato-tetra-methoxy-calix[4]arene. Complete characterization of this current and the corresponding single channel properties could lead to the development of a new therapy to correct the defective airway surface liquid in cystic fibrosis patients.

Chloride secretion across the airway epithelium can be stimulated by a number of secretagogues that activate distinct second messenger transduction mechanisms (reviewed in Refs. 1 and 2). The cystic fibrosis (CF)<sup>1</sup> gene product, the cystic fibrosis transmembrane conductance regulator (CFTR), accounts for the cAMP-regulated apical Cl<sup>-</sup> conductance (3, 4). There is, however, compelling evidence that a separate Ca<sup>2+</sup>-

activated apical Cl<sup>-</sup> conductance (CaCC) exists. A large class of ligands, including histamine (5, 6), bradykinin (7, 8), and extracellular ATP (9–11), has been shown to activate CaCC across the apical membrane of airway epithelia. The unique identity of this pathway in airway epithelia was established in studies of CF nasal epithelia, which demonstrated that Ca<sup>2+</sup> ionophores are effective Cl<sup>-</sup> secretagogues in CF tissues (12–14). Moreover, in the airways of the CFTR(–/–) knockout mouse, which definitively lacks CFTR (15), not only is the CaCC pathway preserved, but it appears to be up-regulated (16).

In the airway epithelium, Cl<sup>-</sup> secretion is dependent on the development of a favorable driving force, because at basal conditions Cl<sup>-</sup> is at or near electrochemical equilibrium across the apical membrane. Ca<sup>2+</sup><sub>i</sub> can stimulate Cl<sup>-</sup> secretion by multiple mechanisms. Elevation of Ca<sup>2+</sup><sub>i</sub> can directly activate an apical membrane-localized Cl<sup>-</sup> conductance and thereby stimulate an apical exit pathway for Cl<sup>-</sup> secretion. Ca<sup>2+</sup> mobilizing agents can also cause a hyperpolarization in the cell to generate a driving force for Cl<sup>-</sup> secretion across the apical membrane by either (or both) inhibiting an apical membrane Na<sup>+</sup> conductance (17) or activating a basolateral K<sup>+</sup> conductance. Thus study of Ca<sup>2+</sup><sub>i</sub>-activated Cl<sup>-</sup> conductance in the apical membrane of a polarized epithelium requires a means to identify the contributions of apical Cl<sup>-</sup> conductance in isolation from other actions.

Previous studies in non-polarized secretory epithelia, *e.g.* airway epithelia or T<sub>84</sub> cells plated as isolated or dissociated cells, have shown outwardly rectifying Cl<sup>-</sup> currents stimulated by intracellular Ca<sup>2+</sup> and sensitive to 4,4'-diisothiocyanostilbene-2,2'-disulfonate (DIDS) (18–24). These descriptions have included such a wide range of Cl<sup>-</sup> channel characteristics that no consensus on the characteristics of this channel can be achieved (25–28). Recently, a family of putative CaCC genes has been cloned (29–32). The single channel properties and the cellular localization of these gene products, however, have not yet been determined. Thus, no indisputably apical Ca<sup>2+</sup>-activated Cl<sup>-</sup> channel has been identified at either the molecular or single channel level.

We have recently identified a CaCC current expressed in immortalized CF and normal murine tracheal epithelial cell lines (33). In the current study we used permeabilization of the basolateral membrane to determine the basic biophysical properties of the CaCC current in a functionally isolated apical membrane of airway epithelial cells. We have accomplished basolateral permeabilization by a novel approach involving stable transfection of the P2X<sub>7</sub> purinoreceptor (P2X<sub>7</sub>-R) into our murine CF tracheal epithelial cell line. The P2X<sub>7</sub>-R is

\* This work was supported by Grant 99PO from the Cystic Fibrosis Foundation and Grant HL62564 from the National Institutes of Health (both to S. E. G.). The costs of publication of this article were defrayed in part by the payment of page charges. This article must therefore be hereby marked "advertisement" in accordance with 18 U.S.C. Section 1734 solely to indicate this fact.

§ To whom correspondence should be addressed: CF/PRT Center & Dept. of Pediatrics, University of North Carolina, Chapel Hill, NC 27599. Tel.: 919-966-7058; Fax: 919-966-7524; E-mail: sgabriel@med.unc.edu.

<sup>1</sup> The abbreviations used are: CF, cystic fibrosis; P2X<sub>7</sub>-R, P2X<sub>7</sub> purinoreceptor; CaCC, Ca<sup>2+</sup><sub>i</sub>-activated Cl<sup>-</sup> conductance; CFTR, cystic fibrosis transmembrane conductance regulator; KBR, Krebs bicarbonate Ringer solution; NFA, niflumic acid; NPPB, 5-nitro-2-(3-phenylpropylamino)benzoic acid; DIDS, 4,4'-diisothiocyanostilbene-2,2'-disulfonate; DPC, diphenylamine-2-carboxylate; TS-TM calixarene, *p*-tetra-sulfonato-tetra-methoxy-calix[4]arene.



unique within its family, because binding of nucleotides ( $\text{ATP}^{4-}$  is the preferred agonist) to this receptor results in the formation of a membrane pore that is capable of conducting molecules as large as 900 daltons (34, 35). The pore is not ion-selective and allows for free diffusion of both cations and anions. Thus, by application of ATP selectively to the basolateral solution, we can selectively permeabilize this barrier.

We report here the characterization of CaCC in the apical membrane of a CF tracheal epithelial cell line when activated by different classes of  $\text{Ca}^{2+}$ -mobilizing agents (UTP and ionomycin). We have determined the halide selectivity and inhibitor sensitivity of this  $\text{Cl}^-$  current unambiguously localized to the apical membrane. Importantly, these observations will provide us with the hallmark characteristics for comparison with subsequent whole cell and single channel studies and will enable us to evaluate CaCC candidate genes. A greater understanding of the characteristics and mechanism of regulation of the CaCC pathway is essential for development of pharmacological therapies designed to use CaCC as an alternate  $\text{Cl}^-$  channel to replace the defective CFTR.

#### EXPERIMENTAL PROCEDURES

**Cell Culture**—These studies utilized the immortalized murine tracheal epithelial cell line (MTE18) derived from the CFTR(−/−) knockout mouse, described previously (33). Cells were maintained and cultured at 33 °C, the permissive temperature for the immortalizing tsA58 Tag activity (33) on “Transwell-col” culture inserts. Culture medium consisted of a 1:1 mix of Ham’s F12 and 3T3 fibroblast-conditioned medium supplemented with the following hormones: transferrin (2.5 mg/ml), insulin (5 mg/ml), epidermal growth factor (12.5 ng/ml), endothelial cell growth supplement (1.875 mg/ml), triiodothyronine (15 nM), hydrocortisone (0.5 mM), and  $\text{CaCl}_2$  (0.5 mM). Cells were harvested for experimental studies by trypsinization and plated at high density ( $2 \times 10^4$  cells per  $\text{mm}^2$ ) onto tissue culture inserts (collagen matrix supports with a 4.5-mm plating diameter) and evaluated for confluence by daily monitoring of transepithelial resistance ( $R_T$ ) and potential difference ( $V_T$ ). Only monolayers generating at least a 1.0-millivolt (mV)  $V_T$  and a  $100\text{-}\Omega\text{-cm}^2$  resistance (after the resistance of the permeable support is subtracted) were used for Ussing chambers studies, typically 5–7 days after plating.

**Ussing Chamber Studies**—Electrical measurements, i.e.  $V_T$ ,  $R_T$ , and short-circuit current ( $I_{SC}$ ), were made on cell monolayers mounted in Ussing chambers. Monolayers were bathed in a Krebs bicarbonate Ringer solution (KBR) on both the luminal and the serosal sides. Serosal  $\text{Ca}^{2+}$  was buffered to 300 nM with the addition of EGTA (achieved by the addition of 1 mM EGTA and 0.925 mM  $\text{Ca}^{2+}$ ). Other alterations to the bathing solutions are listed in the figure legends. All bathing solutions were bubbled with 95%  $\text{O}_2$ , 5%  $\text{CO}_2$  and maintained at 37 °C.  $V_T$  was clamped to zero and pulsed to  $\pm 10$  mV for a 0.5-s duration every minute. Electrometer output was digitized online and  $I_{SC}$ ,  $R_T$ , and calculated transepithelial potential ( $V_T$ ) were displayed on a video monitor and stored on a computer hard drive. Drugs were added from concentrated stock solutions to either luminal and/or serosal sides of the tissue. To eliminate the contribution of apical  $\text{Na}^+$  channels, amiloride ( $10^{-4}$  M) was added to the luminal bath at the outset of all experiments. Data are expressed as mean  $\pm$  S.E. for the number of experiments ( $n$ ). Student’s  $t$  test was used to determine statistical significance between means.

**Permeabilization**—Basolateral membrane permeabilization was achieved by stable transfection of the recombinant P2X<sub>7</sub>-R (a generous gift from Dr. George Dubyak) into the MTE18 cell line. A cDNA construct of the P2X<sub>7</sub>-R was cloned into a retroviral expression vector with a selectable puromycin-resistance gene. Infection of the MTE18 cell line with this retroviral vector and selection of resistant colonies in puromycin-containing media resulted in the identification of several cell clones that were puromycin-resistant and were verified for expression of P2X<sub>7</sub>-R. These P2X<sub>7</sub>-R-expressing cells were plated on membrane supports and used for Ussing chamber studies.

Following recording of stable baseline  $I_{SC}$  and  $R_T$  (15–20 min in symmetrical  $\text{Cl}^-$  KBR solutions), 1 mM  $\text{ATP}^{4-}$  (UTP is not an agonist for the P2X<sub>7</sub>-R) was added to the serosal solution and serosal  $\text{Mg}^{2+}$  was reduced to 100  $\mu\text{M}$  to activate the pore (divalent cations inhibit pore formation). Following successful permeabilization, documented by a drop in the  $I_{SC}$  to 0  $\mu\text{A}/\text{cm}^2$ , the luminal solution was diluted by three

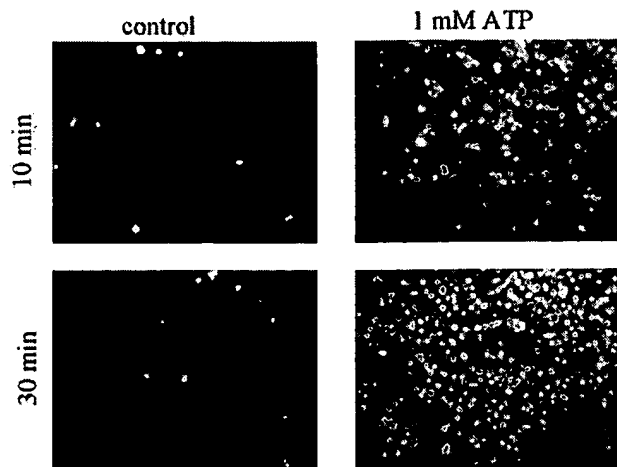


FIG. 1. ATP-mediated permeabilization of the basolateral membrane of P2X<sub>7</sub>-R monolayers. P2X<sub>7</sub>-R-expressing cells were exposed to 10  $\mu\text{M}$  ToPro-1-iodide in the absence (left two panels) or presence (right two panels) of 1 mM ATP for 10 or 30 min. Cells were photographed on a fluorescence inverted microscope with identical exposure times.

successive 1-ml replacements of KBR with a low  $\text{Cl}^-$  containing (4.8 mM  $\text{Cl}^-$ , 110 mM gluconate $^-$ ) KBR. This maneuver generates a gradient for  $\text{Cl}^-$  secretion with a serosal  $\text{Cl}^-$  concentration of 115 mM and a final luminal  $\text{Cl}^-$  concentration of  $\sim 68$  mM.  $\text{Ca}^{2+}$ -mobilizing agents were added to the luminal solution after the final dilution step. Anion selectivity was determined by a similar strategy used to generate the  $\text{Cl}^-$  gradients. Briefly, three successive 1-ml replacements of the luminal solution with a modified KBR solution containing a halide ion ( $\text{I}^-$ ,  $\text{Br}^-$ ) were substituted for  $\text{Cl}^-$  (e.g. 4.8 mM  $\text{Cl}^-$ , 110 mM  $\text{I}^-$ ). The inhibitor profile of CaCC was determined by the addition of inhibitors to the luminal solution after the imposition of the  $\text{Cl}^-$  gradient and prior to stimulation by UTP. All experiments consisted of alterations in the ion composition of the mucosal or serosal solution, followed by CaCC activation by addition of luminal UTP.

In a subset of experiments we used the  $\alpha$ -toxin of *Staphylococcus aureus* to permeabilize MTE18 or MTE7b (CFTR(+/-) cells) monolayers not expressing the P2X<sub>7</sub>-R. 1000 units of  $\alpha$ -toxin was introduced to the serosal compartment bathing MTE18 or MTE7b monolayers and monitored for  $\sim 60$  min until the  $I_{SC}$  dropped to 0  $\mu\text{A}/\text{cm}^2$ , indicating permeabilization. Subsequent dilutions and agonist additions were performed as described for P2X<sub>7</sub>-R monolayers.

**Data Analysis**—In CF and normal airway epithelial cells, mucosal nucleotides, ATP or UTP, acting via purinergic receptors cause an increase in  $I_{SC}$  by reducing the apical membrane resistance with little or no effect on the basolateral or shunt resistance, i.e. by directly activating an apical membrane conductance (11). All experiments were performed under voltage clamp conditions (clamped to 0 mV) and in the presence of a  $\text{Cl}^-$  gradient followed by the addition of mucosal UTP. Our experimental protocol defines the CaCC current as  $\Delta I_{\text{CaCC}} = I_{\text{UTP}} - I_{\text{gradient}}$ . Because the transepithelial potential is clamped to 0 mV, the equilibrium potential for  $\text{Cl}^-$  can be calculated as  $E_{\text{Cl}^-} = \Delta I_{\text{CaCC}} \Delta G_{\text{CaCC}}$  and is determined by the chemical driving force imposed as a result of the  $\text{Cl}^-$  gradient. This measured  $E_{\text{Cl}^-}$  should ideally equal the calculated  $E_{\text{Cl}^-}$  determined by the Nernst equation. We used the measured  $E_{\text{ion}}$  ( $\text{Cl}^-$ ,  $\text{Br}^-$ ,  $\text{I}^-$ ) values to determine a permselectivity sequence. Apparent differences between the measured  $E_{\text{ion}}$  and Nernst equation-calculated  $E_{\text{ion}}$  values are likely caused by ion permeation and accumulation in the unstirred layer closely adjacent to the membrane surface (37).

**Materials**—All biochemicals used were obtained from commercial sources and were of tissue culture grade or better.

#### RESULTS

Transfection and expression of P2X<sub>7</sub>-R in MTE18 cells followed by incubation of monolayers with 1 mM ATP and 10  $\mu\text{M}$  ToPro-1-iodide (a membrane-impermeant dye that fluoresces when bound to DNA,  $M_r = 645$ ) demonstrates efficient membrane permeabilization (Fig. 1). Although cells exposed to ATP for either 10 or 30 min showed distinct intracellular fluores-

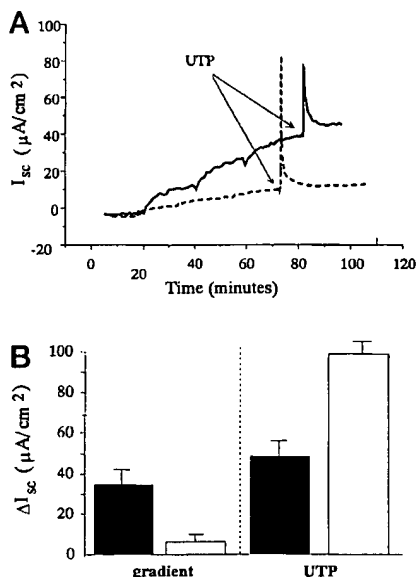


**FIG. 2. Characteristic CaCC current response in  $\text{P2X}_7$ -R permeabilized MTE18 monolayers.** A, typical  $I_{sc}$  responses in  $\text{P2X}_7$ -R-expressing MTE18 monolayers permeabilized by 1-mM serosal ATP (solid line) and non-permeabilized MTE18 monolayers (dashed line). Both permeabilized and non-permeabilized monolayers were treated similarly during the rest of the experimental protocol. Luminal  $\text{Cl}^-$  was successively diluted by replacement with a sodium gluconate solution to achieve a final luminal  $\text{Cl}^-$  concentration of 68 mM, and 10  $\mu\text{M}$  UTP was added to the luminal solution (as indicated by the arrows). B, mean  $\text{Cl}^-$  current responses in permeabilized (filled bars) and non-permeabilized (open bars) MTE18 monolayers. Gradient responses (left two bars) represent the total  $I_{sc}$  response following the final solution change. The  $I_{sc}$  in response to UTP (10  $\mu\text{M}$ ) addition following the imposition of the  $\text{Cl}^-$  gradient is shown in the right two bars. Filled bars represent the mean current response of  $\text{P2X}_7$ -R monolayers exposed to serosal ATP (permeabilized,  $n = 13$ ), and open bars represent  $\text{P2X}_7$ -R monolayers in the absence of serosal ATP (non-permeabilized,  $n = 14$ ). Values represent mean and S.E. for each condition.

cence (Fig. 1, right two panels),  $\text{P2X}_7$ -R-expressing cells not exposed to ATP showed no significant fluorescence beyond background levels (Fig. 1, left two panels). Control MTE18 cells or MTE18 cells expressing the control LISN vector, did not show any intracellular fluorescence in response to a 30-min exposure with 1 mM ATP (data not shown). We used this cell line (murine tracheal CFTR $^{-/-}$ ) epithelial cells, expressing  $\text{P2X}_7$ -R and selective permeabilization of the basolateral membrane to characterize CaCC resident in the apical membrane of airway epithelial cells.

Basolateral membrane permeabilization of murine tracheal epithelial cells followed by imposition of a  $\text{Cl}^-$  gradient and activation by mucosal UTP revealed the presence of an apical membrane  $\text{Cl}^-$  current (Fig. 2). Application of a cell to lumen  $\text{Cl}^-$  gradient resulted in a greater response in monolayers exposed to serosal 1 mM ATP than to cells not permeabilized by ATP (Fig. 2B,  $34.4 \pm 9.2$  versus  $7.5 \pm 2.4$   $\mu\text{A}/\text{cm}^2$ ). Importantly, addition of mucosal UTP to permeabilized cell monolayers was still capable of stimulating an increase in  $I_{sc}$  consistent with  $\text{Cl}^-$  secretion (Fig. 2A, solid line trace, and Fig. 2B, right panel, filled bar). Similar responses to both an imposed  $\text{Cl}^-$  gradient and mucosal UTP addition ( $\Delta I_{sc} = 54 \pm 7.4$  and  $32.1 \pm 8.9$   $\mu\text{A}/\text{cm}^2$ ,  $n = 8$ , respectively) were observed in MTE18 (CF) monolayers permeabilized by *S. aureus*  $\alpha$ -toxin. The magnitude of the  $\text{Cl}^-$  secretory response to the purinergic agonist UTP was significantly greater in  $\alpha$ -toxin-permeabilized MTE18 preparations than in  $\alpha$ -toxin-permeabilized MTE7B (normal) preparations ( $32.1 \pm 8.9$   $\mu\text{A}/\text{cm}^2$ ,  $n = 8$ ;  $10.9 \pm 3.7$   $\mu\text{A}/\text{cm}^2$ ,  $n = 8$ , respectively,  $p < .001$ ). Elevation of intracellular  $\text{Ca}^{2+}$  by

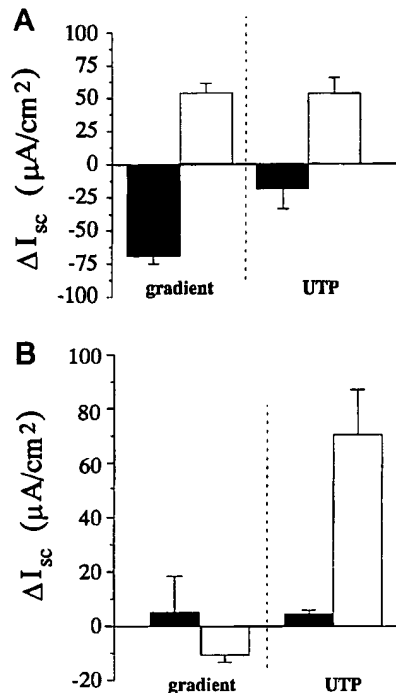


**FIG. 3. Effects of altering the  $\text{Cl}^-$  gradient in  $\text{P2X}_7$ -R monolayers.** A, dilution of the serosal  $\text{Cl}^-$  concentration generates a mucosal to serosal  $\text{Cl}^-$  current. All bars represent  $\text{P2X}_7$ -R monolayers permeabilized by 1 mM serosal ATP.  $\text{Cl}^-$  gradients were generated as described above (i.e. dilution of either the luminal or serosal solution to achieve a  $\text{Cl}^-$  concentration ratio of 115 mM to 68 mM). Filled bars ( $n = 10$ ) represent monolayers with 115 mM mucosal  $\text{Cl}^-$  and 68 mM serosal  $\text{Cl}^-$  concentrations, and open bars ( $n = 13$ ) represent monolayers with 115 mM serosal  $\text{Cl}^-$  and 68 mM mucosal  $\text{Cl}^-$  concentration. The response to 10  $\mu\text{M}$  luminal UTP following the generation of the  $\text{Cl}^-$  gradient is shown in the right two bars. B,  $\text{Cl}^-$  secretion induced with lower serosal  $\text{Cl}^-$  concentrations. All conditions contain 35 mM  $\text{Cl}^-$  in the serosal solution and a final mucosal  $\text{Cl}^-$  concentration of  $\sim 20$  mM. Filled bars represent the mean current response of  $\text{P2X}_7$ -R monolayers exposed to serosal ATP (permeabilized,  $n = 11$ ), and open bars represent  $\text{P2X}_7$ -R monolayers in the absence of serosal ATP (non-permeabilized,  $n = 18$ ). The  $I_{sc}$  response to 10  $\mu\text{M}$  luminal UTP is shown in the right two bars. Values represent mean and S.E. for each condition.

inclusion of the ionophore, ionomycin (1  $\mu\text{M}$ ), showed a similar ability to stimulate  $\text{Cl}^-$  secretion in permeabilized CF monolayers ( $25.8 \pm 6.6$   $\mu\text{A}/\text{cm}^2$ ,  $n = 8$ ).

We have used several solution changes to verify that the observed current in MTE18- $\text{P2X}_7$ -R cells is a  $\text{Cl}^-$  current. As shown above (Fig. 2)  $\text{Cl}^-$  secretion (serosal to mucosal) is stimulated by imposition of a chemical gradient (i.e. lower  $\text{Cl}^-$  concentration in the luminal solution). Reversal of this gradient, by decreasing the serosal  $\text{Cl}^-$  concentration in permeabilized preparations, results in stimulation of " $\text{Cl}^-$  absorption" (mucosal to serosal) (Fig. 3). When the  $\text{Cl}^-$  concentration in the luminal solution was maintained at 115 mM and the serosal solution was sequentially reduced, an absorptive  $\text{Cl}^-$  current was recorded (Fig. 3A). The magnitude of the response was similar to the response observed for  $\text{Cl}^-$  secretion (Fig. 2) but in the opposite direction ( $68.8 \pm 7.4$  versus  $54.1 \pm 8.2$   $\mu\text{A}/\text{cm}^2$ , respectively). Mucosal UTP was likewise able to augment this basal level of  $\text{Cl}^-$  absorption by  $18.2 \pm 15.8$   $\mu\text{A}/\text{cm}^2$ . MTE18- $\text{P2X}_7$ -R cells that were not permeabilized (not exposed to serosal ATP) did not respond to the imposed absorptive gradient (data not shown).

We also studied the magnitude of the  $\text{Cl}^-$  current when the serosal  $\text{Cl}^-$  concentration was reduced to levels that approximate intracellular  $\text{Cl}^-$  ( $\sim 35$  mM). We then imposed an out-

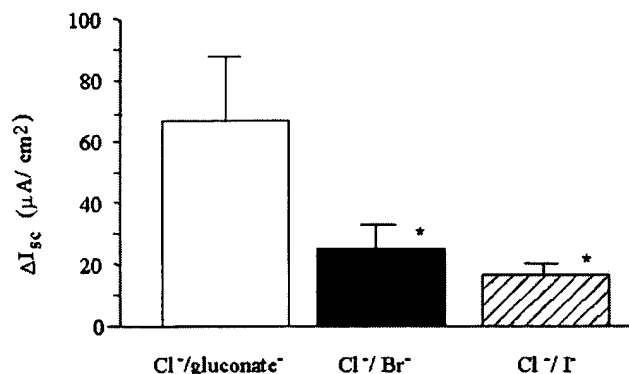


FIG. 4. Halide selectivity sequence in  $\text{P2X}_7\text{-R}$  monolayers. All bars represent  $\text{P2X}_7\text{-R}$  monolayers permeabilized by 1 mM serosal ATP and contain 115 mM serosal  $\text{Cl}^-$ . Mucosal solutions were diluted to achieve a final  $\text{Cl}^-$  concentration of 68 mM with the replacement anion, gluconate (open bars,  $n = 11$ ), bromide (filled bars,  $n = 7$ ), or iodide (hatched bars,  $n = 12$ ). Total luminal anion concentrations were always maintained at 115 mM (e.g. 68 mM  $\text{Cl}^-$  and 47 mM gluconate). Values represent mean  $\pm$  S.E. for each condition. The asterisk represents statistical significance ( $p < 0.01$ ) as determined by the Student's  $t$  test between gluconate and bromide means and gluconate and iodide means.

wardly directed  $\text{Cl}^-$  gradient by reducing luminal  $\text{Cl}^-$  to a similar ratio as previously studied (final mucosal  $\text{Cl}^-$  was diluted to a value of approximately 56% of the serosal concentration). Under these conditions, UTP was still capable of stimulating a characteristically similar  $\text{Cl}^-$  response, although the magnitude of the response was smaller than that observed with higher  $\text{Cl}^-$  concentrations (Fig. 3B).

The previous series of experiments involved dilution of the  $\text{Cl}^-$  concentration by substitution with the less permeant anion gluconate $^-$ . This in effect results in a bi-ionic permselectivity relation, which provides an opportunity to determine the relative permeabilities of  $\text{Cl}^-$  and gluconate. We subsequently performed similar experiments in which  $\text{Cl}^-$  was substituted with  $\text{Br}^-$  or  $\text{I}^-$  (Fig. 4). Substitution of  $\text{Cl}^-$  with gluconate showed an increase in secretory  $\text{Cl}^-$  current (serosal to mucosal) as expected for a  $\text{Cl}^-$  dominated current. Both bromide and iodide substitution significantly attenuated the magnitude of this current, indicating that both of these halides,  $\text{I}^-$  and  $\text{Br}^-$  were more permeable than gluconate but less permeable than  $\text{Cl}^-$ . Simply considering the  $\text{Cl}^-$  concentration on either side of the membrane, the Nernst equation would predict an equilibrium potential of  $-13.6$  mV. With gluconate as the counterion, we calculated an  $E_{\text{Cl}^-}$  of  $\sim -9.8$  mV. When bromide was substituted for  $\text{Cl}^-$ , the calculated  $E_{\text{Cl}^-}$  was  $\sim -6.7$  mV, and when iodide was used as the counterion,  $E_{\text{Cl}^-}$  was calculated to be  $\sim -3.8$  mV. These increasing differences away from the Nernst equilibrium potential describe an anion selectivity sequence that is  $\text{Cl}^- > \text{I}^- > \text{Br}^- > \text{gluconate}^-$ .

Several putative  $\text{Cl}^-$  channel blockers were investigated for inhibition of UTP-stimulated  $\text{Cl}^-$  secretion in  $\text{P2X}_7\text{-R}$ -permeabilized MTE18 cells (Fig. 5). The most efficacious compounds appeared to be niflumic acid (NFA) ( $100 \mu\text{M}$ ) and 5'-nitrophenyl-propylbenzoate (NPPB;  $100 \mu\text{M}$ ), both of which inhibited approximately 90% of the  $\text{CaCC}$ -mediated current. The most routinely used  $\text{Cl}^-$  channel blocker, DIDS ( $100 \mu\text{M}$ ), inhibited slightly more than 60% of the UTP-stimulated current, whereas glybenclamide ( $100 \mu\text{M}$ ), a  $\text{K}^+$  channel blocker that has been shown to have efficacy against CFTR (38), blocked about 40% of the UTP-stimulated current. Finally, TS-TM calixarene ( $1 \mu\text{M}$ ), a reported inhibitor specific for the outward rectifying  $\text{Cl}^-$  channel (36), the anti-estrogen tamoxifen ( $10 \mu\text{M}$ ), shown to inhibit the human CICA2 channel (32), and

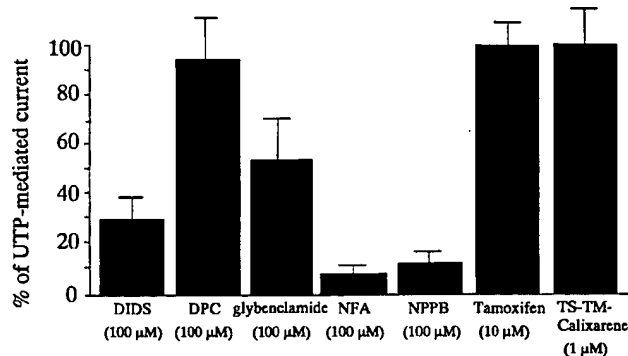


FIG. 5. Inhibitor effects on  $\text{Cl}^-$  currents measured in  $\text{P2X}_7\text{-R}$ -permeabilized monolayers. All monolayers were permeabilized by 1 mM serosal ATP and exposed to the serosal to mucosal  $\text{Cl}^-$  gradient as described above. Inhibitors, DIDS ( $100 \mu\text{M}$ ,  $n = 8$ ), DPC ( $100 \mu\text{M}$ ,  $n = 8$ ), glybenclamide ( $100 \mu\text{M}$ ,  $n = 8$ ), NFA ( $100 \mu\text{M}$ ,  $n = 8$ ), NPPB ( $100 \mu\text{M}$ ,  $n = 8$ ), tamoxifen ( $10 \mu\text{M}$ ,  $n = 8$ ), and TS-TM calixarene ( $1 \mu\text{M}$ ,  $n = 9$ ) were added to the mucosal solution prior to addition of  $10 \mu\text{M}$  UTP. Values represent mean  $\pm$  S.E. of percentage inhibition of the UTP response in comparison to permeabilized monolayers treated with vehicle alone prior to UTP.

diphenylamine-2-carboxylate (DPC) ( $100 \mu\text{M}$ ) were essentially without effect ( $<10\%$  inhibition) on the UTP-stimulated current.

#### DISCUSSION

We have previously shown that UTP, ionomycin, and thapsigargin are all capable of stimulating a  $\text{Cl}^-$  current in both CF and normal murine airway epithelial cells (33). In that study we demonstrated the presence of the  $\text{Ca}^{2+}$ -activated  $\text{Cl}^-$  current and noted that the magnitude of the current was greater in CF (MTE18) than in normal (MTE7b) cells. In this study we have used permeabilization of the basolateral membrane to focus on an "apically isolated" preparation. Efficacy of permeabilization is apparent by the greater response to the imposed gradient observed in the permeabilized versus non-permeabilized preparations (compare filled with open bars in Fig. 2B). Dilutions of the luminal solution in non-permeabilized monolayers leads to only minor changes in current, but subsequent addition of UTP generates a large change in current. In permeabilized preparations, a large increase in current is observed in response to both changes in the  $\text{Cl}^-$  concentration, as well as the addition of UTP. Importantly, nucleotides ATP/UTP acting via the purinoreceptor,  $\text{P2Y}_2$ , have been shown to directly reduce the apical membrane resistance with no effect on the resistance of the tight junction (11). In our experimental design, imposition of a chemical gradient for  $\text{Cl}^-$  is likely to have effects on both the apical membrane conductance and the paracellular pathway, but application of UTP will only stimulate  $\text{Cl}^-$  secretion by activation of an apical membrane  $\text{Cl}^-$  channel. Thus, the response to UTP following permeabilization and imposition of the  $\text{Cl}^-$  gradient is convincing evidence for the existence of a  $\text{Ca}^{2+}$ -activated apical membrane  $\text{Cl}^-$  channel. Furthermore, an increase in  $I_{sc}$  in response to ionomycin is also confirmatory evidence that the  $\text{Ca}^{2+}$ -mediated effects are the result of an apical  $\text{Cl}^-$  conductance rather than an effect on the paracellular pathway.

In an intact preparation,  $\text{Ca}^{2+}$  activation of  $\text{K}^+$  channels in the basolateral membrane likely plays an important role in maintaining the driving force necessary for  $\text{Cl}^-$  secretion. One obvious advantage of a permeabilized preparation is that we can eliminate the need for basolateral  $\text{K}^+$  channels by imposing a gradient by solution changes and thereby directly focus on the apical membrane. With these maneuvers we have shown that a  $\text{Ca}^{2+}$ -activated  $\text{Cl}^-$  conductance is present in the apical

membrane of murine tracheal epithelial cells. Interestingly, UTP and ionomycin regulate this apical membrane  $\text{Cl}^-$  conductance even when  $\text{Ca}^{2+}$  is buffered to moderate levels (300 nM) by EGTA. This suggests that the accessory proteins necessary for regulation are not dialyzed by permeabilization and that the mechanisms for intracellular  $\text{Ca}^{2+}$  release are also well preserved. Somewhat surprising, however, was the observation that UTP consistently activated this  $\text{Cl}^-$  conductance in the presence of 1 mM EGTA. EGTA is relatively slow in terms of buffering  $\text{Ca}^{2+}$  and may not be able to rapidly chelate release from local  $\text{Ca}^{2+}$  stores efficiently (39, 40). This experimental protocol allows us to buffer  $\text{Ca}^{2+}$  to physiological levels and preserves the ability to observe a UTP-mediated current response. These data are consistent with whole cell patch clamp studies that showed ATP-activated  $\text{Cl}^-$  currents in human airway epithelial cells in the presence of 10 mM EGTA (41). We have previously shown that UTP-stimulated currents in non-permeabilized MTE18 cells can be abolished by BAPTA-AM (33). Together, these results suggest that the UTP-stimulated current is  $\text{Ca}^{2+}$ -dependent, but that released  $\text{Ca}^{2+}$  is capable of activating a target before it can be chelated by EGTA.

Heterologous expression of P2X<sub>7</sub>-R in MTE18 cells provides a reliable, consistent, and rapid technique to generate an apically isolated preparation. Characteristically, the  $\text{Cl}^-$  secretory response to the imposed  $\text{Cl}^-$  gradient and to the luminal addition of UTP is similar to the responses observed in  $\alpha$ -toxin permeabilized monolayers. Challenging P2X<sub>7</sub>-R-expressing monolayers with ATP and the fluorescent DNA-intercalating agent, ToPro-1-iodide, demonstrated that P2X<sub>7</sub>-R effectively forms a pore sufficient for dialysis of the intracellular ion solution. These studies show that nearly every cell was expressing P2X<sub>7</sub>-R and that receptor expression alone did not confer an increase in cell conductance, but rather that receptor occupancy by ATP was an absolute requirement for pore formation. Reversal of the  $\text{Cl}^-$  gradient confirmed that the preparation was permeabilized and also established that the current was  $\text{Cl}^-$ -selective. Stable expression of P2X<sub>7</sub>-R allows us an opportunity to determine the characteristics of the  $\text{Ca}^{2+}$ -activated  $\text{Cl}^-$  conductance of the apical membrane in CF murine tracheal epithelial cells. This novel protocol for membrane permeabilization (transfection and activation of P2X<sub>7</sub>-R) has the further advantage of serving as a self-contained control for permeabilization. By not exposing the cells to millimolar basolateral ATP, the cells function as an intact monolayer, thus the same monolayer preparation can be used for both non-permeabilized and permeabilized protocols.

We have characterized apical membrane CaCC in these preparations in terms of ion selectivity and inhibitor sensitivity. As mentioned earlier, several reports have provided differing characteristics for the CaCC. We believe that characterization in the CF murine airway apical membrane will provide the hallmark characteristics for this channel for subsequent whole cell and single channel analyses. Initial studies in P2X<sub>7</sub>-R-permeabilized monolayers (Figs. 2 and 3) demonstrated a  $\text{Cl}^-$  current in response to a gradient that was generated by partial replacement of the mucosal  $\text{Cl}^-$  with the less permeant anion, gluconate. Although this fundamentally important experiment demonstrates the presence of the apical membrane  $\text{Cl}^-$  conductance, it also in fact serves as the first in a series of ion replacement studies. Although gluconate is often used as an "impermeant" anion, it is really only less permeant than the halide series. Therefore, a bi-ionic solution of  $\text{Cl}^-$  and gluconate can be evaluated for permselectivity based on the magnitude of the current response and a calculated equilibrium potential. As observed in Fig. 4, not surprisingly,  $\text{Cl}^-$  is more permeant than gluconate and results in a  $\text{Cl}^-$  current from serosal to mucosal

solution. In contrast, when the mucosal  $\text{Cl}^-$  is partially replaced with iodide or bromide, we observed a smaller UTP-induced secretion and a greater shift from the ideal equilibrium potential, suggesting an ion series for this apical  $\text{Cl}^-$  conductance of  $\text{Cl}^- > \text{I}^- > \text{Br}^- > \text{gluconate}^-$ . This anion selectivity sequence is somewhat similar to other reports of  $\text{Ca}^{2+}$ -activated  $\text{Cl}^-$  channels (14, 41–43) but importantly differs from the selectivity sequence for CFTR (3, 4, 14, 42) or from the CLC superfamily of  $\text{Cl}^-$  channels (44).

$\text{Cl}^-$  channel blockers were investigated to determine a "sensitivity sequence" for the CaCC channel. Pretreatment of permeabilized monolayers with the  $\text{Cl}^-$  channel blockers was used to determine a percentage inhibition of the UTP-mediated  $\text{Cl}^-$  current. The rank order of potency for channel inhibitors appears to be NFA, NPPB ( $\approx 90\%$ ) > DIDS ( $\approx 60\%$ ) > glybenclamide ( $\approx 40\%$ ) >> tamoxifen, TS-TM calixarene, and DPC (0–10%). The very low, nearly non-existent effect of TS-TM calixarene was consistent with previous studies that defined this compound as a specific inhibitor of the outward rectifying  $\text{Cl}^-$  channel (36). The moderate effect of glybenclamide on CaCC was a bit surprising, because this sulfonylurea compound was thought to be fairly specific for K-ATP and CFTR channels (45, 46). In many studies DIDS is reported to be a highly effective inhibitor of  $\text{Ca}^{2+}$ -activated  $\text{Cl}^-$  conductance (18–20, 41, 47), and although we observed moderate inhibition, it was not as effective as NFA. Higher doses of DIDS may generate higher levels of inhibition, but we are sensitive to the concerns of cross-linking that are associated with this compound. In our studies NFA was the most potent inhibitor of CaCC but like many  $\text{Cl}^-$  channel blockers lacks specificity, as it has been shown to also inhibit CFTR in human airways (47, 48). These studies serve to confirm the notion that  $\text{Cl}^-$  channel blockers are notoriously nonspecific, and inhibitor studies should be used simply as another characteristic to define the observed current. That is, an inhibitor order of potency or sensitivity sequence should serve an analogous function as a halide permselectivity sequence. The identity of the current should be defined by a combination of those characteristic sequences rather than any single effect.

Tamoxifen has recently been shown to have inhibitory effects against the human ClCA2 channel (32). Interestingly, tamoxifen was without effect in our CF murine tracheal epithelial cells. Furthermore, we have not been able to detect the murine homologue of this channel, mClCA1, by Northern blot analysis in our CF murine tracheal epithelial cells, suggesting that the apical membrane  $\text{Ca}^{2+}$ -activated  $\text{Cl}^-$  conductance is mediated by a thus far unidentified gene or protein.

We propose to utilize the activation, inhibition, and selectivity characteristics determined in this study for future experiments studying whole cell currents and single channel properties and ensure that the channel characteristics are consistent at each level of investigation. This systematic approach will result in the unambiguous identification of the murine airway CaCC localized to the apical membrane. Identification of CaCC along with a determination of regional distribution within the lung will permit us to develop strategies to activate CaCC and stimulate  $\text{Cl}^-$  and fluid secretion and thereby ameliorate the dehydration that is foremost in the pathology of cystic fibrosis.

**Acknowledgments**—We thank Drs. J. Stutts and B. Grubb (University of North Carolina) for excellent advice, discussion, and review of this manuscript. We are especially grateful to Dr. George Dubyak (Case Western Reserve) for his kind gift of the cDNA for the P2X<sub>7</sub>-R. We also thank Dr. John Olsen (University of North Carolina) for assistance with retroviral expression of the P2X<sub>7</sub>-R. Thanks also to Drs. B. Bridges and A. Singh (University of Pittsburgh) for the generous gift of TS-TM calixarene.

## REFERENCES

1. Boucher, R. C. (1994) *Am. J. Respir. Crit. Care Med.* **150**, 581–593
2. Boucher, R. C. (1994) *Am. J. Respir. Crit. Care Med.* **150**, 271–281
3. Kartner, N., Hanrahan, J. W., Jensen, T. J., Naismith, A. L., Sun, S., Ackerley, C. A., Reyes, E. F., Tsui, L. C., Rommens, J. M., Bear, C. E., and Riordan, J. R. (1991) *Cell* **64**, 681–691
4. Bear, C. E., Li, C., Kartner, N., Bridges, R. J., Jensen, T. J., Ramjeesingh, M., and Riordan, J. R. (1992) *Cell* **68**, 809–818
5. Clarke, L. L., Paradiso, A. M., and Boucher, R. C. (1992) *Am. J. Physiol.* **263**, C1190–C1199
6. Noah, T. L., Paradiso, A. M., Madden, M. C., McKinnon, K. P., and Devlin, T. B. (1991) *Am. J. Respir. Cell Mol. Biol.* **5**, 484–492
7. Clarke, L. L., Paradiso, A. M., Mason, S. J., and Boucher, R. C. (1992) *Am. J. Physiol.* **262**, C644–C655
8. Paradiso, A. M., Cheng, E. H. C., and Boucher, R. C. (1991) *Am. J. Physiol.* **261**, L63–L69
9. Mason, S. J., Paradiso, A. M., and Boucher, R. C. (1991) *Br. J. Pharmacol.* **103**, 1649–1656
10. Knowles, M. R., Clarke, L. L., and Boucher, R. C. (1991) *N. Engl. J. Med.* **325**, 533–538
11. Clarke, L. L., and Boucher, R. C. (1992) *Am. J. Physiol.* **263**, C348–C356
12. Willumsen, N. J., and Boucher, R. C. (1989) *Am. J. Physiol.* **256**, C226–C233
13. Boucher, R. C., Cheng, E. H. C., Paradiso, A. M., Stutts, M. J., Knowles, M. R., and Earp, H. S. (1989) *J. Clin. Invest.* **84**, 1424–1431
14. Anderson, M. P., and Welsh, M. J. (1991) *Proc. Natl. Acad. Sci. U. S. A.* **88**, 6003–6007
15. Snouwaert, J. N., Brigman, K. K., Latour, A. M., Malouf, N. N., Boucher, R. C., Smithies, O., and Koller, B. H. (1992) *Science* **257**, 1083–1088
16. Grubb, B. R., Vick, R. N., and Boucher, R. C. (1994) *Am. J. Physiol.* **266**, C1478–C1483
17. Devor, D. C., and Pilewski, J. M. (199) *Am. J. Physiol.* **276**, C827–C837
18. Egan, M., Flotte, T., Afione, S., Solow, R., Zeitlin, P. L., Carter, B. J., and Guggino, W. B. (1992) *Nature* **358**, 581–584
19. Hanrahan, J. W., and Tabcharani, J. A. (1989) *Ann. N. Y. Acad. Sci.* **574**, 30–43
20. Tabcharani, J. A., and Hanrahan, J. W. (1991) *Am. J. Physiol.* **261**, G992–G999
21. Hanrahan, J. W., and Tabcharani, J. A. (1990) *J. Membr. Biol.* **116**, 65–77
22. Tabcharani, J. A., Jensen, T. J., Riordan, J. R., and Hanrahan, J. W. (1989) *J. Membr. Biol.* **112**, 109–122
23. McCann, J. D., Li, M., and Welsh, M. J. (1989) *J. Gen. Physiol.* **94**, 1015–1036
24. McCann, J. D., Bhalla, R. C., and Welsh, M. J. (1989) *Am. J. Physiol.* **257**, L116–L124
25. Ishikawa, T., and Cook, D. I. (1993) *J. Membr. Biol.* **135**, 261–271
26. Duszyk, M., and Man, S. F. P. (1992) *Biophys. J.* **61**, 583–587
27. Morris, A. P., and Frizzell, R. A. (1993) *Am. J. Physiol.* **264**, C968–C976
28. Kunzelmann, K., Kubitz, R., Grolik, M., Warth, R., and Greger, R. (1992) *Pfluegers Arch.* **421**, 238–246
29. Gruber, A. D., Elble, R. C., Ji, H. L., Schreier, K. D., Fuller, C. M., and Pauli, B. U. (1998) *Genomics* **54**, 200–214
30. Gandhi, R., Elble, R. C., Gruber, A. D., Schreier, K. D., Ji, H. L., Fuller, C. M., and Pauli, B. U. (1998) *J. Biol. Chem.* **273**, 32096–32101
31. Romio, L., Musante, L., Cinti, R., Seri, M., Moran, O., Zegar-Moran, O., and Galletta, L. J. V. (1999) *Gene* **228**, 181–188
32. Gruber, A. D., Schreier, K. D., Ji, H. L., Fuller, C. M., and Pauli, B. U. (1999) *Am. J. Physiol.* **276**, C1261–C1270
33. Gabriel, S. E., Thomas, E. J., Makhilina, M., Hardy, S. P., and Lethem, M. I. (1999) *Am. J. Physiol.*, in press
34. Humphreys, B. D., Virginio, C., Surprenant, A., Rice, J., and Dubyak, G. R. (1998) *Mol. Pharmacol.* **54**, 22–32
35. Rassendren, F., Buell, G. N., Virginio, C., Collo G., North A., and Surprenant A. (1997) *J. Biol. Chem.* **272**, 5482–5486
36. Singh, A. K., Venglarik, C. J., and Bridges, R. J. (1995) *Kidney Int.* **48**, 985–993
37. Illek, B., Tam, A. W., Fischer, H., and Machen, T. E. (1999) *Pfluegers Arch.* **437**, 812–822
38. Sheppard, D. N., and Robinson, K. A. (1997) *J. Physiol. (Lond.)* **503**, 333–346
39. Adler, E. M., Augustine, G. J., Duffy, S. N., and Charlton, M. P. (1991) *J. Neurosci.* **11**, 1496–1507
40. Nichols, R. A., and Suplick, G. R. (1996) *Neurosci. Lett.* **211**, 135–137
41. Stutts, M. J., Fitz, J. G., Paradiso, A. M., and Boucher, R. C. (1994) *Am. J. Physiol.* **267**, C1442–C1451
42. Cliff, W. H., and Frizzell, R. A. (1990) *Proc. Natl. Acad. Sci. U. S. A.* **87**, 4956–4960
43. Hwang, T. H., Schwiebert, E. M., and Guggino, W. B. (1996) *Am. J. Physiol.* **270**, C1611–C1623
44. Lorenz, C., Pusch, M., and Jentsch, T. J. (1996) *Proc. Natl. Acad. Sci. U. S. A.* **93**, 13362–13366
45. Sheppard, D. N., and Welsh, M. J. (1992) *J. Gen. Physiol.* **100**, 573–591
46. Schultz, B. D., DeRoos, A. D. G., Venglarik, C. J., Singh, A. K., Frizzell, R. A., and Bridges, R. J. (1996) *Am. J. Physiol.* **271**, L192–L200
47. Gabriel, S. E., Boucher, R. C., and Stutts, M. J. (1993) *Pediatr. Pulmonol.* **9**(Suppl.), 223–224
48. Zegar-Moran, O., Sacco, O., Romano, L., Rossi, G. A., and Galletta, L. J. V. (1997) *J. Membr. Biol.* **156**, 297–305

# Neutrophils as early immunologic effectors in hemorrhage- or endotoxemia-induced acute lung injury

EDWARD ABRAHAM, AARON CARMODY, ROBERT SHENKAR, AND JOHN ARCAROLI  
*Division of Pulmonary Sciences and Critical Care Medicine, University of Colorado  
Health Sciences Center, Denver, Colorado 80262*

Received 9 March 2000; accepted in final form 10 June 2000

**Abraham, Edward, Aaron Carmody, Robert Shenkar, and John Arcaroli.** Neutrophils as early immunologic effectors in hemorrhage- or endotoxemia-induced acute lung injury. *Am J Physiol Lung Cell Mol Physiol* 279: L1137–L1145, 2000.—Acute lung injury is characterized by accumulation of neutrophils in the lungs, accompanied by the development of interstitial edema and an intense inflammatory response. To assess the role of neutrophils as early immune effectors in hemorrhage- or endotoxemia-induced lung injury, mice were made neutropenic with cyclophosphamide or anti-neutrophil antibodies. Endotoxemia- or hemorrhage-induced lung edema was significantly reduced in neutropenic animals. Activation of the transcriptional regulatory factor nuclear factor- $\kappa$ B after hemorrhage or endotoxemia was diminished in the lungs of neutropenic mice compared with nonneutropenic controls. Hemorrhage or endotoxemia was followed by increases in pulmonary mRNA and protein levels for interleukin-1 $\beta$  (IL-1 $\beta$ ), macrophage inflammatory protein-2 (MIP-2), and tumor necrosis factor- $\alpha$  (TNF- $\alpha$ ). Endotoxin-induced increases in proinflammatory cytokine expression were greater than those found after hemorrhage. The amounts of mRNA or protein for IL-1 $\beta$ , MIP-2, and TNF- $\alpha$  were significantly lower after hemorrhage in the lungs of neutropenic versus nonneutropenic mice. Neutropenia was associated with significant reductions in IL-1 $\beta$  and MIP-2 but not in TNF- $\alpha$  expression in the lungs after endotoxemia. These experiments show that neutrophils play a central role in initiating acute inflammatory responses and causing injury in the lungs after hemorrhage or endotoxemia.

cytokines; nuclear factor- $\kappa$ B; interleukin-1 $\beta$ ; tumor necrosis factor- $\alpha$ ; macrophage inflammatory protein-2

ACUTE LUNG INJURY is characterized by the accumulation of large numbers of neutrophils into the lungs and a pulmonary inflammatory response in which there is increased production of immunoregulatory cytokines (13, 18, 26, 27). Macrophages, neutrophils, endothelial cells, and other pulmonary cell populations have all been demonstrated to express proinflammatory cytokines, but the relative importance of each of these cell populations in contributing to the development of acute lung injury has not been well defined. Interleukin (IL)-1 $\beta$  appears to be the most important proinflamma-

tory cytokine in bronchoalveolar lavage specimens from patients with acute respiratory distress syndrome (ARDS), the most severe form of acute lung injury (25). Tumor necrosis factor- $\alpha$  (TNF- $\alpha$ ) and IL-8 also appear to have central roles in the initiation and potentiation of acute lung injury (8, 11, 19, 24).

Blood loss and sepsis are major risk factors for the development of acute lung injury (5, 15). Experimental models of hemorrhage or endotoxin administration demonstrate that both of these pathophysiological insults produce acute inflammatory lung injury (9, 17, 31). Neutrophils appear to be important in the genesis of acute lung injury since induced neutropenia followed by endotoxin challenge or complement activation attenuates increases in vascular permeability and other indexes of pulmonary damage (14, 32). However, the *in vivo* mechanisms by which neutrophils mediate lung injury after hemorrhage or endotoxemia remain incompletely understood.

Neutrophils can express proinflammatory cytokines, including IL-1 $\alpha$ , IL-1 $\beta$ , IL-8, and TNF- $\alpha$  (2, 7, 23, 30, 34). After hemorrhage or endotoxemia, neutrophils are major contributors to lung IL-1 $\beta$  production (23). Expression of TNF- $\alpha$  and macrophage inflammatory protein-2 (MIP-2), a murine homologue of IL-8, is also increased in lung neutrophils after blood loss or endotoxin administration (2, 30, 33). Binding sites for the transcriptional regulatory factor nuclear factor- $\kappa$ B (NF- $\kappa$ B) are present in the promoters of IL-1 $\beta$ , TNF- $\alpha$ , and MIP-2, and activation of NF- $\kappa$ B is important in modulating the expression of these as well as other immunoregulatory mediators (3, 4, 28). After hemorrhage or endotoxemia, NF- $\kappa$ B activation is increased in lung but not in blood neutrophils, providing an explanation for the enhanced expression of proinflammatory cytokines in pulmonary neutrophil populations (30).

Although neutrophils are an important component of the inflammatory response that characterizes acute lung injury, limited information is available concerning their role as early immune effectors in this process. To examine this issue, we performed a series of experiments in which neutrophils were depleted and then pulmonary cytokine expression, NF- $\kappa$ B activation, and

Address for reprint requests and other correspondence: E. Abraham, Div. of Pulmonary Sciences and Critical Care Medicine, Box C272, Univ. of Colorado Health Sciences Center, 4200 E. Ninth Ave., Denver, Colorado 80262 (E-mail: edward.abraham@uchsc.edu).

The costs of publication of this article were defrayed in part by the payment of page charges. The article must therefore be hereby marked "advertisement" in accordance with 18 U.S.C. Section 1734 solely to indicate this fact.

parameters of lung injury were examined after either hemorrhage or endotoxemia. These studies demonstrate that activated neutrophils have an important role in initiating the inflammatory processes involved in the development of hemorrhage- or endotoxemia-induced acute lung injury.

## METHODS

**Mice.** Male BALB/c mice, 8–12 wk of age, were purchased from Harlan Sprague Dawley (Indianapolis, IN). The mice were kept on a 12:12-h light-dark cycle with free access to food and water. All experiments were conducted in accordance with institutional review board-approved protocols.

**Models of hemorrhage and endotoxemia.** The murine hemorrhage model used in these experiments was developed in our laboratory and reported on previously (1, 2, 23, 29–31). With this model, 30% of the calculated blood volume (~0.55 ml for a 20-g mouse) is withdrawn over a 60-s period by cardiac puncture from a methoxyflurane-anesthetized mouse. The period of methoxyflurane anesthesia is <2 min in all cases. The mortality rate with this hemorrhage protocol is ~12%.

The model of endotoxemia used was reported previously (2, 23, 30). Mice received an intraperitoneal injection of lipopolysaccharide at dose of 1 mg/kg in 200  $\mu$ l of PBS. This dose produces neutrophil infiltration into the lungs and acute neutrophilic alveolitis in mice, histologically consistent with acute lung injury.

**Generation of neutropenia.** In designated experiments, mice were given 150 mg/kg cyclophosphamide intraperitoneally in 0.2 ml of PBS as previously reported (23). Control mice were given 0.2 ml of PBS intraperitoneally at the same time points. The effects of cyclophosphamide treatment on neutrophil numbers were determined by preparing Wright's stains using blood withdrawn from the tail of each mouse. In mice treated with this dose of cyclophosphamide 4 days and 1 day before hemorrhage or administration of endotoxin, there was >95% reduction in neutrophil numbers compared with that in control mice. Mice given a single dose of cyclophosphamide 1 day before endotoxin administration or hemorrhage had neutrophil counts that were not different from those in controls.

Neutropenia also was produced by treating mice with absorbed rabbit anti-neutrophil antibodies (Accurate Chemicals, Westbury, NY) (12). In these experiments, mice were treated intraperitoneally with anti-neutrophil antibodies diluted 1:15 in 0.2 ml of PBS on days 3 and 4 before endotoxin administration or hemorrhage, followed by 2 days of treatment with 0.2 ml of undiluted antibodies. Wright's staining of tail blood was used in each mouse to determine the degree of neutropenia achieved with this regimen. In each case, >95% of neutrophils, compared with that in PBS-treated controls, were eliminated with such anti-neutrophil antibody treatment.

**Myeloperoxidase assay.** Myeloperoxidase activity was assayed as reported previously (2, 23). Excised lungs from three to four mice per treatment group were frozen in liquid nitrogen, weighed, and stored at -86°C. Lungs were homogenized for 30 s in 1.5 ml of 20 mM potassium phosphate, pH 7.4, and centrifuged at 4°C for 30 min at 40,000 *g*. The pellet was resuspended in 1.5 ml of 50 mM potassium phosphate, pH 6.0, containing 0.5% hexadecyltrimethylammonium bromide, sonicated for 90 s, incubated at 60°C for 2 h, and centrifuged. The supernatant was assayed for peroxidase activity corrected to lung weight.

**Wet-to-dry lung weight ratios.** All mice used for lung wet-to-dry weight ratios were of identical ages. Lungs were ex-

cised, rinsed briefly in PBS, blotted, and then weighed to obtain the "wet" weight. Lungs were then dried in an oven at 80°C for 7 days to obtain the "dry" weight.

**Cytokine ELISA.** After the lung vascular bed had been flushed by injecting 5 ml of chilled (4°C) PBS into the right ventricle, the lungs were homogenized for 30 s in lysis buffer containing 10 mM HEPES, 150 mM NaCl, 1 mM EDTA, 0.6% ipegal, 5 mM phenylmethylsulfonyl fluoride, 1  $\mu$ g/ml leupeptin, 1  $\mu$ g/ml aprotinin, 10  $\mu$ g/ml soybean trypsin inhibitor, and 1  $\mu$ g/ml pepstatin. The homogenates were centrifuged at 10,000 rpm at 4°C for 10 min, and the supernatants were collected. Protein content of the supernatants was determined using the bicinchoninic acid protein assay kit from Pierce Chemical (Pittsburgh, PA). Immunoreactive IL-1 $\beta$ , TNF- $\alpha$ , and MIP-2 were quantitated with commercially available ELISA kits (R&D Systems, Minneapolis, MN). With these assays, the threshold of sensitivity for IL-1 $\beta$  and MIP-2 is 3 pg/ml, and for TNF- $\alpha$ , it is 10 pg/ml.

**Quantitative PCR.** Groups of five mice, with results obtained from individual mice, were used for each experimental condition. PCR was used in these studies because the amount of RNA obtained from each mouse was insufficient to prepare Northern blots for cytokine analysis. The animals were anesthetized with methoxyflurane and then killed by cervical dislocation. The thorax was opened with two lateral incisions along the rib cage. The right heart was injected with cold, sterile PBS (3–5 ml) until the lungs had been flushed thoroughly. The lungs were excised with care to avoid the peritracheal lymph nodes and rinsed in PBS. The lungs were briefly blotted. The lungs were homogenized for 30 s on ice in 300  $\mu$ l of buffer RLT (QIAGEN, Valencia, CA) with 3  $\mu$ l of  $\beta$ -mercaptoethanol (Sigma, St. Louis, MO). RNA was isolated using the RNeasy kit (QIAGEN) following the manufacturer's protocol. Briefly, proteinase K was added to each sample, incubated at 55°C for 10 min, and then centrifuged at 12,000 rpm for 3 min. Ethanol (100%) was added to clear the lysate, and the samples were centrifuged at 12,000 rpm for 15 s. After washes, the samples were treated with DNase for 15 min at room temperature and the membrane was dried in buffer RPE. RNA was eluted from the membrane in 30  $\mu$ l RNase-free water, and the quantity of RNA was determined at 260-nm absorbance.

Primers and probes for IL-1 $\beta$ , TNF- $\alpha$ , and MIP-2 were designed using Primer Express software supplied by Perkin-Elmer (Foster City, CA). The IL-1 $\beta$  primer and probe sequence consisted of forward primer, 5'-GCTGAAAGCTCTCCACCTCAA-3'; reverse primer, 5'-TCGTTGCTTGTTCTCCTTGTA-3'; and probe, 5'-CAGAATATCAACCAACAAGTGATATTCTCCATGAGC-3'. The TNF- $\alpha$  primer and probe consisted of forward primer, 5'-CTGTAGCCACGTCGTAGTCAA-3'; reverse primer, 5'-CTCCTGGTATGAGATAGCAAATCG-3'; and probe, 5'-TGCCCCGACTACGTGCTCCTCAC-3'. The MIP-2 primers and probes consisted of forward primer, 5'-TGTGACGCCCCAGGA-3'; reverse primer, 5'-AACTTTTGTGACCGCCCTTGAG-3'; and probe, 5'-TGCGCCAGACAGAGTCATAGCCA-3'.

To optimize the primer sets, a primer optimization experiment was performed as described in the manufacturer's protocol. Based on the primer optimization, the concentration of primers and probe for IL-1 $\beta$  and TNF- $\alpha$  contained 200 nM for the probe, forward primer, and reverse primer. The primer and probe concentrations for MIP-2 consisted of 10 nM for the forward primer, 450 nM for the reverse primer, and 200 nM for the probe. In each experiment, ribosomal RNA control probe, forward primer, and reverse primer (Perkin-Elmer) at concentrations of 50 nM were used to normalize the amount of RNA in each sample.



All reagents used in the one-step RT-PCRs were purchased from Perkin-Elmer. Each one-step RT-PCR contained a total volume of 50  $\mu$ l. The RT reaction was performed for 30 min at 48°C with MultiScribe reverse transcriptase with a final concentration of 0.25 U/ $\mu$ l. After the RT step, AmpliTaq Gold polymerase, at a final concentration of 0.025 U/ $\mu$ l, was activated by an increase in temperature to 95°C for 10 min followed by 40 cycles of amplification (95°C for 15 s and 60°C for 1 min) with a GeneAmp 5700 sequence detection system (ABI Prism, Foster City, CA). The quantity of cytokine mRNA was determined from a standard curve with 10-fold dilutions of known amounts of target RNA with each primer and probe set. RNA amounts were determined using software provided with the GeneAmp 5700 sequence detection system. Quantification was determined by dividing the amount of 18S ribosomal RNA by the target amount for each cytokine sample.

**Preparation of nuclear extracts.** Nuclear extracts were prepared as previously described (17, 18). In brief, lungs were snap-frozen in liquid nitrogen and then homogenized in buffer A. After cytoplasm was removed from the nuclei by 15 passages through a 25-gauge needle, nuclei were centrifuged at 4°C for 6 min at 600 *g*. After the nuclear pellet was incubated on ice for 15 min in buffer C, the extract was centrifuged at 4°C for 10 min at 12,000 *g*. The supernatant was collected, divided into aliquots, and stored at -86°C. Protein concentration was determined using Coomassie Plus protein assay reagent (Pierce Chemical) standardized to bovine serum albumin according to the manufacturer's protocol.

**Electrophoretic mobility shift assay analysis.** Activation of the transcriptional factor NF- $\kappa$ B was determined by electrophoretic mobility shift assay (EMSA) analysis, as described previously in our laboratory (22, 29, 30). The  $\kappa$ B DNA sequence of the immunoglobulin gene was used. Synthetic DNA sequences (with enhancer motifs underlined) were annealed, forming double-strand DNA probes with single-strand ends consisting of sequences of four thymidines, allowing the ends to be labeled by base pairing with [ $\alpha$ -<sup>32</sup>P]dATP using Sequenase DNA polymerase:  $\kappa$ B, 5'-TTTTCGAGCTCGGGACTT-TCCGAGC-3' and 3'-GCTCGAGCCCTGAAAGGCTCGTT-TT-5'.

DNA binding reaction mixtures of 20  $\mu$ l contained 1  $\mu$ g of nuclear extract, 10 mM Tris-Cl, pH 7.5, 50 mM EDTA, 0.5 mM dithiothreitol, 1 mM MgCl<sub>2</sub>, 4% glycerol, 0.08  $\mu$ g of poly(dI-dC)-poly(dI-dC), and 0.7 fmol of <sup>32</sup>P-labeled double-stranded oligonucleotide. After the samples were incubated at room temperature for 20 min, they were loaded onto a 4% polyacrylamide gel (acrylamide-bis-acrylamide, 80:1; 2.5% glycerol in Tris-borate-EDTA) at 10 V/cm. Each gel was then dried and subjected to autoradiography.

Supershift studies using anti-p50 or anti-p65 antiserum (Santa Cruz Biotechnology, Santa Cruz, CA) as previously described (29, 30) were used to demonstrate specificity of  $\kappa$ B oligonucleotide binding. Specificity of binding also was confirmed by ablation of the  $\kappa$ B band through incubation with a 500-fold excess of unlabeled oligonucleotide.

**In situ immunolocalization of TNF- $\alpha$ .** Immunohistochemistry was performed as described previously (24). Briefly, control mice or endotoxin-treated mice were prepared as previously described. After the right ventricle was perfused with 5 ml of PBS (4°C), the lungs were gently infiltrated through the trachea with 1% low-melting-point agarose (Seakem, Rockland, ME) at 42°C. Lungs were then removed en bloc and fixed in 4% paraformaldehyde-0.23 M sucrose solution overnight. Tissue was then embedded and treated with 0.2 M glucose and 1.5 U/ml glucose oxidase in PBS for 30

min followed by 10% hydrogen peroxide in PBS for 15 min, after which 5- $\mu$ m sections were prepared. Immunohistochemistry was conducted using either rabbit polyclonal anti-mouse TNF- $\alpha$  antibodies or control rabbit serum (PharMingen, San Diego, CA) at a dilution of 1:1,000 using the Vectastain immunohistochemistry kit following the manufacturer's protocol (Vector, Burlingame, CA).

**Statistical analysis.** For each experimental condition, the entire group of animals was prepared and studied at the same time. Mice in all groups had the same birth date and had been housed together. Separate groups of mice were used for myeloperoxidase assays, PCR, and EMSA. For PCR, each animal was analyzed individually before group data. Data are presented as means  $\pm$  SD for each experimental group were calculated. One-way ANOVA and the Tukey-Kramer multiple comparisons test were used when more than two experimental groups were compared. Student's *t*-test was used for comparisons between two data groups. *P* < 0.05 was considered significant.

## RESULTS

**Elimination of neutrophils reduces hemorrhage- or endotoxemia-induced lung injury.** Hemorrhage or endotoxemia results in accumulation of neutrophils in the lungs (Fig. 1) and increased wet-to-dry weight ratios (Fig. 2). Endotoxemia- or hemorrhage-induced lung edema was significantly reduced in mice made neutropenic by treatment with cyclophosphamide (Fig. 2A). The ameliorative effects of cyclophosphamide treatment on hemorrhage- or endotoxemia-associated increases in lung wet-to-dry weight ratios appeared to be due to neutropenia, but not to other effects of cyclophosphamide, since there was no effect on lung edema in nonneutropenic cyclophosphamide-treated animals (i.e., given cyclophosphamide 1 day before endotoxin administration or hemorrhage).

To confirm the role of neutrophils in contributing to lung injury after hemorrhage or endotoxemia, mice were made neutropenic with anti-neutrophil antibodies. As was the case with cyclophosphamide-induced neutropenia, anti-neutrophil treatment significantly reduced lung edema produced by hemorrhage or endotoxemia (Fig. 2B).

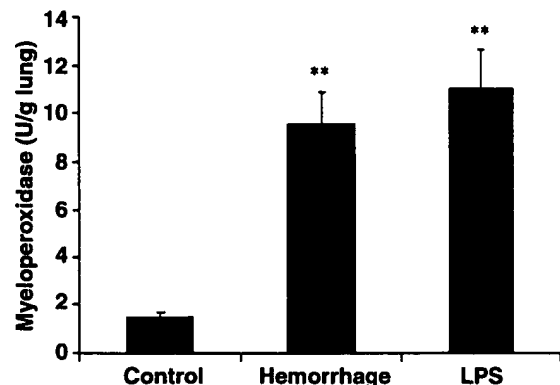


Fig. 1. Myeloperoxidase activity in lungs of mice (*n* = 6 in each group) that were either hemorrhaged, given endotoxin [lipopolysaccharide (LPS)] 1 h previously, or unmanipulated (control). \*\**P* < 0.01 vs. control.



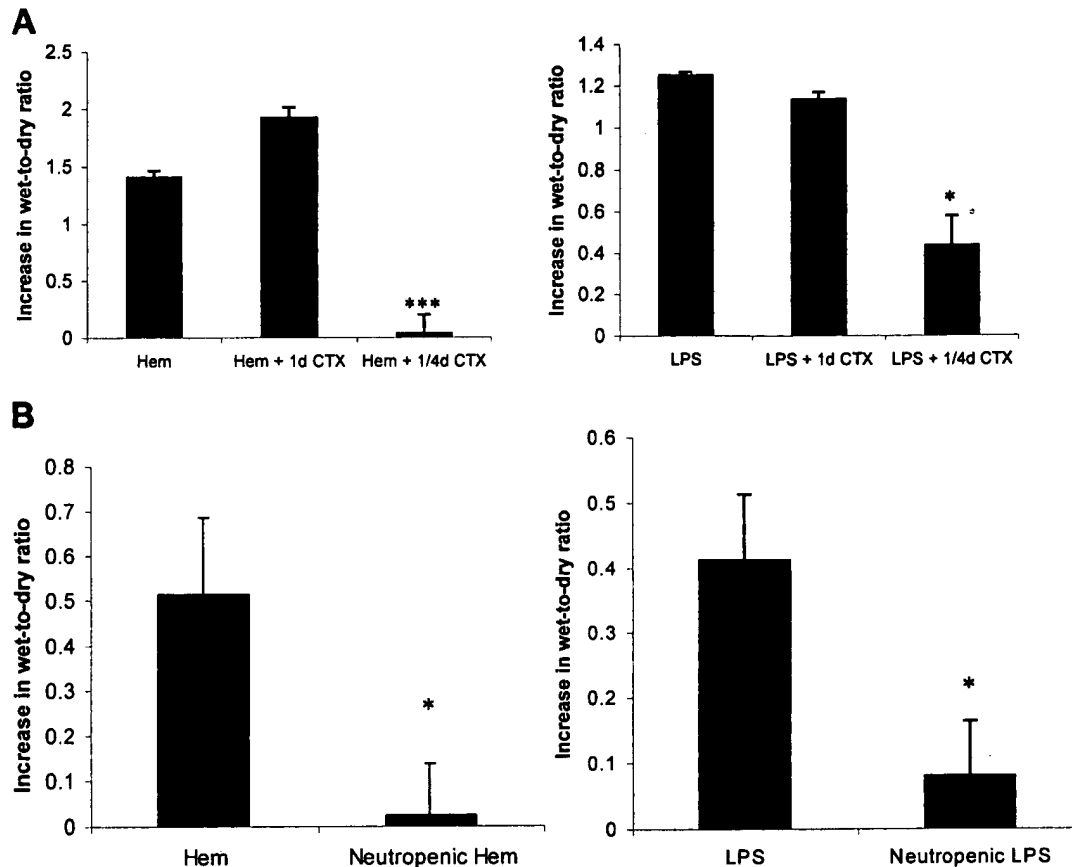


Fig. 2. Endotoxemia- or hemorrhage-induced lung injury was significantly reduced in mice ( $n = 6$  in each group) rendered neutropenic by treatment with cyclophosphamide (CTX; A) or polyclonal rabbit anti-neutrophil antibodies (B). The wet-to-dry weight ratio of each endotoxin-treated or hemorrhaged (Hem) animal was corrected by subtracting the mean value for normal animals, and the increased mean of the untreated and CTX and anti-neutrophil antibody-treated groups was plotted. The increase in wet-to-dry weight ratio in LPS-treated or hemorrhaged animals or nonneutropenic CTX-treated animals [i.e., given CTX 1 day before LPS administration or hemorrhage (1d CTX)] compared with sham animals was significant ( $P < 0.001$ ). The decrease in wet-to-dry weight ratio in mice made neutropenic with anti-neutrophil antibodies or CTX (i.e., given CTX 1 and 4 days before LPS administration or hemorrhage [1/4d CTX]) was significant compared with nonneutropenic controls ( $*P < 0.05$  and  $***P < 0.001$ ). Effective neutropenia was  $>98\%$  in mice treated with anti-neutrophil antibodies or with CTX on days 1 and 4 before hemorrhage or endotoxin administration. In contrast, administration of CTX 1 day before hemorrhage or endotoxemia caused a  $<10\%$  change in neutrophil counts compared with untreated or PBS-treated animals.

*Effects of neutrophils on NF- $\kappa$ B activation in the lungs after hemorrhage or endotoxemia.* The transcriptional regulatory factor NF- $\kappa$ B was activated in the lungs after hemorrhage or endotoxemia but to a greater extent by endotoxemia than by hemorrhage (Fig. 3). To determine the relative importance of neutrophils in affecting pulmonary NF- $\kappa$ B activation, we treated mice with either cyclophosphamide or anti-neutrophil antibodies and then examined nuclear translocation of NF- $\kappa$ B in whole lung extracts obtained after endotoxin administration or hemorrhage (Fig. 3). The increases in lung NF- $\kappa$ B activation produced by hemorrhage or endotoxemia were reduced in mice made neutropenic by administration of either cyclophosphamide or anti-neutrophil antibodies. Mice treated with a single dose of cyclophosphamide 1 or 4 days before hemorrhage or endotoxin administration

or with anti-neutrophil antibodies for 2 days before hemorrhage or endotoxin administration were not neutropenic and showed levels of NF- $\kappa$ B activation similar to those found in control mice not given either cyclophosphamide or anti-neutrophil antibodies.

*Role of neutrophils in hemorrhage- or endotoxemia-induced increases in lung cytokine expression.* Hemorrhage or endotoxemia resulted in increased pulmonary mRNA levels for IL-1 $\beta$ , MIP-2, and TNF- $\alpha$  (Fig. 4). Although the amounts of mRNA for these proinflammatory cytokines were significantly elevated compared with control level after hemorrhage, the increases produced by endotoxin injection were  $\sim 10$ - to 100-fold greater than those occurring after hemorrhage.

No significant increases in lung IL-1 $\beta$  expression, compared with those in unmanipulated nonneutropenic control mice, were present after hemorrhage or

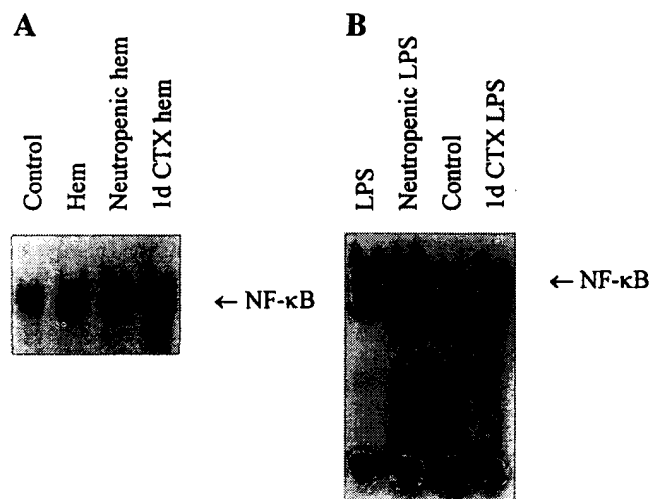


Fig. 3. Depletion of neutrophil-decreased hemorrhage (A)- or endotoxin (B)-induced activation of nuclear factor- $\kappa$ B (NF- $\kappa$ B) in the lung. Nuclear extracts were obtained from whole lungs of mice that were unmanipulated (control), given LPS 1 h previously (LPS), hemorrhaged 1 h previously (Hem), treated with CTX 1 day before LPS administration (1d CTX LPS) or hemorrhage (1d CTX hem) or treated with CTX 1 and 4 days before LPS administration (neutropenic LPS) or hemorrhage (neutropenic hem). Effective neutropenia was >98% in mice treated with CTX on *days 1* and *4* before hemorrhage or endotoxin administration. In contrast, administration of CTX 1 day before hemorrhage or endotoxemia caused a <10% change in neutrophil counts compared with those in unmanipulated animals. Similar results were found in mice made neutropenic by treatment with polyclonal rabbit anti-neutrophil antibodies. Three additional experiments with separate sets of mice gave similar results.

endotoxemia in neutropenic mice (Fig. 4). Neutropenia also significantly diminished levels of MIP-2 mRNA after hemorrhage or endotoxemia but not to control levels. The amounts of TNF- $\alpha$  mRNA in the lungs after hemorrhage, but not after endotoxemia, were also reduced in neutropenic mice.

IL-1 $\beta$ , MIP-2, and TNF- $\alpha$  proteins were significantly elevated in the lungs after hemorrhage or endotoxemia compared with unmanipulated, control conditions (Fig. 5). Mice treated with a single dose of cyclophosphamide 1 or 4 days before hemorrhage or endotoxin administration or with anti-neutrophil antibodies for 2 days before hemorrhage or endotoxin administration were not neutropenic and had increases in pulmonary MIP-2, IL-1 $\beta$ , and TNF- $\alpha$  proteins that were similar to those found in control mice not given either cyclophosphamide or anti-neutrophil antibodies. As was the case for mRNA levels, endotoxemia-induced increases in pulmonary IL-1 $\beta$  and MIP-2 proteins were more than 10-fold greater than those produced by hemorrhage.

The amounts of MIP-2 and IL-1 $\beta$  proteins in the lungs were significantly lower after hemorrhage or endotoxemia in neutropenic compared with nonneutropenic animals (Fig. 5). However, as with TNF- $\alpha$  mRNA, neutropenia reduced hemorrhage- but not endotoxemia-induced elevations in pulmonary TNF- $\alpha$  protein.

The present experiments are consistent with our previous study (23), where neutrophils were demon-

strated to be a major cellular source of IL-1 $\beta$  in the lungs after endotoxemia. However, the above experiments, which showed that neutropenia had no effect on endotoxin-induced elevations in pulmonary TNF- $\alpha$  expression, suggested that cell sources other than neutrophils were responsible for endotoxin-associated increases in lung TNF- $\alpha$ . To examine this issue we performed immunohistochemical studies on lung sections obtained 1 h after endotoxin administration (Fig. 6). These experiments showed that alveolar macrophages and not neutrophils were the major pulmonary cell population expressing TNF- $\alpha$  after endotoxin treatment.

## DISCUSSION

In these experiments, neutrophils were demonstrated to have a central role in initiating an acute inflammatory response and in causing injury to the lungs after hemorrhage or endotoxemia. Elimination of neutrophils using two techniques with different mechanisms for producing neutropenia, cyclophosphamide or anti-neutrophil antibody therapy, diminished hemorrhage- or endotoxin-induced lung edema, activation of NF- $\kappa$ B, and expression of IL-1 $\beta$  and MIP-2. TNF- $\alpha$  generation in the lungs after hemorrhage but not after endotoxin administration also appeared to be neutrophil dependent.

Previous experiments have shown that neutrophil depletion prevented endotoxin-induced lung edema (14). However, the role that neutrophils have in producing lung injury after hemorrhage has not been well explored previously. In the present studies, both hemorrhage and endotoxemia induced NF- $\kappa$ B activation and proinflammatory cytokine expression in the lungs. However, the magnitude of NF- $\kappa$ B activation and enhancement of cytokine expression was greater after endotoxemia than after hemorrhage. For example, in the case of pulmonary IL-1 $\beta$  mRNA or protein, the increase from baseline, control conditions produced by hemorrhage was less than fivefold, whereas levels rose more than 20-fold after endotoxemia. Similar differences between hemorrhage- and endotoxemia-induced effects were found for MIP-2 and TNF- $\alpha$ . These results indicate that the magnitude of induction of signaling pathways initiated by endotoxemia and leading to NF- $\kappa$ B activation and proinflammatory cytokine expression is substantially greater than that produced by hemorrhage.

In a previous study (30), we found that the enhanced expression of IL-1 $\beta$ , TNF- $\alpha$ , and MIP-2 in lung neutrophils is dependent on activation of xanthine oxidase after hemorrhage but not after endotoxemia. Additionally, activation of the transcription factor cAMP-responsive element binding protein was regulated by xanthine oxidase-dependent pathways after hemorrhage but not after endotoxemia. Our previous study (30), coupled with the present results in which both the magnitude and patterns of endotoxin-induced increases in pulmonary cytokine expression differed from those present after hemorrhage, indicated that the

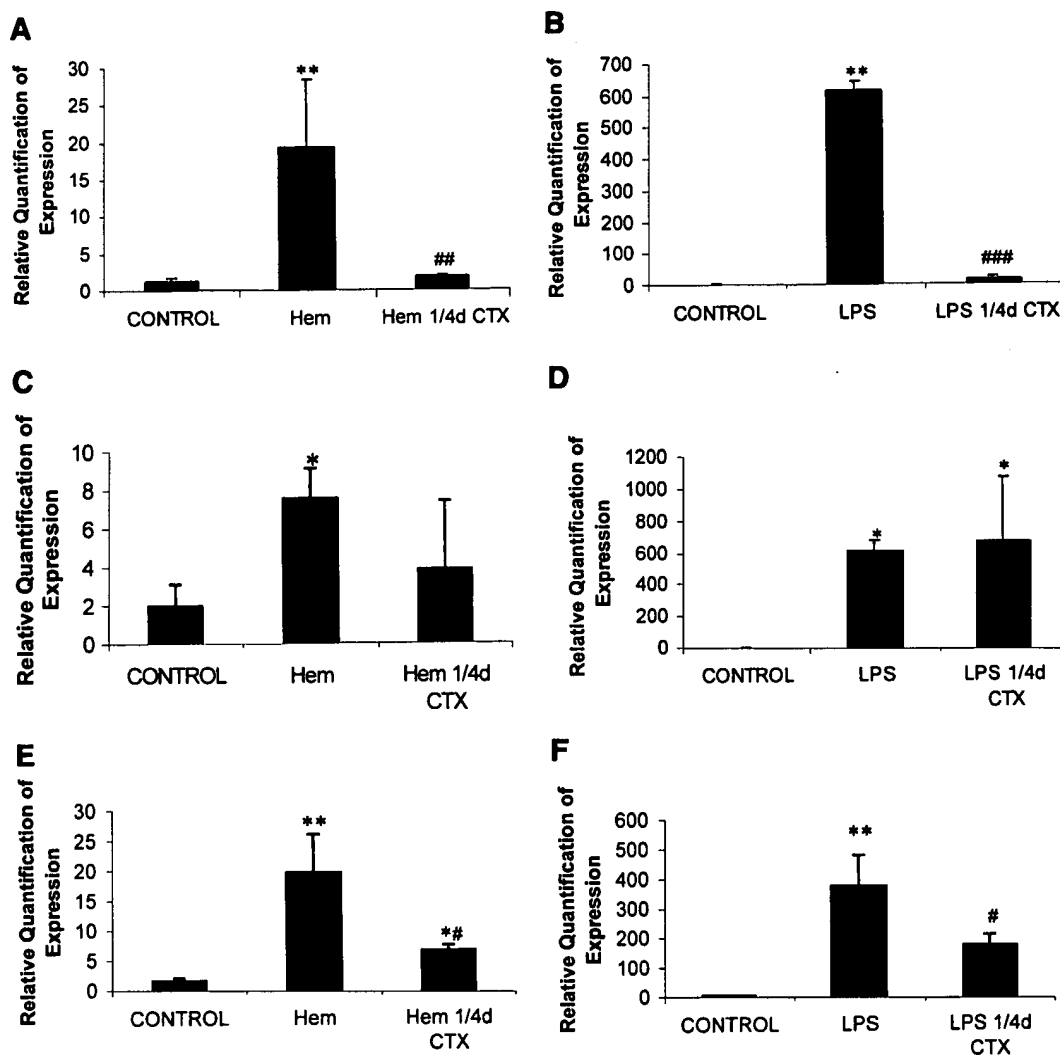


Fig. 4. Effects of neutrophil depletion on cytokine mRNA expression in the lung. *A* and *B*: interleukin-1 $\beta$  (IL-1 $\beta$ ). *C* and *D*: tumor necrosis factor- $\alpha$  (TNF- $\alpha$ ). *E* and *F*: macrophage inflammatory protein-2 (MIP-2). mRNA was isolated from whole lungs of mice ( $n = 6$  in each group) that were unmanipulated (control), given LPS 1 h previously (LPS), hemorrhaged 1 h previously (Hem), or treated with CTX 1 and 4 days before LPS administration (LPS 1/4d CTX) or hemorrhage (Hem 1/4d CTX). \* $P < 0.05$  and \*\* $P < 0.01$  vs. control. \* $P < 0.05$ , \*\* $P < 0.01$ , and \*\*\* $P < 0.001$  vs. nonneutropenic hemorrhage or LPS.

intracellular signaling pathways initiated by endotoxemia and leading to increased expression of proinflammatory cytokines in lung neutrophils are distinct from those associated with hemorrhage.

Despite differences between endotoxemia or hemorrhage on NF- $\kappa$ B activation and cytokine expression, the magnitude of increase in lung edema was similar with the two conditions. Although these results are consistent with there being a threshold effect for pulmonary damage, with no additional injury occurring even if there are further increases in NF- $\kappa$ B activation and proinflammatory cytokine release, it is possible that histopathological alterations, other than the measured increase in lung edema, may differ between hemorrhage and endotoxemia, reflecting the more pronounced effect of endotoxemia on NF- $\kappa$ B activation and

cytokine expression. An alternate explanation for the present findings is that additional potent neutrophil-derived proinflammatory mediators not measured in these experiments were released after hemorrhage in amounts similar to those after endotoxemia and that such mediators were more important than IL-1 $\beta$  or MIP-2 in causing lung injury.

Neutrophil depletion prevented lung edema but did not decrease pulmonary TNF- $\alpha$  mRNA or protein levels after endotoxemia. These findings, like those of our previous experiments (30), indicate that transcriptional regulatory pathways activated in the lungs by hemorrhage and leading to enhanced proinflammatory cytokine expression are distinct from those associated with endotoxemia. These results also suggest that TNF- $\alpha$  does not have a central role in producing acute lung injury after endotox-

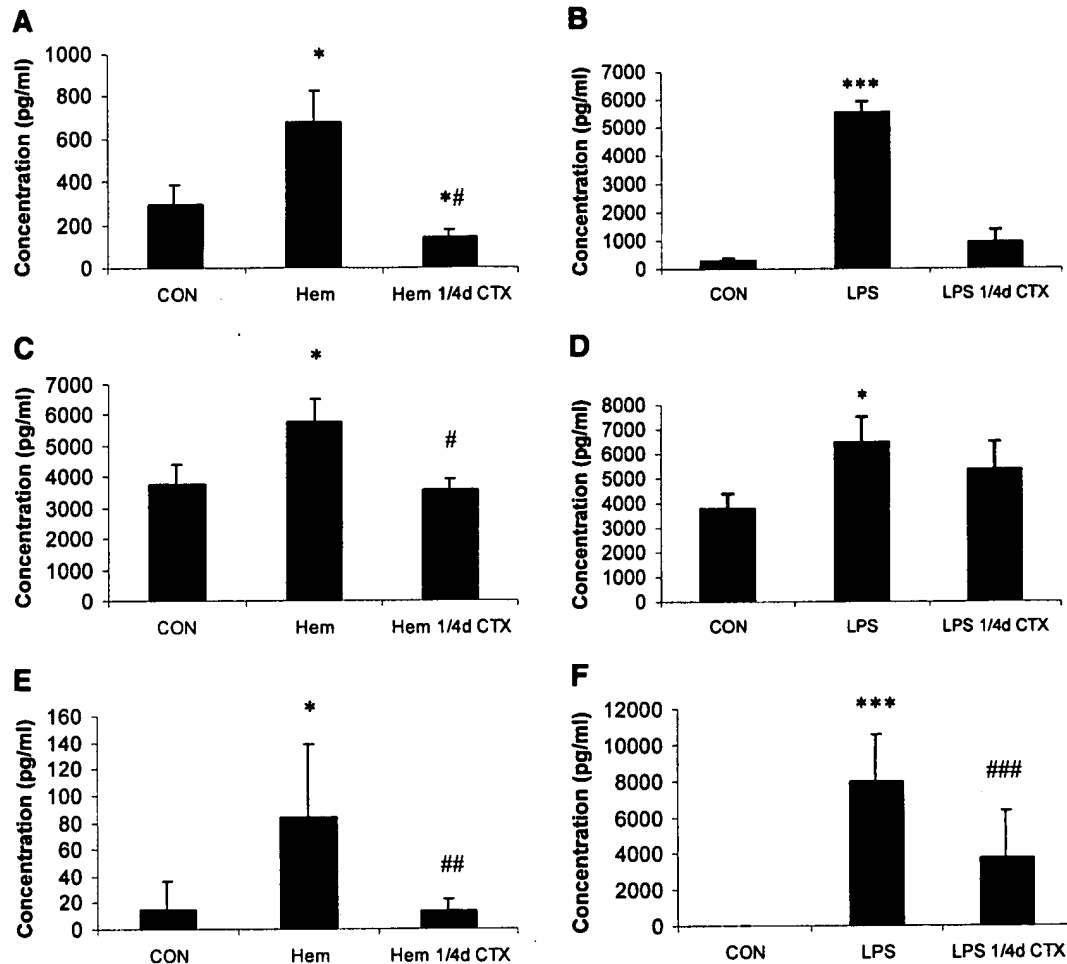


Fig. 5. Effects of neutrophil depletion on cytokine protein in the lung. A and B: IL-1 $\beta$ . C and D: TNF- $\alpha$ . E and F: MIP-2. Lung homogenates were obtained from mice ( $n = 6$  in each group) that were unmanipulated (control), given LPS 1 h previously (LPS), hemorrhaged 1 h previously (Hem), or treated with CTX 1 and 4 days before LPS administration (LPS 1/4d CTX) or hemorrhage (Hem 1/4d CTX). \* $P < 0.05$  and \*\*\* $P < 0.001$  vs. control. # $P < 0.05$ , ## $P < 0.01$ , and ### $P < 0.001$  vs. nonneutropenic Hem or LPS.

emia. Such findings are consistent with those in humans with ARDS, where IL-1 $\beta$  was demonstrated to be the most potent proinflammatory mediator in bronchoalveolar lavage, with TNF- $\alpha$  being much less significant (25).

Activation of the transcriptional factor NF- $\kappa$ B is important in modulating acute inflammatory responses (3, 4, 28). Association of NF- $\kappa$ B heterodimers with  $\kappa$ B binding sites in the promoters of cytokines such as



Fig. 6. TNF- $\alpha$  is localized to alveolar macrophages after endotoxemia. Mice were either given PBS with LPS (A) or PBS alone (B) intraperitoneally. One hour later, the lungs were infiltrated with 1% agarose, removed en bloc, sectioned, and stained using rabbit anti-TNF- $\alpha$  antiserum. Photographs represent 1,000 magnifications of the sections. Arrows identify alveolar macrophages, which are positively stained for TNF- $\alpha$  in LPS-treated mice.

IL-1 $\beta$ , TNF- $\alpha$ , and MIP-2, as well as of other proinflammatory mediators, including intercellular adhesion molecule-1 and tissue factor, enhances expression of these proteins. Increased activation of NF- $\kappa$ B occurs among lung cell populations in models of acute lung injury due to hemorrhage or endotoxemia (6, 20, 21, 29, 30). NF- $\kappa$ B activation is also enhanced in alveolar macrophages from patients with ARDS (22). Previous experiments showed that inhibition of NF- $\kappa$ B activation prevented hemorrhage- or endotoxin-induced proinflammatory cytokine expression and neutrophil accumulation in the lungs (6, 20, 30).

In these experiments, hemorrhage- or endotoxemia-induced NF- $\kappa$ B activation was diminished in the lungs of neutropenic mice. We previously demonstrated that NF- $\kappa$ B is activated in lung neutrophils after hemorrhage or endotoxemia (30). One explanation for the present results is that most of the activation of NF- $\kappa$ B occurring in the lungs after hemorrhage or endotoxemia is in infiltrating neutrophils. In that case, neutrophil depletion decreases NF- $\kappa$ B activation in whole lung extracts simply by eliminating the major cell population in which such activation of NF- $\kappa$ B occurs. However, an alternate explanation is that neutrophils, by generating reactive oxygen intermediates, cytokines, or other proinflammatory mediators, initiate an inflammatory response in the lungs through which NF- $\kappa$ B becomes activated in other pulmonary cell populations. In this scenario, neutrophils are the initiators of an inflammatory response but are not the major cell population in which NF- $\kappa$ B is activated. Further in situ studies will resolve this issue.

Inhibition of neutrophil accumulation in the lungs, such as through the use of anti-adhesion molecule therapies, decreases the severity of lung injury after endotoxin administration, ischemia-reperfusion, or other pathophysiological insults (10, 16). The benefit of such interventions generally has been ascribed to inhibiting the effector functions of neutrophils, primarily the release of reactive oxygen intermediates and proteolytic mediators by which the lungs are directly damaged. However, neutrophils may have an alternate role in which they initiate inflammatory responses. Neutrophils are transcriptionally active and can produce a range of immunoregulatory molecules, such as cytokines, that are capable of potentiating inflammatory responses (2, 7, 30, 33). The present experiments are consistent with this early immunomodulatory role for neutrophils because they show that neutrophils are responsible for the initial activation of NF- $\kappa$ B, as well as of the increases in proinflammatory cytokines that occur in the lungs after hemorrhage or endotoxemia.

This work was supported by the National Heart, Lung, and Blood Institute Grants HL-50284 and HL-62221.

## REFERENCES

1. Abraham E, Jesmok G, Tuder R, Allbee JJ, and Chang Y-H. Contribution of tumor necrosis factor  $\alpha$  to pulmonary cytokine expression and lung injury following hemorrhage and resuscitation. *Crit Care Med* 23: 1319-1326, 1995.
2. Abraham E, Kaneko DJ, and Shenkar R. Effects of endogenous and exogenous catecholamines on LPS-induced neutrophil trafficking and activation. *Am J Physiol Lung Cell Mol Physiol* 276: L1-L8, 1999.
3. Baeuerle PA and Baltimore D. NF- $\kappa$ B: ten years after. *Cell* 87: 13-20, 1996.
4. Baeuerle PA and Henkel T. Function and activation of NF- $\kappa$ B in the immune system. *Annu Rev Immunol* 12: 141-179, 1994.
5. Bernard GR, Artigas A, Brigham KL, Carlet J, Falke K, Hudson L, Lamy M, LeGall JR, Morris AM, and Spragg R. The American-European consensus conference on ARDS: definitions, mechanisms, relevant outcomes, and clinical trial coordination. *Am J Respir Crit Care Med* 149: 818-824, 1994.
6. Blackwell TS, Blackwell TR, Holden EP, Christman BW, and Christman JW. In vivo antioxidant treatment suppresses nuclear factor- $\kappa$ B activation and neutrophilic lung inflammation. *J Immunol* 157: 1630-1637, 1996.
7. Cassatella MA. The production of cytokines by polymorphonuclear neutrophils. *Immunol Today* 16: 21-28, 1995.
8. Cholle Martin S, Jourdain B, Gibert C, Elbim C, Chastre J, and Gougerot-Pocidalo MA. Interactions between neutrophils and cytokines in blood and alveolar spaces during ARDS. *Am J Respir Crit Care Med* 154: 594-601, 1996.
9. Denis M, Guojian L, Widmer M, and Cantin A. A mouse model of lung injury induced by microbial products: implication of tumor necrosis factor. *Am J Respir Cell Mol Biol* 10: 658-664, 1994.
10. Doerschuk CM, Quinlan WM, Doyle NA, Bullard DC, Vestweber D, Jones ML, Takei F, Ward PA, and Beaudet AL. The role of P-selectin and ICAM-1 in acute lung injury as determined using blocking antibodies and mutant mice. *J Immunol* 157: 4609-4614, 1996.
11. Donnelly SC, Strieter RM, Kunkel SL, Walz A, Robertson CR, Carter DC, Grant IS, Pollok AJ, and Haslett C. Interleukin-8 and development of adult respiratory distress syndrome in at-risk patient groups. *Lancet* 341: 643-647, 1993.
12. Folz RJ, Abushama AM, and Suliman HB. Extracellular superoxide dismutase in the airways of transgenic mice reduces inflammation and attenuates lung toxicity following hyperoxia. *J Clin Invest* 103: 1055-1066, 1999.
13. Goodman RB, Streiter RM, Martin DP, Steinberg KP, Milberg JA, Maunder RJ, Kunkel SL, Walz A, Hudson LD, and Martin TR. Inflammatory cytokines in patients with persistence of the acute respiratory distress syndrome. *Am J Respir Crit Care Med* 154: 602-611, 1996.
14. Heflin AC and Brigham KL. Prevention by granulocyte depletion of increased vascular permeability of sheep lung following endotoxemia. *J Clin Invest* 68: 1253-1260, 1981.
15. Hudson LD, Milberg JA, Anardi D, and Maunder RJ. Clinical risks for development of the acute respiratory distress syndrome. *Am J Respir Crit Care Med* 151: 293-301, 1995.
16. Kamochi M, Kamochi F, Yim YB, Sawh S, Sanders JM, Sarembock I, Green S, Young JS, Ley K, Fu SM, and Rose CE. P-selectin and ICAM-1 mediate endotoxin-induced neutrophil recruitment and injury to the lung and liver. *Am J Physiol Lung Cell Mol Physiol* 277: L310-L319, 1999.
17. Kelley DM, Lichtenstein A, Wang J, Taylor AN, and Dubinett SM. Corticotropin-releasing factor reduces lipopolysaccharide-induced pulmonary vascular leak. *Immunopharmacol Immunotoxicol* 16: 139-148, 1994.
18. Kollef MH and Schuster DP. The acute respiratory distress syndrome. *N Engl J Med* 332: 27-37, 1995.
19. Kurdowska A, Miller EJ, Noble JM, Baughman RP, Matthay MA, Brelsford WG, and Cohen AB. Anti-IL-8 autoantibodies in alveolar fluid from patients with the adult respiratory distress syndrome. *J Immunol* 157: 2699-2706, 1996.
20. Liu SF, Ye X, and Malik AB. In vivo inhibition of nuclear factor- $\kappa$ B activation prevents inducible nitric oxide synthase expression and systemic hypotension in a rat model of septic shock. *J Immunol* 159: 3976-3983, 1997.
21. Manning AM, Bell FP, Rosenbloom CL, Chosay JG, Simmons CA, Northrup JL, Shebuski RJ, Dunn CJ, and Anderson DC. NF- $\kappa$ B is activated during acute inflammation in vivo in association with elevated endothelial cell adhesion mol-

- ecule gene expression and leukocyte recruitment. *J Inflamm* 45: 283–296, 1995.
22. Moine P, McIntyre R, Schwartz MD, Kaneko D, Shenkar R, le Tulzo Y, Moore EE, and Abraham E. NF- $\kappa$ B regulatory mechanisms in alveolar macrophages from patients with acute respiratory distress syndrome. *Shock* 13: 85–91, 2000.
  23. Parsey MV, Tudor R, and Abraham E. Neutrophils are major contributors to intraparenchymal lung IL-1 $\beta$  expression after hemorrhage and endotoxemia. *J Immunol* 160: 1007–1013, 1998.
  24. Pittet JF, Mackersie RL, Martin TR, and Matthay MA. Biological markers of acute lung injury: prognostic and pathogenetic significance. *Am J Respir Crit Care Med* 255: 1187–1205, 1997.
  25. Pugin J, Ricou B, Steinberg KP, Suter PM, and Martin TR. Proinflammatory activity in bronchoalveolar lavage fluids from patients with ARDS, a prominent role for interleukin-1. *Am J Respir Crit Care Med* 153: 1850–1856, 1996.
  26. Repine JE. Scientific perspectives on the adult respiratory distress syndrome. *Lancet* 339: 466–469, 1992.
  27. Repine JE and Abraham E. Challenges in treating ARDS. *Curr Opin Crit Care* 2: 73–78, 1996.
  28. Sha WC. Regulation of immune responses by NF- $\kappa$ B/Rel transcription factors. *J Exp Med* 187: 143–146, 1998.
  29. Shenkar R and Abraham E. Hemorrhage induces rapid in vivo activation of CREB and NF- $\kappa$ B in murine intraparenchymal lung mononuclear cells. *Am J Respir Cell Mol Biol* 16: 145–152, 1997.
  30. Shenkar R and Abraham E. Mechanisms of lung neutrophil activation after hemorrhage or endotoxemia: roles of reactive oxygen intermediates, NF- $\kappa$ B, and CREB. *J Immunol* 163: 954–962, 1999.
  31. Shenkar R, Coulson WF, and Abraham E. Hemorrhage and resuscitation induce alterations in cytokine expression and the development of acute lung injury. *Am J Respir Cell Mol Biol* 10: 290–297, 1994.
  32. Till GO, Johnson KT, Kunkel S, and Ward PA. Intravascular activation of complement and acute lung injury: dependency on neutrophils and toxic oxygen intermediates. *J Clin Invest* 69: 1126–1135, 1982.
  33. Xing Z, Jordana M, Kirpalani H, Driscoll KE, Schall TJ, and Gauldie J. Cytokine expression by neutrophils and macrophages in vivo: endotoxin induces tumor necrosis factor- $\alpha$ , macrophage inflammatory protein-2, interleukin-1 beta, and interleukin-6 but not RANTES or transforming growth factor-beta 1 mRNA express in acute lung inflammation. *Am J Respir Cell Mol Biol* 10: 148–153, 1994.



# Trypsin activates pancreatic duct epithelial cell ion channels through proteinase-activated receptor-2

Toan D. Nguyen,<sup>1</sup> Mark W. Moody,<sup>1</sup> Martin Steinhoff,<sup>2</sup> Charles Okolo,<sup>1</sup> Duk-Su Koh,<sup>3</sup> and Nigel W. Bunnett<sup>2</sup>

<sup>1</sup>Department of Medicine, University of Washington and Veterans Affairs Puget Sound Health Care System, Seattle, Washington 98108, USA

<sup>2</sup>Departments of Surgery and Physiology, University of California, San Francisco, California 94143, USA

<sup>3</sup>Department of Physiology and Biophysics, University of Washington, Seattle, Washington 98195, USA

Address correspondence to: Toan D. Nguyen, GI Section (111 GI), Veterans Affairs Medical Center, 1660 S. Columbian Way, Seattle, Washington 98108, USA. Phone: (206) 764-2285; Fax: (206) 764-2232; E-mail: t1nguyen@u.washington.edu

Received for publication December 16, 1997, and accepted in revised form November 17, 1998.

Proteinase-activated receptor-2 (PAR-2) is a G protein-coupled receptor that is cleaved by trypsin within the NH<sub>2</sub>-terminus, exposing a tethered ligand that binds and activates the receptor. We examined the secretory effects of trypsin, mediated through PAR-2, on well-differentiated nontransformed dog pancreatic duct epithelial cells (PDEC). Trypsin and activating peptide (AP or SLIGRL-NH<sub>2</sub>, corresponding to the PAR-2 tethered ligand) stimulated both an <sup>125</sup>I- efflux inhibited by Ca<sup>2+</sup>-activated Cl<sup>-</sup> channel inhibitors and a <sup>86</sup>Rb<sup>+</sup> efflux inhibited by a Ca<sup>2+</sup>-activated K<sup>+</sup> channel inhibitor. The reverse peptide (LRGILS-NH<sub>2</sub>) and inhibited trypsin were inactive. Thrombin had no effect, suggesting absence of PAR-1, PAR-3, or PAR-4. In Ussing chambers, trypsin and AP stimulated a short-circuit current from the basolateral, but not apical, surface of PDEC monolayers. In monolayers permeabilized basolaterally or apically with nystatin, AP activated apical Cl<sup>-</sup> and basolateral K<sup>+</sup> conductances. PAR-2 agonists increased [Ca<sup>2+</sup>]<sub>i</sub> in PDEC, and the calcium chelator BAPTA inhibited the secretory effects of AP. PAR-2 expression on dog pancreatic ducts and PDEC was verified by immunofluorescence. Thus, trypsin interacts with basolateral PAR-2 to increase [Ca<sup>2+</sup>]<sub>i</sub> and activate ion channels in PDEC. In pancreatitis, when trypsinogen is prematurely activated, PAR-2-mediated ductal secretion may promote clearance of toxins and debris.

*J. Clin. Invest.* 103:261-269 (1999).

## Introduction

Proteinase-activated receptor-2 (PAR-2) is the second member of the new family of G protein-coupled receptors that are activated by proteolysis rather than binding to a soluble ligand (reviewed in ref. 1). PAR-1, PAR-3, and PAR-4 are receptors for thrombin (2-5); PAR-2 is a receptor for pancreatic trypsin and mast cell tryptase (6, 7). Trypsin and tryptase cleave within the extracellular NH<sub>2</sub>-terminus of PAR-2 at SKGR↓SLIGRL, yielding a tethered ligand (SLIGRL) that binds to and activates the cleaved receptor. Synthetic peptides corresponding to this tethered ligand domain selectively activate PAR-2 without proteolysis. They are thus valuable reagents for studying receptor function without the use of proteases, which may cleave other proteins.

The gene encoding PAR-2 has been cloned in humans, and PAR-2 has been found to be highly expressed in the pancreas and kidney as well as intestine, liver, prostate, heart, lung, and trachea (8). High pancreatic expression is supported by abundant PAR-2 expression in several cell lines derived from pancreatic acinar and duct cells. However, although the tissue distribution of PAR-2 has been examined, its precise cellular localization, ligands, and physiological function are unknown for most tissues.

The very high level of PAR-2 expression in the pancreas is intriguing, as trypsin, the protease that cleaves and triggers PAR-2 with highest potency and efficacy, is syn-

thesized and secreted by pancreatic acinar cells. Although trypsin is traditionally considered as a digestive enzyme, we have recently reported (9) that physiological concentrations of trypsin in the intestinal lumen cleave and activate PAR-2 at the apical membrane of enterocytes, suggesting that trypsin also acts as a signaling molecule that specifically targets cells through PAR-2. It is therefore possible that trypsin also activates PAR-2 in the pancreas and thereby regulates pancreatic function. However, trypsin is mostly secreted as its inactive zymogen precursor, trypsinogen, which is inactive until it is cleaved by enterokinase in the intestinal lumen. Although small amounts of active trypsin are formed within the pancreas under normal circumstances, trypsin is prematurely autoactivated within the inflamed pancreas and is believed to contribute to pancreatitis (10). Indeed, the genetic defects of hereditary pancreatitis are amino acid mutations of trypsin that render it resistant to degradation following premature autoactivation (11, 12). Therefore, trypsin may cleave and activate PAR-2 within the inflamed pancreas. A role for PAR-2 in inflammation is also supported by the finding that tryptase, a prominent component of secretory granules of most subsets of human mast cells that is released upon degranulation, also activates PAR-2 (7, 13). Tryptase may also trigger PAR-2 in the pancreas during inflammation, when mast cells are present (Nguyen,

T.D., *et al.*, unpublished observations). However, the localization of PAR-2 in the exocrine pancreas and the consequences of receptor activation are unknown.

The principal cell types within the exocrine pancreas are acinar cells, which secrete digestive enzymes, and pancreatic duct epithelial cells (PDEC), which secrete fluid and electrolytes, mainly bicarbonate. Recently, Oda *et al.* developed methods to isolate and culture dog PDEC that are nontransformed, well-differentiated, and polarized, and which retain many of the characteristics of PDEC, such as mucin secretion (14) and the presence of cAMP- and  $\text{Ca}^{2+}$ -activated  $\text{Cl}^-$  channels (15), and  $\text{Ca}^{2+}$ -activated  $\text{K}^+$  channels (16). They are thus ideally suited for detailed examination of the regulation of ion channels by specific receptors (17, 18). In the present investigation, we examined the hypothesis that trypsin regulates PDEC through PAR-2. Our aims were to (a) determine that trypsin and PAR-2 agonists affect channel activities of PDEC, (b) identify the channels thus regulated, (c) define the signaling pathway mediating PAR-2 effects on PDEC, (d) delimit the apical and/or basolateral expression of functional PAR-2, and (e) localize PAR-2 within the pancreas and PDEC.

## Methods

**Chemicals and reagents.** Bovine trypsin XII-S (11,900 benzoyl-arginine ethyl ester [BAEE] units/mg protein) and ovomucoid trypsin inhibitor (III-O, inhibiting 13,000 BAEE units/mg protein) were from Sigma Chemical Co. (St. Louis, Missouri, USA). Indo-1/AM was from Molecular Probes (Eugene, Oregon, USA). Activating peptide (AP, SLIGRL-NH<sub>2</sub>) corresponding to the tethered ligand of mouse PAR-2, and reverse peptide (RP, LRGLS-NH<sub>2</sub>), were synthesized by solid-phase methods and purified by high-pressure liquid chromatography. Analogues of these peptides, highly selective for PAR-1 (AF[PF]RChaCitY-NH<sub>2</sub>) or PAR-2 (tc-LGRLO-NH<sub>2</sub>), were a gift from M. Hollenberg (University of Calgary, Calgary, Alberta, Canada) (19–21). The sources of other reagents have been described (15–18).

**Antibodies.** Rabbit antibody PAR-2 B5, raised against a fragment of rat PAR-2 (<sup>30</sup>GPNSKGR↓SLIGRLDT<sup>46</sup>P-YGGC, ↓ =

trypsin cleavage site), was a gift from M. Hollenberg and was used at a dilution of 1:500–1:2,000 (9, 13). Rabbit antibody PAR-2 C, raised against a fragment of human PAR-2 (↓<sup>37</sup>SLIGKVDGTSHVTGKG<sup>53</sup>V), was a gift from C. Derian (R.W. Johnson Pharmaceutical Research Institute, Spring House, Pennsylvania, USA) and was used at 2 µg/ml (22). Mouse monoclonal antibody to von Willebrand factor was from DAKO Corp. (Carpenteria, California, USA) and used at 1:50. Goat anti-rabbit IgG conjugated to FITC and goat anti-mouse IgG conjugated to Texas-Red were from Cappel Research Products (Durham, North Carolina, USA) and Jackson Immuno Research Laboratories Inc. (West Grove, Pennsylvania, USA); they were used at a dilution of 1:200.

**PDEC culture.** PDEC were isolated from the accessory pancreatic duct of a dog and cultured as described previously (14). The cells used in this report were between passages 9 and 30.

**Efflux studies.** Cellular <sup>125</sup>I- and <sup>86</sup>Rb<sup>+</sup> effluxes were measured to study activation of  $\text{Cl}^-$  and  $\text{K}^+$  conductance, as described for T84 cells (23) and extended to PDEC (15, 16). In brief, confluent PDEC and supporting membranes were excised, washed in experimental buffer (140 mM NaCl, 4.7 mM KCl, 1.2 mM  $\text{CaCl}_2$ , 10 mM glucose, 10 mM HEPES, pH 7.4), and incubated for 45 min with buffer containing either ~2 µCi/ml  $\text{Na}^{125}\text{I}$  or ~1 µCi/ml <sup>86</sup>RbCl. Isotope efflux was measured by sequential addition and removal of 1 ml of isotope-free buffer at 15-s intervals for 5 min. After a basal period of 1 min, agonists were added to all solutions for 4 min. Inhibitors were added at the beginning of the experiment, except for 1,2-bis(2-aminophenoxy)ethane-N,N,N',N'-tetraacetic acid, tetra(acetoxymethyl) ester (BAPTA/AM), which was also added during the <sup>125</sup>I- loading period. The efflux rate coefficient for a certain time interval was calculated using the formula:  $r = [\ln(R_1) - \ln(R_2)] / (t_1 - t_2)$ , where  $R_1$  and  $R_2$  are the percent of counts initially loaded remaining in the cells at times  $t_1$  and  $t_2$ . In certain experiments in which the peak effluxes were compared, we also considered the increase of the efflux rate coefficient above the baseline efflux rate coefficient. The baseline rate coefficient is determined as the lowest efflux rate coefficient immediately before addition of AP or trypsin (15–18).

**Ussing chamber studies.** Ion transports across confluent PDEC monolayers or across their apical or basolateral membranes were determined in Ussing chambers as described previously

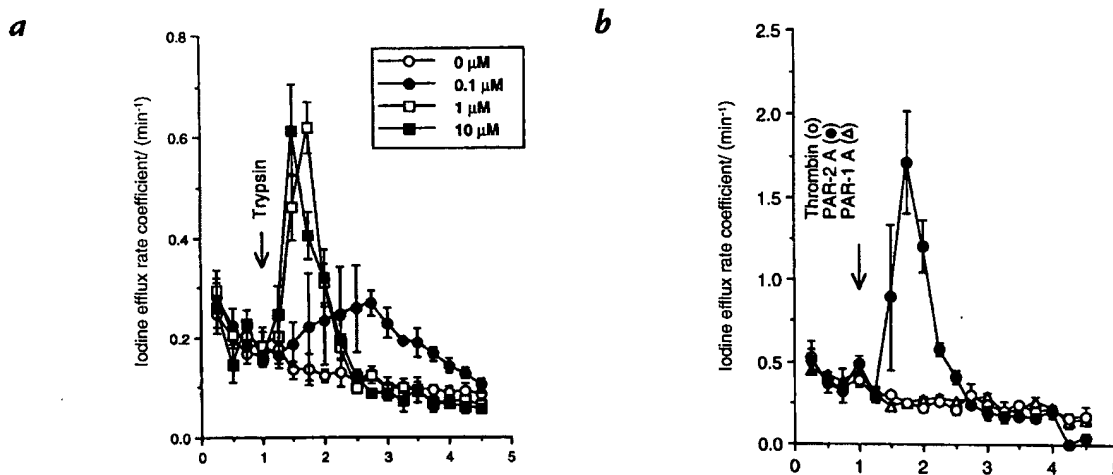


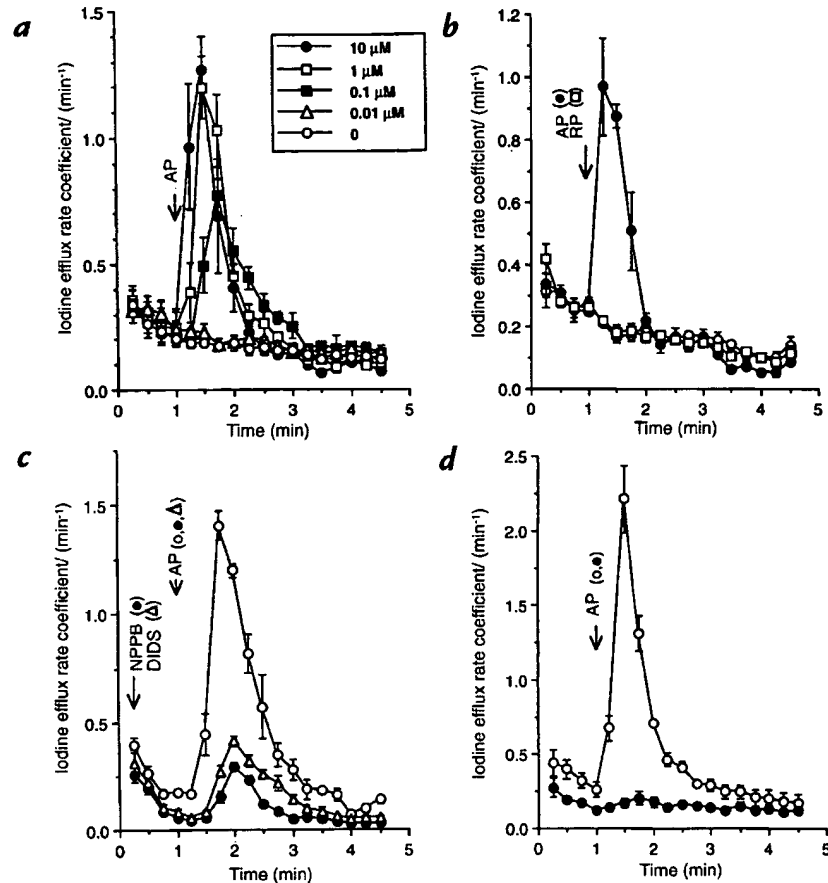
**Figure 1**

Stimulation of <sup>125</sup>I- efflux by trypsin. <sup>125</sup>I- efflux was monitored as detailed in Methods and the efflux rate coefficient shown (means ± SEM, n = 3). (a) After 1 min for baseline determination, trypsin was added at the final concentrations shown. (b) After 1 min, 1 µM of either thrombin (open circle), the PAR-1 agonist, AF[PF]RChaCitY-NH<sub>2</sub> (PAR-1 A, open circle), or the PAR-2 agonist, tc-LGRLO-NH<sub>2</sub> (PAR-2 A, filled circle), was added.



**Figure 2**

Stimulation of  $^{125}\text{I}^-$  efflux by AP.  $^{125}\text{I}^-$  efflux was monitored as detailed in Methods and the efflux rate coefficient shown (means  $\pm$  SEM,  $n = 3$ ). (a) After 1 min for baseline determination, AP was added at the final concentrations shown. (b) After 1 min,  $1\ \mu\text{M}$  of either activating peptide (closed circle) or reversed activating peptide (RP, open square) was added. Control efflux without peptide is indicated by an open circle. (c) After 1 min,  $1\ \mu\text{M}$  AP was added in the absence (open circle) or presence of  $500\ \mu\text{M}$  NPPB (closed circle) or DIDS (open triangle). (d) After 1 min,  $1\ \mu\text{M}$  AP was added to cells pretreated with  $50\ \mu\text{M}$  BAPTA/AM (closed circle) or untreated control cells (open circle). AP, activating peptide; BAPTA/AM, 1,2-bis(2-aminophenoxy)ethane-N,N,N',N'-tetraacetic acid, tetra(acetoxymethyl) ester DIDS, 4,4'-diisothiocyanatostilbene-2,2'-disulfonic acid; NPPB, 5-nitro-2-(3-phenylpropylamino)benzoic acid.



(16–18). To study apical  $\text{Cl}^-$  conductance, the basolateral cell membrane was permeabilized to small monovalent ions with nystatin ( $0.36\ \text{mg/ml}$  in the serosal compartment for  $\geq 20\ \text{min}$ ). A  $135\text{-mM}$  serosal-to-luminal  $\text{Cl}^-$  gradient was generated using a serosal buffer ( $135\ \text{mM NaCl}$ ,  $1.2\ \text{mM CaCl}_2$ ,  $1.2\ \text{mM MgCl}_2$ ,  $2.4\ \text{mM K}_2\text{HPO}_4$ ,  $0.6\ \text{mM KH}_2\text{PO}_4$ ,  $10\ \text{mM HEPES}$ ,  $10\ \text{mM glucose}$ ) and a luminal buffer in which the  $\text{NaCl}$  was substituted with  $\text{Na-gluconate}$ . To study basolateral  $\text{K}^+$  conductance, the apical membrane was permeabilized using nystatin. A  $114\text{-mM}$  luminal-to-serosal  $\text{K}^+$  gradient was generated with a luminal buffer of ( $10\ \text{mM NaCl}$ ,  $1.25\ \text{mM CaCl}_2$ ,  $1\ \text{mM MgCl}_2$ ,  $118\ \text{K gluconate}$ ,  $10\ \text{mM HEPES}$ ,  $10\ \text{mM glucose}$ , titrated to  $\text{pH } 7.4$  with  $\text{NaOH}$ ) and a serosal buffer in which the  $118\ \text{K gluconate}$  was substituted with  $4\ \text{K gluconate}$  and  $114\ \text{N-methyl-D-glucamine}$ . In the latter case, ouabain ( $100\ \mu\text{M}$ ) was used to inhibit the  $\text{Na}^+, \text{K}^+$ -ATPase pump and maintain intracellular ATP.

**Cytosolic  $\text{Ca}^{2+}$  studies.** PDEC were cultured to subconfluence on glass coverslips coated with Vitrogen and loaded with  $1\ \mu\text{M}$  of the membrane-permeant Indo-1 AM at room temperature for  $30\ \text{min}$  and perfused with experimental buffer (solution exchange within  $2\ \text{s}$ ). Fluorescence in single cells was detected using an inverted epifluorescence microscope (Diaphor; Nikon, Melville, New York, USA), fitted with a  $100\text{-W}$  mercury lamp, and two photon-counting photomultiplier tubes (Hamamatsu H3460-04; Hamamatsu Photonic Systems, Bridgewater, New Jersey, USA). Cells were excited at  $365\ \text{nm}$ , and emission was measured every  $2\ \text{s}$  at  $405$  and  $500\ \text{nm}$ . Correction was made for background fluorescence.

Intracellular free  $\text{Ca}^{2+}$  concentration ( $[\text{Ca}^{2+}]_i$ ) was calculated as:  $K^* (R - R_{\text{min}}) / (R_{\text{max}} - R)$ , where  $R$  is the ratio of cellular fluorescence at  $405\ \text{nm}$ /fluorescence at  $500\ \text{nm}$ ,  $R_{\text{min}}$  the corre-

sponding cellular ratio in a  $\text{Ca}^{2+}$ -free buffer, and  $R_{\text{max}}$  the ratio obtained with  $\text{Ca}^{2+}$ -bound dye (25).  $K^*$  was calculated using cells perfused with the experimental buffer containing  $5\ \mu\text{M}$  ionomycin plus either  $50\ \text{mM EGTA}$  ( $R_{\text{min}}$ ),  $20\ \text{mM Ca}^{2+}$  ( $R_{\text{max}}$ ), or  $15\ \text{mM Ca}^{2+}$  and  $20\ \text{mM EGTA}$  (calculated  $[\text{Ca}^{2+}]_i$  was  $251\ \text{nM}$ ). Values for  $R_{\text{min}}$ ,  $R_{\text{max}}$ , and  $K^*$  were  $0.44$ ,  $4.46$ , and  $1770\ \text{nM}$ , respectively ( $n = 8\text{--}13$  cells for each measurement).

**Immunostaining.** Pancreas from an adult dog was fixed in  $4\%$  paraformaldehyde in  $100\ \text{mM PBS}$  for  $48\text{--}72\ \text{h}$  at  $4^\circ\text{C}$  and placed in  $25\%$  sucrose in  $\text{PBS}$  for  $24\ \text{h}$  at  $4^\circ\text{C}$ . Specimens were either (a) embedded in OCT (Miles, Slough, United Kingdom) and  $10\text{-}\mu\text{m}$  frozen sections prepared and postfixed in  $4\%$  paraformaldehyde in  $\text{PBS}$  for  $20\ \text{min}$  or (b) dehydrated, embedded in paraffin, and sectioned at  $5\ \mu\text{m}$ . PDEC, cultured on filters for  $8$  days, were fixed in  $4\%$  paraformaldehyde in  $\text{PBS}$  for  $20\ \text{min}$ , at  $4^\circ\text{C}$ , dehydrated, embedded in paraffin, and sectioned at  $5\ \mu\text{m}$ . Paraffin sections were deparaffinized in xylene and rehydrated.

Sections were processed to localize PAR-2 by indirect immunofluorescence, as described previously (9, 13). In controls, diluted antibodies were preincubated for  $24\ \text{h}$  at  $4^\circ\text{C}$  with  $1\text{--}100\ \mu\text{M}$  of the peptide fragment used for immunization, or nonspecific rabbit IgG were substituted. To localize PAR-2 and endothelial cells simultaneously, slides were concurrently incubated with rabbit polyclonal antibody B5 and mouse monoclonal antibody against von Willebrand factor, followed by secondary antibodies conjugated to contrasting fluorophores. Serial sections of tissues were also stained with hematoxylin and eosin, to assist in identifying pancreatic ducts, acini, and blood vessels. Slides were observed using a Zeiss Axioplan microscope (Carl Zeiss Inc., Thornwood, New York, USA) and an MRC 1000 laser scanning confocal microscope (Bio-Rad Laboratories Inc.,

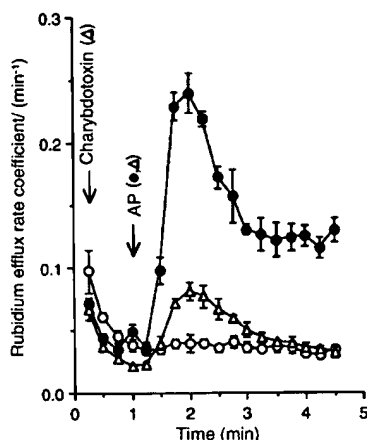


**Figure 3**

Stimulation of  $^{86}\text{Rb}^+$  efflux by activating peptide.  $^{86}\text{Rb}^+$  efflux was monitored as detailed in Methods and the efflux rate coefficient shown (means  $\pm$  SEM,  $n = 3$ ). After 1 min for baseline determination, 1  $\mu\text{M}$  AP was added in the presence (open triangle) or absence (closed circle) of 100 nM charybdotoxin. Control efflux without AP is indicated (open circle).

Hercules, California, USA) (26).

**Statistics.** Results, based on at least three experiments, were expressed as means and SEM, unless specified otherwise. Statistical significance was determined using unpaired two-tailed Student's *t* tests.

## Results

**Iodide efflux studies.** Trypsin activation of ion channels of PDEC was first evaluated. Trypsin stimulated  $^{125}\text{I}^-$  efflux in a concentration-dependent manner, with efflux peak rate coefficients of  $0.268 \pm 0.25/\text{min}$  (peak increase above baseline:  $0.085/\text{min}$ ),  $0.620 \pm 0.051/\text{min}$  (peak increase:  $0.436/\text{min}$ ), and  $0.615 \pm 0.089/\text{min}$  (peak increase:  $0.456/\text{min}$ ) observed, respectively, 105, 45, and 30 seconds after the addition of 0.1, 1, and 10  $\mu\text{M}$  trypsin (Fig. 1a). Thus, increasing concentrations of trypsin stimulated  $^{125}\text{I}^-$  effluxes with larger peak efflux rate coefficients and of quicker onsets. When trypsin was neutralized for 45 minutes at  $37^\circ\text{C}$  with ovomucoid trypsin inhibitor

(4.2-fold excess of inhibitory potential based on estimates of BAEE units), its ability to stimulate  $^{125}\text{I}^-$  efflux was abolished (data not shown), suggesting that its effect was dependent on its enzymatic activity.

Although trypsin is the most effective activator for PAR-2, it also is a weak activator of PAR-1 and PAR-3 and a strong activator of PAR-4 (2–5), the latter highly expressed in the pancreas (4). To evaluate whether the stimulation of  $^{125}\text{I}^-$  efflux by trypsin may be mediated by proteinase-activated receptors other than PAR-2, we assessed the effect of thrombin, which strongly activates PAR-1, PAR-3, and PAR-4 (2–5). Thrombin (1  $\mu\text{M}$ ) had no effect on  $^{125}\text{I}^-$  efflux (Fig. 1b).  $\text{AF(PF)RChaCitY-NH}_2$ , a selective agonist of PAR-1, at 1  $\mu\text{M}$ , had no effect on  $^{125}\text{I}^-$  efflux, whereas the same concentration of the PAR-2 agonist,  $\text{tc-LIGRLO-NH}_2$ , stimulated a robust response (Fig. 1b). Together, these results suggest that PAR-1, PAR-3, and PAR-4 do not mediate the stimulation of  $^{125}\text{I}^-$  efflux; by exclusion, trypsin most likely acts through PAR-2.

AP, a synthetic activating peptide (SLIGRL-NH<sub>2</sub>) that corresponds to the tethered ligand of PAR-2, directly activates the receptor (6). AP stimulated  $^{125}\text{I}^-$  efflux in a concentration-dependent manner: 0.01  $\mu\text{M}$  produced no response, 0.1  $\mu\text{M}$  produced an intermediate response, with a peak efflux rate coefficient of  $0.775 \pm 0.067/\text{min}$  (peak increase above baseline:  $0.566/\text{min}$ ), and 1  $\mu\text{M}$  and 10  $\mu\text{M}$  produced maximal responses with peak efflux rate coefficients of  $1.197 \pm 0.122/\text{min}$  (peak increase:  $0.954/\text{min}$ ) and  $1.268 \pm 0.131$  (peak increase:  $1.018/\text{min}$ ), respectively (Fig. 2a). A peptide with the reverse sequence of AP (RP) did not stimulate an increased  $^{125}\text{I}^-$  efflux (Fig. 2b).

To verify that the increased  $^{125}\text{I}^-$  efflux occurred through activated  $\text{Cl}^-$  conductances, the effect of different inhibitors of  $\text{Cl}^-$  channels was studied. While the control peak efflux rate coefficient produced by 1  $\mu\text{M}$  AP was  $1.405 \pm 0.066/\text{min}$  (peak increase above baseline:  $1.24/\text{min}$ ), it was significantly inhibited to  $0.292 \pm 0.018/\text{min}$  (peak increase:  $0.235/\text{min}$ ) with 500  $\mu\text{M}$  5-nitro-2-(3-phenylpropylamino)benzoic acid (NPPB) and to  $0.412 \pm 0.026/\text{min}$  (peak increase:  $0.329/\text{min}$ ) with 500  $\mu\text{M}$  4,4'-diisothiocyanatostilbene-2,2'-disulfonic acid (DIDS) ( $P < 0.001$  compared with control for both inhibitors) (Fig. 2c).

Of the two  $\text{Cl}^-$  channels previously identified on the dog PDEC, the cAMP-activated cystic fibrosis transmembrane conductance regulator (CFTR) and the  $\text{Ca}^{2+}$ -activated  $\text{Cl}^-$  channel, only the latter channel was sensitive to DIDS (15). Sensitivity of AP-stimulated  $^{125}\text{I}^-$  to DIDS is consistent with its mediation through the  $\text{Ca}^{2+}$ -activated  $\text{Cl}^-$  channel, stimulated by an increased  $[\text{Ca}^{2+}]_i$ . This possibility was further verified using BAPTA/AM, a cell-permeant  $\text{Ca}^{2+}$  chelator. As shown in Fig. 2d, in cells treated with BAPTA/AM, AP no longer increased  $^{125}\text{I}^-$  efflux.

**Rubidium efflux studies.** Through measurements of  $^{86}\text{Rb}^+$  efflux, we recently observed that PDEC express  $\text{Ca}^{2+}$ -activated  $\text{K}^+$  channels (16). Should PAR-2 mediate  $[\text{Ca}^{2+}]_i$  mobilization, it may also activate these  $\text{K}^+$  channels. As shown in Fig. 3, 1  $\mu\text{M}$  AP stimulated an increased  $^{86}\text{Rb}^+$  efflux, with a peak efflux rate coefficient of  $0.239 \pm 0.016/\text{min}$  (peak increase above baseline:  $0.205/\text{min}$ ,  $n = 3$ ), 1 min after its addition. This effect was inhibited by 100 nM charybdotoxin, an

**Table 1**

Effect of trypsin and AP on  $[\text{Ca}^{2+}]_i$

Treatment	Basal $[\text{Ca}^{2+}]_i$ (nM)	Peak $[\text{Ca}^{2+}]_i$ (nM)	n
Trypsin	$52 \pm 11$	$487 \pm 100^A$	6
Trypsin + charybdotoxin <sup>B</sup>	$53 \pm 6$	$715 \pm 99^A$	4
AP	$51 \pm 7$	$303 \pm 41^A$	4
AP + charybdotoxin <sup>C</sup>	$72 \pm 6$	$703 \pm 127^A$	3
AP + DIDS <sup>B</sup>	$62 \pm 14$	$370 \pm 50^A$	3

The effects of 1  $\mu\text{M}$  trypsin or AP on  $[\text{Ca}^{2+}]_i$  of PDEC, in the presence or absence charybdotoxin (100 nM) or DIDS (500  $\mu\text{M}$ ), were determined as described in Methods. Basal  $[\text{Ca}^{2+}]_i$  and peak  $[\text{Ca}^{2+}]_i$  following agonist addition are shown (mean  $\pm$  SEM). Charybdotoxin and DIDS were added 2 min before AP or trypsin. When DIDS was used, the results were corrected for its background fluorescence. <sup>A</sup>Significant difference between basal  $[\text{Ca}^{2+}]_i$  and stimulated peak  $[\text{Ca}^{2+}]_i$ , at  $P < 0.05$ . Peak  $[\text{Ca}^{2+}]_i$  stimulated by AP and trypsin were not significantly different ( $P > 0.1$ ), and the peak  $[\text{Ca}^{2+}]_i$  stimulated by AP or trypsin was not significantly different in the presence or absence of charybdotoxin or DIDS. <sup>B</sup> $P > 0.1$ . <sup>C</sup> $P > 0.05$ . PDEC, pancreatic duct epithelial cell.

inhibitor of  $\text{Ca}^{2+}$ -activated  $\text{K}^+$  channels, to a peak efflux rate coefficient of  $0.081 \pm 0.007/\text{min}$  (peak increase:  $0.059/\text{min}$ ,  $P < 0.001$  compared with control).

**Intracellular  $\text{Ca}^{2+}$  determination.** To mediate activation of the  $\text{Ca}^{2+}$ -activated  $\text{Cl}^-$  and  $\text{K}^+$  channels, PAR-2 action must be coupled to an increased  $[\text{Ca}^{2+}]_i$ . This signaling mechanism is also consistent with BAPTA inhibition and observations obtained in other systems (8). The effects of trypsin and AP on  $[\text{Ca}^{2+}]_i$  were determined using Indo-1, a  $\text{Ca}^{2+}$ -sensitive dye. Trypsin ( $1 \mu\text{M}$ ) stimulated a biphasic  $[\text{Ca}^{2+}]_i$  response with a sharp increase within the first 4 seconds, followed by a slower increase that was sustained over time (Fig. 4*a*);  $1 \mu\text{M}$  AP stimulated a similar increase in  $[\text{Ca}^{2+}]_i$ , except that the initial sharp response was often blunted. The average peak responses stimulated by AP and trypsin and the lack of inhibition of this response by DIDS and charybdotoxin are shown in Table 1. In addition, AP was also able to stimulate an increased  $[\text{Ca}^{2+}]_i$  in cells treated with  $500 \mu\text{M}$  NPPB (from a basal concentration of  $50 \text{ nM}$  to a stimulated concentration of  $277 \text{ nM}$ ,  $n = 2$ ).

**Ussing chamber studies.** Because these dog PDEC are polarized and form confluent monolayers with high transepithelial resistance, they were mounted in Ussing chambers to assess PAR-2 expression on their basolateral or apical surface. As shown in Fig. 5*a*,  $1 \mu\text{M}$  trypsin stimulated an increased short-circuit current (Isc) when added to the serosal compartment, contiguous with the basolateral side of the cell. In contrast, when added to the luminal compartment on the apical side of the cell, trypsin produced no Isc change. Preincubation of trypsin with trypsin inhibitor abolished the ability of trypsin to stimulate an increased Isc (Fig. 5*b*). Similarly,  $1 \mu\text{M}$  AP stimulated an increased Isc only when added to the serosal, but not luminal, compartment of the Ussing chamber (data not shown). Together, these observations suggest that functional PAR-2 is expressed on the basolateral membrane of PDEC. In additional experiments, we also observed that  $1 \mu\text{M}$  thrombin did not stimulate an increased Isc when added to either serosal or luminal compartment (Fig. 5*c*) and that the PAR-1 agonist,  $\text{AF}(\text{PF})\text{RChaCitY-NH}_2$ , stimulated a very modest response compared with the PAR-2 agonist,  $\text{tc-LIGRLO-NH}_2$  (Fig. 5*d*).

Because we have not yet fully defined the mechanism accounting for the net transepithelial electrogenic ion transport reflected by the Isc, we determined whether AP stimulated apical membrane  $\text{Cl}^-$  conductances and basolateral membrane  $\text{K}^+$  conductances. PDEC were mounted in Ussing chambers, and their basolateral or apical membrane permeabilized with nystatin. To study  $\text{Cl}^-$  flow through apical  $\text{Cl}^-$  conductances, the basolateral membrane was permeabilized, and a  $135\text{-mM}$  serosal-to-luminal  $\text{Cl}^-$  gradient was used to drive  $\text{Cl}^-$  flow across the apical membrane. Activation of apical  $\text{Cl}^-$  conductances thus promotes an intra-to-extracellular  $\text{Cl}^-$  flow across the membrane, manifested by an Isc increase. In this system, serosal, but not luminal, addition of  $1 \mu\text{M}$  AP stimulated an increased Isc (Fig. 6*a*), providing electrophysiologic support for AP interaction with basolateral PAR-2 to activate apically located  $\text{Cl}^-$  conductances.

Conversely, to study  $\text{K}^+$  flow through basolateral  $\text{K}^+$

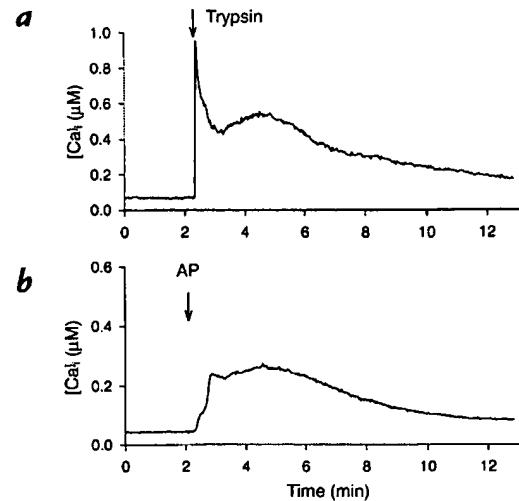


**Figure 4** Effects of trypsin and AP on  $[\text{Ca}^{2+}]_i$  of PDEC. Pancreatic duct epithelial cells were loaded with Indo-1, and the fluorescences emitted at 405 nm and 500 nm while excited at 365 nm were measured.  $[\text{Ca}^{2+}]_i$ , calculated as described in Methods, was monitored following addition of  $1 \mu\text{M}$  trypsin (*a*) or AP (*b*). The traces shown are representative of six (trypsin) and four (AP) experiments. PDEC, pancreatic duct epithelial cells.

channels, the apical membrane was permeabilized with nystatin, and a  $114\text{-mM}$  luminal-to-serosal  $\text{K}^+$  gradient was generated across the basolateral membrane. In this instance, activation of basolateral  $\text{K}^+$  conductances promotes intra-to-extracellular  $\text{K}^+$  flow across the membrane, resulting in an increased Isc. Serosal, but not luminal, addition of AP also stimulated an increased Isc in this setting (Fig. 6*b*). These findings verify that AP interacts with basolateral PAR-2 to activate basolateral  $\text{K}^+$  conductances.

**Immunostaining.** We localized PAR-2 by immunofluorescence to provide further evidence for its expression on pancreatic duct cells. In the intact pancreas, immunoreactive PAR-2 was prominent on epithelial cells of the intralobular and interlobular ducts in all regions (Fig. 7*a*, arrows). The intensity of the staining of the epithelium was similar for intralobular and interlobular ducts. Examination by confocal microscopy indicated that staining of the epithelial cells of pancreatic ducts was often granular in appearance and that these granules were localized in the basal area of the cell (Fig. 7, *c* and *d*, arrowheads). There was very weak staining of acinar cells in certain regions of the pancreas (not shown). Simultaneous staining with antibodies to PAR-2 and to von Willebrand's factor indicated that PAR-2 was predominantly expressed by epithelial cells of pancreatic ducts rather than endothelial cells of blood vessels, which stained only weakly for PAR-2 (not shown).

In PDEC in culture, PAR-2 immunoreactivity was prominently localized to large vesicles in the basal region of the cells near the nucleus (Fig. 7*e*, arrows) and in numerous small vesicles that were uniformly distributed throughout the cytoplasm. It was not possible to determine unequivocally whether immunoreactive PAR-2 was present at the basolateral membrane of PDEC, possibly

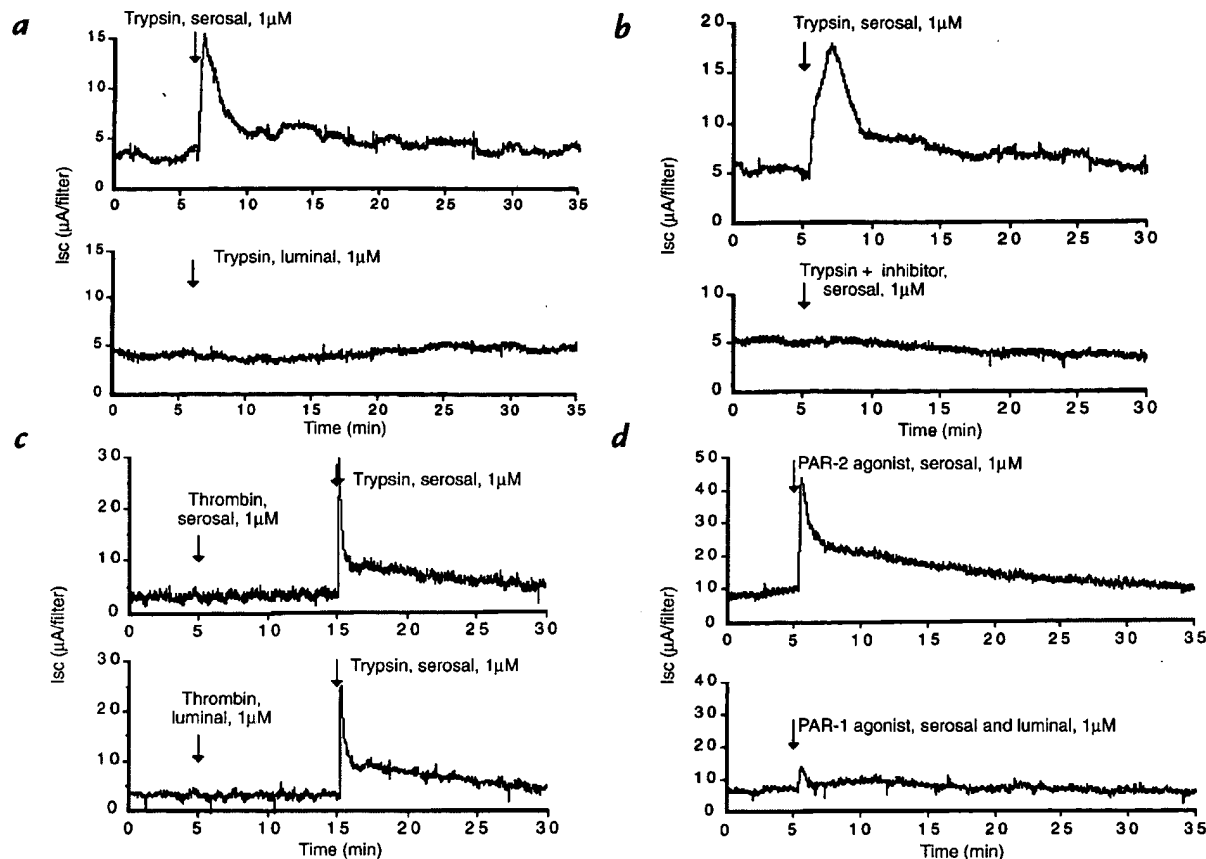


**Figure 5** PAR-2 mediated effects on net electrogenic ion transport across PDEC monolayers. PDEC were mounted in Ussing chambers as described in Methods and the Isc ( $\mu\text{A}/\text{filter}$  of  $0.95\text{ cm}^2$ ) shown. The traces in each panel, obtained from monolayers cultured and studied at the same time, are representative of at least three experiments. (a) After 5 min for baseline determination, trypsin ( $1\text{ }\mu\text{M}$ ) was added to the serosal (top trace) or luminal compartment (bottom trace). (b) After 5 min,  $1\text{ }\mu\text{M}$  of trypsin (top trace) or trypsin pretreated with trypsin inhibitor (bottom trace) was added to the serosal compartment. (c) After 5 min,  $1\text{ }\mu\text{M}$  thrombin was added to the serosal (top trace) or luminal compartment (bottom trace). After an additional 10 min,  $1\text{ }\mu\text{M}$  trypsin was added to the serosal compartment as control. (d) After 5 min,  $1\text{ }\mu\text{M}$  of the PAR-2 agonist, tc-LGRLO-NH<sub>2</sub> (top trace), or PAR-1 agonist, AF(PF)RChaCitY-NH<sub>2</sub> (bottom trace), was added to the serosal compartment (top trace) or to both compartments (bottom trace).

because the close proximity of the filter prevented clear observation of the membranes.

Staining of tissue sections and PDEC was abolished when the primary antibodies were preincubated with the peptides used for immunization (Fig. 7, *b* and *f*) and when the primary antibodies were replaced with an unrelated rabbit IgG (not shown), both indicating specificity. Thus, immunoreactive PAR-2 is expressed by epithelial cells of pancreatic ducts in the intact pancreas, and PDEC continue to express immunoreactive PAR-2 in culture.

## Discussion

PDEC mediate the secretion of fluid and electrolytes by the exocrine pancreas. Trypsin, a proteolytic enzyme secreted by acinar cells, is usually considered to have a role limited to nutrient digestion in the intestinal lumen. In this report, we demonstrate that trypsin can activate ion channels in PDEC by cleaving and triggering PAR-2. Both anatomical and functional evidence indicate that PAR-2 is expressed by PDEC, and our results indicate that trypsin cleaves and triggers PAR-2 on the basolateral

membrane of these cells. Furthermore, PAR-2 activation increases  $[\text{Ca}^{2+}]_i$  and stimulates  $\text{Ca}^{2+}$ -activated  $\text{Cl}^-$  and  $\text{K}^+$  conductances. Thus trypsin, prematurely activated in the inflamed pancreas, may act in a paracrine manner to regulate ion transport by duct cells during pancreatitis. To our knowledge, this is the first direct report that PAR-2 regulates ion channel activity.

Measurements of  $^{125}\text{I}^-$  and  $^{86}\text{Rb}^+$  effluxes to study  $\text{Cl}^-$  and  $\text{K}^+$  channels, validated with T84 colonocytes (23), have been used to demonstrate, on cultured PDEC, the expression of the CFTR  $\text{Cl}^-$  channel sensitive to NPPB but resistant to DIDS, a  $\text{Ca}^{2+}$ -activated  $\text{Cl}^-$  channel sensitive to both DIDS and NPPB, and a  $\text{K}^+$  channel sensitive to charybdotoxin (15, 16). In this report, we observed that trypsin and AP stimulated an  $^{125}\text{I}^-$  efflux that could be inhibited by NPPB and DIDS and a  $^{86}\text{Rb}^+$  efflux that could be inhibited by charybdotoxin. These inhibitory profiles are consistent with the respective mediation of the  $^{125}\text{I}^-$  and  $^{86}\text{Rb}^+$  effluxes by the  $\text{Ca}^{2+}$ -activated  $\text{Cl}^-$  and  $\text{K}^+$  channels previously identified on these PDEC.

Several observations are consistent with the hypothesis

that the secretory effects of trypsin are mediated by PAR-2. First, we specifically localized immunoreactive PAR-2 to pancreatic duct cells in the intact pancreas and in culture, using antibodies to two different epitopes within the extracellular NH<sub>2</sub> terminus in the region of the trypsin cleavage site. Despite the lack of information about the sequence of canine PAR-2, residues around the trypsin cleavage site are highly conserved in mouse, rat, and human (6, 8, 27). Although we cannot exclude the possibility that the antibodies interact with proteins other than PAR-2, our results suggest that staining of duct epithelial cells is specific for this receptor. Immunoreactive PAR-2 was predominantly detected in intracellular pools in PDEC both in intact tissues and in culture. The precise intracellular location of PAR-2 within PDEC remains to be determined, but PAR-2 is present in prominent Golgi stores in cell lines and in enterocytes, which are important for resensitization of cellular responses to proteases (8, 9, 28). Second, the stimulatory effect of trypsin on <sup>125</sup>I<sup>-</sup> efflux and I<sub>sc</sub> was abolished after incubation with a trypsin inhibitor. The dependence of trypsin effect on its proteolytic activity is consistent with trypsin action through PAR-2 cleavage. Third, the action of trypsin's was mimicked by a peptide corresponding to the tethered ligand domain of PAR-2. This observation is compatible with the known effects of trypsin, which cleaves PAR-2 to expose a tethered ligand that binds to and activates the cleaved receptor. Fourth, the PAR-2 agonist, tc-LIGRLO-NH<sub>2</sub> (19–21), also stimulated <sup>125</sup>I<sup>-</sup> efflux from PDEC. Because trypsin also activates the newly discovered PAR-4 and (albeit weakly) the thrombin receptors PAR-1 and PAR-3, the potential role of these receptors was also examined. The lack of a response to thrombin, which activates PAR-1, PAR-2, and PAR-4, and the lack of a response to the PAR-1 agonist, AF(PF)RChaCitY-NH<sub>2</sub>, exclude a secretory role for these receptors. Although these receptors may still be expressed on PDEC, they do not mediate the secretory effects of trypsin.

Our results suggest that the tethered ligand domain of canine PAR-2 may be similar to rodent and human PAR-2 because mouse and rat AP (SLIGRL-NH<sub>2</sub>) was able to activate PAR-2 in dog PDEC. Of note, in dog PDEC, PAR-2 was activated with concentrations of trypsin and AP as low as 0.1 μM. In previous studies, the EC<sub>50</sub>s of trypsin and AP for the rat PAR-2 were, respectively, 25 nM and 17 μM; for the human PAR-2, the corresponding EC<sub>50</sub>s were 2.3 nM and 18 μM (8). These different potencies may reflect slight interspecies differences of PAR-2 or the different biologic responses evaluated.

Confluent PDEC monolayers display transepithelial electrical resistance adequate for electrophysiologic studies. Indeed, using intact PDEC monolayers in Ussing chambers, we defined the polar distributions of the histamine H<sub>1</sub> and purinergic P2Y<sub>2</sub> receptors on PDEC (17, 18); with permeabilized PDEC, we verified the presence of apical Cl<sup>-</sup> and basolateral K<sup>+</sup> conductances (16, 17). In the present investigation, we studied basolaterally permeabilized cells subject to a Cl<sup>-</sup> gradient to show that PAR-2 stimulates apical Cl<sup>-</sup> conductances. Similarly, we use apically permeabilized cells subject to a K<sup>+</sup> gradient to verify that PAR-2 stimulates basolateral K<sup>+</sup> conductances. In addition, with intact PDEC monolayers, the serosal, but not luminal, addition of trypsin and AP stimulated an increased I<sub>sc</sub>, reflecting a net electrogenic ion transport. Consistent with the efflux studies, this effect of trypsin was inhibited by trypsin inhibitor, was reproduced by AP and the PAR-2 agonist, tc-LGRLO-NH<sub>2</sub>, and was not reproduced with thrombin or the PAR-1 agonist, AF(PF)RChaCitY-NH<sub>2</sub>. In addition to confirming that trypsin interacts with PAR-2 in PDEC, these results provide functional evidence for localization of PAR-2 at the basolateral membrane of PDEC, as the effects of trypsin and AP were observed only with application to the serosal surface. At the present time, we have not determined all the component ion transport pathways on PDEC that contribute to the I<sub>sc</sub> generated by intact monolayers. It is

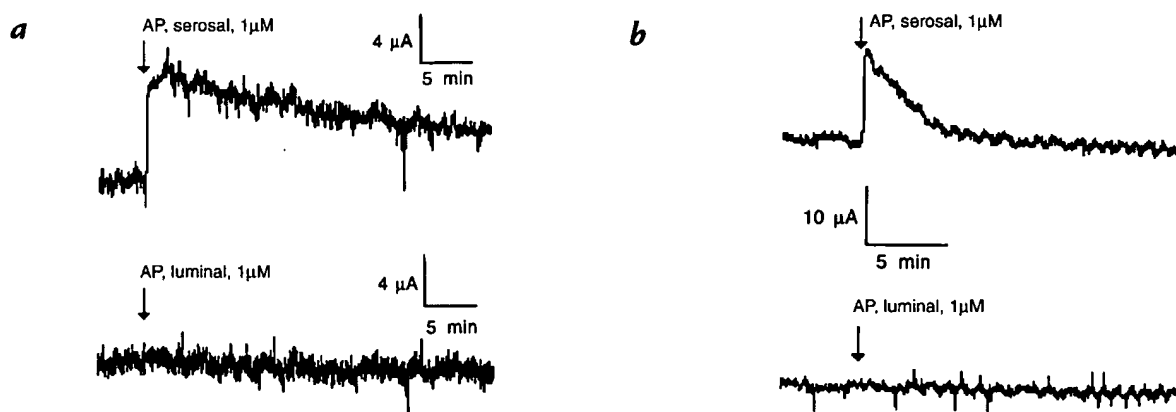
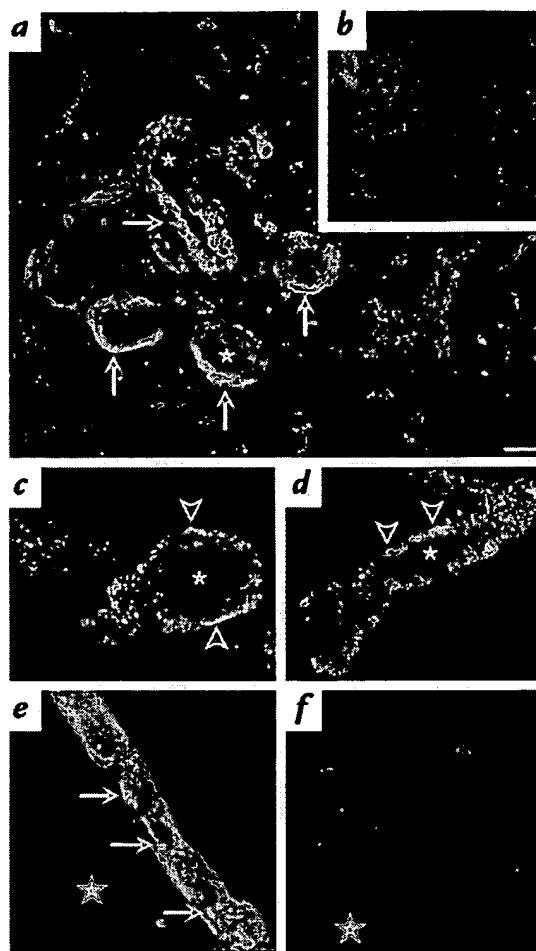


**Figure 6**

Effect of AP on permeabilized PDEC mounted in Ussing chambers. PDEC were mounted in Ussing chambers and either apical or basolateral membrane permeabilized with nystatin. The traces shown in each panel, obtained from monolayers cultured and studied at the same time, are representative of at least three experiments. (a) The basolateral membrane was permeabilized and a 135-mM serosal-to-luminal Cl<sup>-</sup> gradient maintained. The I<sub>sc</sub>, shown on the ordinate (μA/filter of 0.95 cm<sup>2</sup>), reflects the effect of serosal (top trace) or luminal (bottom trace) addition of 1 μM AP on apical membrane Cl<sup>-</sup> conductances. (b) The apical membrane was permeabilized and a 114-mM luminal-to-serosal K<sup>+</sup> gradient maintained. The I<sub>sc</sub>, shown on the ordinate (μA/filter of 0.95 cm<sup>2</sup>), reflects the effect of serosal (top trace) or luminal (bottom trace) addition of 1 μM AP on basolateral membrane K<sup>+</sup> conductances.

**Figure 7**

Localization of PAR-2 in PDEC by immunofluorescence. (a–d) PAR-2 localization in sections of the body of the intact pancreas using antibody PAR-2 B5. Arrows in *a* identify intensely stained PDEC. Arrowheads in *c* and *d* show granular staining in the basal area of the cells. Asterisk denotes the lumen of the pancreatic ducts. (e and f) PAR-2 localization in sections of PDEC grown on Transwell filters using antibody PAR-2 C. The arrows in *e* indicate the prominent intracellular pools of PAR-2 in the basolateral region of the cells. Stars indicate the filter. *b* and *f* are controls in which the antibodies were preabsorbed with the receptor fragments that were used for immunization. Each image is a sum of three to four optical sections cut at intervals of 0.5–0.7  $\mu\text{m}$ . Bar, 50  $\mu\text{m}$  in *a*; 20  $\mu\text{m}$  in *b* and *c*; 28  $\mu\text{m}$  in *d*; 13  $\mu\text{m}$  in *e* and *f*.



possible that additional ion transport pathways may be regulated directly or indirectly by PAR-2. These other pathways may function in concert with  $\text{Cl}^-$  and  $\text{K}^+$  conductances to contribute to the net electrogenic ion transport reflected by an increased  $I_{\text{sc}}$ .

In most systems, PAR-2 couples to phospholipase  $\text{C}_\beta$  forming inositol triphosphate, which mobilizes  $[\text{Ca}^{2+}]_i$  (1). We directly demonstrated that PAR-2 agonists increase  $[\text{Ca}^{2+}]_i$  in PDEC using the  $\text{Ca}^{2+}$ -sensitive probe Indo-1. BAPTA/AM, a cell-permeant  $\text{Ca}^{2+}$  chelator, also inhibited AP-stimulated  $^{125}\text{I}^-$  efflux, which further suggests that PAR-2 couples to  $\text{Ca}^{2+}$  mobilization in PDEC. The ability of PAR-2 activation to increase  $[\text{Ca}^{2+}]_i$  further suggests that the  $\text{Cl}^-$  and  $\text{K}^+$  conductances observed are indeed the  $\text{Ca}^{2+}$ -activated  $\text{Cl}^-$  and  $\text{K}^+$  channels. Of note, DIDS, NPPB, and charybdotoxin did not inhibit this  $[\text{Ca}^{2+}]_i$  response, suggesting that these inhibitors acted directly on the  $\text{Cl}^-$  or  $\text{K}^+$  channels. The increased  $[\text{Ca}^{2+}]_i$  obtained with trypsin and AP are qualitatively slightly different: trypsin elicited a clear biphasic response, whereas the first phase of the response was blunted with AP. This difference may reflect the varying mechanisms by which trypsin and AP activate PAR-2. Exogenous AP may not exactly reproduce the intramolecular interaction between the tethered ligand exposed by trypsin and the cleaved receptor molecule. Furthermore, trypsin may

have additional interactions with PDEC that are not mediated through PAR-2.

Under normal circumstances, it is unlikely that pancreatic trypsin cleaves PAR-2 at the serosal membrane of duct epithelial cells. Although a small amount of trypsinogen is normally activated within the pancreas, trypsinogen is mainly activated in the intestinal lumen by enterokinase. Furthermore, pancreatic juice is contained within the duct lumen. However, the array of proteases that trigger PAR-2 remains to be clarified, and it is possible that trypsinlike proteases from the vasculature and interstitium could cleave serosal PAR-2.

Interaction between trypsin and pancreatic ductal PAR-2 may occur in certain pathologic states. A fraction of trypsinogen is prematurely autoactivated to trypsin within pancreatic acini under normal conditions; defective neutralization of this trypsin is the cause of hereditary pancreatitis (12). Trypsin is also prematurely activated when acinar cell function is impaired, such as in inflammation (10, 29, 30). Trypsin produced in these circumstances may leak into the interstitium from damaged acinar cells and cleave PAR-2 at the basal membrane of PDEC. The resulting increased PDEC secretion may flush toxic components from the inflamed pancreas and, thus, be of benefit.

Further support for a role of PAR-2 in inflammation comes from the observation that PAR-2 agonists strong-

ly stimulate release of arachidonic acid and secretion of prostaglandins from enterocytes (9) and induce expression of cyclooxygenase 2 (Bunnett, N.W., unpublished observations), which generates proinflammatory and mitogenic eicosanoids. Furthermore, PAR-2 is upregulated in human umbilical vein and endothelial cells after stimulation with proinflammatory mediators such as tumor necrosis factor- $\alpha$ , interleukin-1 $\alpha$ , and bacterial lipopolysaccharide (31). Besides trypsin, tryptase also activates PAR-2 (7, 13). Mast cells are present in both normal and inflamed pancreatic tissue (Nguyen, T.D., *et al.*, unpublished observations). It is tempting to postulate that these mast cells may also regulate PDEC ion transport through tryptase release and PAR-2 activation.

In conclusion, this report describes a novel pathway for the regulation of ion transport in PDEC. Besides illustrating the utility of the cultured dog PDEC as a model for ductal secretion, these findings may have important implications for pancreatic pathophysiology.

### Acknowledgments

The authors thank Sum Lee (University of Washington, Seattle, Washington, USA) for his advice on culture and characterization of PDEC, Phillip Ursell (University of California, San Francisco, California, USA) for help with interpreting staining of the pancreas, Rix Kuester (Veterans Affairs Puget Sound Health Care System, Seattle, Washington, USA) for harvesting dog pancreas, and M. Hollenberg and C. Derian for gifts of antibodies and PAR agonists. This research was supported by funds from the Cystic Fibrosis Foundation (to T.D. Nguyen), the Department of Veterans Affairs (to T.D. Nguyen), the National Institute of Arthritis, Diabetes, Digestive and Kidney Diseases (to N.W. Bunnett), and the Crohn's and Colitis Foundation (to N.W. Bunnett). C. Okolo is funded through National Institutes of Health (NIH) GI Training Grant DK-07742, and D.S. Koh is funded by NIH grant NS08174 to Bertil Hille.

1. Dery, O., Corvera, C.U., Steinhoff, M., and Bunnett, N.W. 1998. Proteinase-activated receptors: novel mechanisms of signaling by serine proteases. *Am. J. Physiol.* 274:C1429-1452.
2. Vu, T.-K.H., Hung, D.T., Wheaton, V.I., and Coughlin, S.R. 1991. Molecular cloning of a functional thrombin receptor reveals a novel proteolytic mechanism of receptor activation. *Cell*. 64:1057-1068.
3. Ishihara, H., *et al.* 1997. Protease-activated receptor 3 is a second thrombin receptor in humans. *Nature*. 386:502-506.
4. Xu, W.-F., *et al.* 1998. Cloning and characterization of human protease-activated receptor 4. *Proc. Natl. Acad. Sci. USA*. 95:6642-6646.
5. Kahn, M.L., *et al.* 1998. A dual thrombin receptor system for platelet activation. *Nature*. 394:690-694.
6. Nystedt, S., Emilsson, K., Wahlestedt, C., and Sundelin, J. 1994. Molecular cloning of a potential proteinase activated receptor. *Proc. Natl. Acad. Sci. USA*. 91:9208-9212.
7. Molino, M., *et al.* 1997. Interactions of mast cell tryptase with thrombin receptors and PAR-2. *J. Biol. Chem.* 272:4043-4049.
8. Böhm, S.K., *et al.* 1996. Molecular cloning, expression and potential func-

- tions of the human proteinase-activated receptor-2. *Biochem. J.* 314:1009-1016.
9. Kong, W., *et al.* 1997. Luminal trypsin may regulate enterocytes through proteinase-activated receptor 2. *Proc. Natl. Acad. Sci. USA*. 94:8884-8889.
10. Hofbauer, B., *et al.* 1998. Intra-acinar cell activation of trypsinogen during caerulein-induced pancreatitis in rats. *Am. J. Physiol.* 275:G352-G362.
11. Gorry, M.C., *et al.* 1997. Mutations in the cationic trypsinogen gene are associated with recurrent acute and chronic pancreatitis. *Gastroenterology*. 113:1063-1068.
12. Whitcomb, D.C., *et al.* 1996. Hereditary pancreatitis is caused by a mutation in the cationic trypsinogen gene. *Nat. Genet.* 14:141-145.
13. Corvera, C.U., *et al.* 1997. Mast cell tryptase regulates colonic myocytes through proteinase-activated receptor-2. *J. Clin. Invest.* 100:1383-1393.
14. Oda, D., *et al.* 1996. Dog pancreatic duct epithelial cells: long-term culture and characterization. *Am. J. Pathol.* 148:977-985.
15. Nguyen, T.D., *et al.* 1997. Characterization of two distinct chloride channels in cultured dog pancreatic duct epithelial cells. *Am. J. Physiol.* 272:G172-G180.
16. Nguyen, T.D., and Moody, M.W. 1998. Calcium-activated potassium conductances on cultured non-transformed dog pancreatic duct epithelial cells. *Pancreas*. 17:348-358.
17. Nguyen, T.D., Moody, M.W., Savard, C.E., and Lee, S.P. 1998. Secretory effects of ATP on non-transformed dog pancreatic duct epithelial cells. *Am. J. Physiol.* 275:G104-G113.
18. Nguyen, T.D., Okolo, C., and Moody, M.W. 1998. Histamine stimulates secretion by non-transformed pancreatic duct epithelial cells. *Am. J. Physiol.* 275:G76-G84.
19. Hollenberg, M.D., Saifeddine, M., al-Ani, B., and Kawabata, A. 1997. Proteinase-activated receptors: structural requirements for activity, receptor cross-reactivity, and receptor selectivity of receptor-activating peptides. *Can. J. Physiol. Pharmacol.* 75:832-841.
20. Roy, S.S., Saifeddine, M., Loutzenhiser, R., Triggie, C.R., and Hollenberg, M.D. 1998. Dual endothelium-dependent vascular activities of proteinase-activated receptor-2-activating peptides: evidence for receptor heterogeneity. *Br. J. Pharmacol.* 123:1434-1440.
21. Vergnolle, N., *et al.* 1998. Proteinase-activated receptor 2 (PAR2)-activating peptides: identification of a receptor distinct from PAR2 that regulates intestinal transport. *Proc. Natl. Acad. Sci. USA*. 95:7766-7771.
22. D'Andrea, M., *et al.* 1998. Characterization of proteases activated receptor-2 immunoreactivity in normal human tissues. *J. Histochem. Cytochem.* 46:1-8.
23. Venglarik, C.J., Bridges, R.J., and Frizzell, R.A. 1990. A simple assay for agonist-regulated Cl and K conductances in salt-secreting epithelial cells. *Am. J. Physiol.* 259:C358-C364.
24. Nguyen, T.D., and Canada, A.T. 1994. Modulation of human colonic T84 cell secretion by hydrogen peroxide. *Biochem. Pharmacol.* 47:403-410.
25. Grynkiewicz, G., Peonie, M., and Tsien, R.Y. 1985. A new generation of Ca<sup>2+</sup> indicators with greatly improved fluorescence properties. *J. Biol. Chem.* 260:3440-3450.
26. Grady, E.F., *et al.* 1996. Endocytosis and recycling of NK1 tachykinin receptors in enteric neurons. *Neuroscience*. 16:1239-1254.
27. Saifeddine, M., Al-Ani, B., Chen, C., Wang, L., and Hollenberg, M. 1996. Rat proteinase-activated receptor-2 (PAR-2): cDNA sequence and activity of receptor-derived peptides and in gastric and vascular tissue. *Br. J. Pharm.* 118:521-530.
28. Böhm, S.K., *et al.* 1996. Mechanisms of desensitization and resensitization of proteinase-activated receptor-2. *J. Biol. Chem.* 271:22003-22016.
29. Yamaguchi, H., Kimura, T., Mimura, K., and Nawata, H. 1989. Activation of proteases in cerulein-induced pancreatitis. *Pancreas*. 4:565-571.
30. Geokas, M.C., and Rinderknecht, H. 1974. Free proteolytic enzymes in pancreatic juice of patients with acute pancreatitis. *Am. J. Dig. Dis.* 19:591-598.
31. Nystedt, S., Ramakrishnan, V., and Sundelin, J. 1996. The proteinase-activated receptor 2 is induced by inflammatory mediators in human endothelial cells. Comparison with the thrombin receptor. *J. Biol. Chem.* 271:14910-14915.

# Intestinal Type 2 Proteinase-Activated Receptors: Expression in Opioid-Sensitive Secretomotor Neural Circuits That Mediate Epithelial Ion Transport<sup>1</sup>

BENEDICT T. GREEN, NIGEL W. BUNNETT, ANJALI KULKARNI-NARLA, MARTIN STEINHOFF, and DAVID R. BROWN

Department of Veterinary Pathobiology, College of Veterinary Medicine, University of Minnesota, St. Paul, Minnesota (B.T.G., A.K.-N., D.R.B.); and Departments of Physiology and Surgery, School of Medicine, University of California, San Francisco, California (N.W.B., M.S.)

Accepted for publication June 9, 2000 This paper is available online at <http://www.jpet.org>

## ABSTRACT

Trypsin and mast cell tryptase cleave within the extracellular N terminus of proteinase-activated receptor-2 (PAR-2), exposing a tethered ligand (SLIGRL) that binds and activates the cleaved receptor. We examined the neuronal expression of PAR-2 and its role in intestinal ion transport. Short-circuit current elevations in response to trypsin or the receptor-activating peptide SLIGRL-NH<sub>2</sub> were measured in sheets of mucosa-submucosa from porcine ileum. SLIGRL-NH<sub>2</sub> or trypsin rapidly elevated short-circuit current after their contraluminal application with respective 50% effective concentrations of 184 and 769 nM. Their actions were attenuated after contraluminal administration of the neuronal conduction blocker saxitoxin (0.1 μM); the cyclooxygenase inhibitor indomethacin (10 μM); or the Na<sup>+</sup>/K<sup>+</sup>/Cl<sup>−</sup> cotransport inhibitor furosemide (10 μM), but not by atropine (0.1 μM), a muscarinic cholinergic antagonist. In addition, soybean trypsin inhibitor (5 μg/ml) reduced mucosal

responses to trypsin. The δ-opioid agonist [D-Pen<sup>2,5</sup>]-enkephalin (0.1 μM) inhibited trypsin action, an effect that was prevented by naltrindole (0.1 μM), a δ-opioid antagonist. PAR-2 immunofluorescence was localized in the mucosa using a receptor-specific antibody. PAR-2-like immunoreactivity was detected in myenteric and submucosal neurons, nerve fibers innervating ileal smooth muscle and mucosa, and in enteroendocrine cells. Some neurons coexpressed PAR-2 and choline acetyltransferase-like immunoreactivity. These results indicate that PAR-2 is expressed on cholinergic and noncholinergic submucosal neurons in porcine ileum. PAR-2 agonists stimulate active anion secretion by a neurogenic mechanism that is modulated by prostanoids and opioids. These receptors may have a potentially important role in intestinal neuroimmunomodulation.

Because of its direct contact with the external environment and its vast surface area, the mammalian gastrointestinal (GI) tract is vulnerable to colonization by many pathogens. To combat enteric pathogens such as *Salmonella*, the GI tract has evolved several nonspecific defenses that are mediated by mast cell products. Activated mast cells release inflammatory mediators that include proteinases, eicosanoids, histamine, and cytokines (Marone et al., 1998). Through its dilution of luminal pathogens and facilitation of the movement of secretory IgA, defensins, mucins, and other protective factors to the surface of the intestinal epithelium, active transepithelial anion secretion is an important component of primary mucosal defense. It can be evoked by several classes

of inflammatory mediators acting at receptors located on enteric neurons (Perdue and McKay, 1994). There is a particularly strong association between mucosal mast cells and enteric secretomotor neurons in the neuroimmune modulation of intestinal ion transport (Berin et al., 1999).

Proteinase-activated receptors (PARs) are members of a newly discovered subfamily of G-protein-coupled receptors that play important roles in responses to injury, including inflammation and repair (Déry et al., 1998; Hollenberg, 1999). Proteinases cleave within the extracellular N-terminal tails of PARs to expose tethered ligand domains that bind to and activate the cleaved receptors. Thrombin cleaves and activates PAR-1, PAR-3, and PAR-4, which mediate platelet aggregation and the inflammatory and proliferative effects of thrombin in multiple tissues (Déry et al., 1998; Hollenberg, 1999). In the mouse and rat, trypsin and mast cell tryptase cleave PAR-2 to expose the tethered ligand sequence SLIGRL-NH<sub>2</sub>. PAR-2 is highly expressed in the GI tract where it has been detected in enterocytes (Kong et al., 1997), myo-

Received for publication April 11, 2000.

<sup>1</sup> This study was funded in part by National Institutes of Health Grant DA-10200 (to D.R.B.) and NIH Grants DK-57840, DK-39957, and DK-43207, and an award from the Crohn's and Colitis Foundation of America (to N.W.B.). Salary support for B.T.G. and A.K.-N. was provided by Alcohol, Drug Abuse, and Mental Health Administration/National Institute on Drug Abuse Psychoneuroimmunology and Substance Abuse training Grant T32 DA07239.

**ABBREVIATIONS:** GI, gastrointestinal; PAR, proteinase-activated receptor; DPDPE, [D-Pen<sup>2,5</sup>]-enkephalin; Isc, short-circuit current; G<sub>t</sub>, tissue conductance; SBTI, soybean trypsin inhibitor; ChAT, choline acetyltransferase; PGP9.5, protein gene product 9.5.



cytes (Corvera et al., 1997), and enteric neurons (Corvera et al., 1999). Trypsin, trypsinase, and analogs of the tethered ligand (i.e., activating peptides) stimulate eicosanoid secretion in intestinal epithelial cells (Kong et al., 1997), inhibit colonic motility (Corvera et al., 1997), and excite enteric neurons (Corvera et al., 1999) and spinal afferent neurons (Steinhoff et al., 2000).

In the rat jejunum, trypsin and SLIGRL-NH<sub>2</sub>, but not thrombin, have been found to stimulate active ion transport (Vergnolle et al., 1998). It has not been determined whether these effects extend to other animal species or intestinal segments. Moreover, the mechanisms underlying PAR-2-mediated intestinal secretion have not been documented. Because it can be activated by mast cell trypsinase, PAR-2 may be involved in intestinal inflammatory reactions to infection or tissue damage. Therefore, in this investigation we tested the hypothesis that PAR-2 is expressed on enteric neurons that mediate active anion secretion. Moreover, we examined the involvement of prostanoids in the effects associated with PAR-2 activation. Finally, because  $\delta$ -opioid receptors associated with secretomotor neural pathways inhibit active secretion in the porcine intestinal mucosa (Quito and Brown, 1991), the ability of a  $\delta$ -opioid receptor agonist to modify PAR-2-mediated intestinal secretion was investigated.

## Materials and Methods

**Chemicals and Drugs.** Trypsin (TPCK treated) was obtained from Worthington Biochemical Corp. (Freehold, NJ). Peptidase inhibitors (captopril, amastatin, and phosphoramidon), atropine, indomethacin, furosemide, soybean trypsin inhibitor, and carbamylcholine chloride (carbachol) were obtained from Sigma Chemical Co. (St. Louis, MO). Saxitoxin and naltrindole were purchased from Research Biochemicals International (Natick, MA); [D-Pen<sup>2,5</sup>]-enkephalin (DPDPE) was purchased from Peninsula Laboratories (Belmont, CA). The PAR-2 agonist SLIGRL-NH<sub>2</sub> and its reversed peptide analog LRGILS-NH<sub>2</sub> were synthesized by solid phase methods and purified by HPLC.

**Animals.** Yorkshire pigs of each sex, 6 to 8 weeks old, were obtained from the University of Minnesota Research Animal Resources and University of Minnesota Agricultural Experiment Station (Rosemount, MN) breeding facilities. Pigs received nonmedicated pig feed ad libitum and were not fasted before sacrifice. The pigs were initially sedated with an i.m. injection of tiletamine hydrochloride-zolazepam (Telazol, 8 mg/kg; Fort Dodge Laboratories, Fort Dodge, IA), in combination with xylazine (8 mg/kg). The animals were euthanized by barbiturate overdose (Beuthanasia-D, 30 mg/lb i.v.; Schering-Plough Animal Health Corp., Kenilworth, NJ) in accordance with approved University of Minnesota Animal Care Committee protocols. A midline laparotomy was performed, and a 20- to 30-cm segment of ileum was obtained that extended from the ileocecal junction to 10 cm oral to the termination of the ileocecal ligament. Each intestinal segment was excised along its antimesenteric aspect, intestinal contents removed, and the tissue was placed in ice-cold oxygenated physiological salt solution modified to approximate the composition of porcine extracellular fluid (Chandan et al., 1991).

**Measurement of Transepithelial Ion Transport.** The circular and longitudinal muscle layers were removed by blunt dissection, and sheets of ileal mucosa with attached submucosa were mounted in Ussing chambers (flux area = 1 or 2 cm<sup>2</sup>) under short-circuit conditions. The tissues were continuously bathed at 39°C (porcine core temperature) in oxygenated physiological salt solution with 10 mM mannitol or D-glucose added to the luminal or contraluminal sides of the tissue, respectively. Short-circuit current (Isc) and open-circuit transmural potential difference were measured across muco-

sal sheets, and tissue conductance (G<sub>t</sub>) was calculated from these electrical parameters by Ohm's law as previously described (Chandan et al., 1991). Tissues were incubated for 25 to 35 min until the baseline Isc stabilized, and drugs and other substances were then added to either the luminal or contraluminal side of each sheet. Changes in Isc and potential difference were measured after drug administration. At the end of each experiment after Isc returned to baseline values, 10 mM glucose was added to the luminal aspect of each tissue, and subsequent changes in mucosal Isc were measured in response to glucose-coupled sodium absorption to assess tissue viability.

In determinations of concentration-effect relationships with SLIGRL-NH<sub>2</sub> or its reversed analog LRGILS-NH<sub>2</sub>, tissues were pretreated with a cocktail of protease inhibitors containing 10  $\mu$ M captopril, 100  $\mu$ M amastatin, and 1  $\mu$ M phosphoramidon. The cocktail was added to the contraluminal side 5 min before peptide addition. In some experiments, 5  $\mu$ g/ml soybean trypsin inhibitor (SBTI), 0.1  $\mu$ M saxitoxin, 10  $\mu$ M indomethacin, or 10  $\mu$ M furosemide was added to the contraluminal side 5 min before trypsin or SLIGRL-NH<sub>2</sub> addition. In other experiments, tissues were pretreated contraluminally with 100 nM DPDPE for 5 min before trypsin addition; in some cases, the  $\delta$ -opioid antagonist naltrindole was present in the contraluminal bathing medium 5 min before DPDPE was added.

**Localization of PAR-2 Immunoreactivity.** To localize PAR-2 immunoreactivity, an antiserum to PAR-2-B5, raised in rabbits to a peptide fragment of rat PAR-2 (<sup>30</sup>GPNSKGR<sup>1</sup>SLIGRLDT<sup>46</sup>P-YGGC; arrow denotes trypsin cleavage site) and conjugated to keyhole limpet hemocyanin (Saifeddine et al., 1996) was generously provided by Dr. Morley D. Hollenberg (University of Calgary, Canada). To identify cholinergic neurons, an antibody to choline acetyltransferase (ChAT) was purchased from Chemicon International, Inc. (Temecula, CA). Protein gene product 9.5 (PGP9.5; Chemicon International, Inc.) was used as a general neuronal marker. Donkey anti-rabbit IgG-indocarbocyanine- and donkey anti-goat IgG-fluorescein isothiocyanate-conjugated secondary antibodies were purchased from Jackson ImmunoResearch Laboratories, Inc. (West Grove, PA).

Ileal segments from three pigs were isolated and immersed in ice-cold 2% paraformaldehyde in PBS at pH 7.4 for 2 h. All tissues were cryoprotected in increasing (10–30%) concentrations of sucrose in PBS, embedded in Tissue Tek O.C.T. compound (Baxter Healthcare Corp., McGaw Park, IL), and frozen. Coronal sections of ileum (15  $\mu$ m in thickness) were thaw-mounted onto Superfrost-plus slides (Fisher Scientific, Pittsburgh, PA) and stored at –20°C until use.

A standard immunofluorescence staining protocol was followed. Briefly, tissue sections were rehydrated in PBS (pH 7.4) for 15 min, and then incubated in 0.4% Triton X-100 (Sigma Chemical Co.) and 2% BSA (Sigma Chemical Co.) in PBS for 30 min to block nonspecific binding. Sections were simultaneously incubated in antibodies to PAR-2-B5 (1:250 dilution) and ChAT (1:30 dilution) in 0.4% Triton X-100 and 2% BSA overnight at 4°C. After three rinses in PBS, sections were further incubated with appropriate secondary antibodies (donkey anti-rabbit indocarbocyanine-conjugated IgG at 1:400 dilution; or donkey anti-goat fluorescein isothiocyanate-conjugated IgG at 1:40 dilution) in PBS for 1 h in the dark. After three rinses in PBS for 15 min, coverslips were mounted with Vectashield (Vector Laboratories, Burlingame, CA), and the edges were sealed with nail polish. Antibody to PGP9.5 (1:150 dilution, overnight incubation) was used as general neuronal marker to confirm the neuronal morphology.

Controls consisted of omission of primary antibody from the staining protocol, replacing the primary antibody with another unrelated primary antibody or preabsorbing the primary antibodies against the antigen that resulted in complete absence of specific immunoreactivity. Omission of PAR-2 antibody resulted in absence of specific immunoreactivity pattern. ChAT immunoreactivity was substantially reduced when anti-ChAT antiserum was preincubated with 2  $\mu$ g/ml of ChAT antigen; however, a nonspecific punctate staining pattern persisted.

Sections were scanned using a Bio-Rad confocal laser scanning microscope (CLSM, model 1000) that was attached to a Nikon fluorescence microscope. Images were obtained using Comos software (version 6.05.8; Comos Bio-Rad, Hercules, CA) and further processed using NIH Image (version 1.59) and Adobe Photoshop (version 4.0) software.

**Data Analysis.** Data are expressed as mean  $\pm$  S.E. of peak changes in *I*<sub>sc</sub> relative to baseline values occurring in response to drug administration. Tissues from at least three pigs were used in all experiments, with the exception of experiments with LRGILS-NH<sub>2</sub>, which used three tissues from two pigs. Determinations of agonist concentration-effect relationships through nonlinear regression methods and statistical analyses of trypsin and SLIGRL-NH<sub>2</sub> data were performed using the PRISM computer software program (GraphPad, San Diego, CA). Comparisons between a single control mean and treatment mean were made with an unpaired, two-tailed Student's *t* test; comparisons of a control mean with multiple treatment means were made by ANOVA followed by Tukey's test. In all cases, the limit for statistical significance was set at *P* < .05.

## Results

**Effects of Trypsin and the PAR-2-Activating Peptide SLIGRL-NH<sub>2</sub> on Transepithelial Conductance and *I*<sub>sc</sub>.** After their contraluminal addition at single concentrations, trypsin and SLIGRL-NH<sub>2</sub> produced rapid increases in *I*<sub>sc</sub>. Contraluminally applied LRGILS-NH<sub>2</sub>, however, did not significantly affect either *I*<sub>sc</sub> or *G*<sub>t</sub> (Fig. 1). When added in cumulatively increasing contraluminal concentrations, trypsin and SLIGRL-NH<sub>2</sub> were equieffective in elevating *I*<sub>sc</sub> (Fig. 2). Maximal mucosal responses to cumulative additions of trypsin or SLIGRL-NH<sub>2</sub> were not significantly different from those produced by the administration of these substances at single concentrations (based on comparisons of responses to 1.0  $\mu$ M trypsin or 0.1  $\mu$ M SLIGRL-NH<sub>2</sub>; one-way ANOVA,

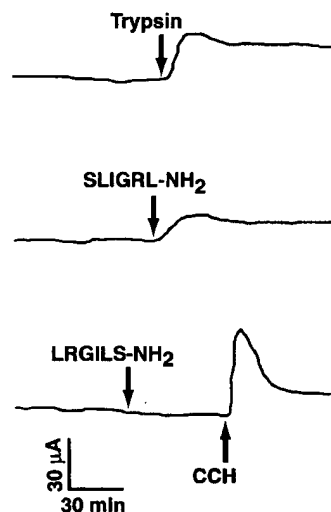


**Fig. 1.** Chart records depicting the effects of trypsin (1.0  $\mu$ M), the PAR-2-activating peptide SLIGRL-NH<sub>2</sub> (0.1  $\mu$ M), and the reverse peptide analog LRGILS-NH<sub>2</sub> (0.1  $\mu$ M) on *I*<sub>sc</sub> after their contraluminal addition to porcine ileal mucosal sheets. Total flux area of chambers was 1 cm<sup>2</sup>. The records are representative of mucosal responses in 7 tissues from 6 pigs for trypsin, 21 tissues from 7 pigs for SLIGRL-NH<sub>2</sub>, and 3 tissues from 2 pigs for LRGILS-NH<sub>2</sub>. As an additional control, 10  $\mu$ M carbachol (CCH) was added to the LRGILS-NH<sub>2</sub>-treated tissue to confirm tissue viability. Average respective changes in *I*<sub>sc</sub> and *G*<sub>t</sub> produced by these substances were as follows: trypsin =  $36 \pm 6 \mu\text{A} \cdot \text{cm}^{-2}$  and  $-3 \pm 1 \text{mS} \cdot \text{cm}^{-2}$ ; SLIGRL-NH<sub>2</sub> =  $13 \pm 3 \mu\text{A} \cdot \text{cm}^{-2}$  and  $-6 \pm 3 \text{mS} \cdot \text{cm}^{-2}$ ; and LRGILS-NH<sub>2</sub> =  $0 \pm 1 \mu\text{A} \cdot \text{cm}^{-2}$  and  $2 \pm 1 \text{mS} \cdot \text{cm}^{-2}$ . mS, millisiemens.

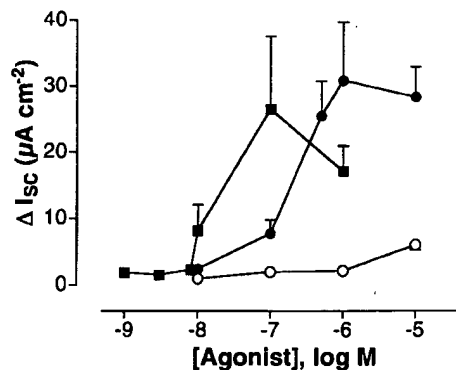


**Fig. 2.** Cumulative concentration-effect relationships for trypsin and SLIGRL-NH<sub>2</sub> in porcine ileal mucosa. Trypsin was added to either the contraluminal (●) or luminal (○) aspects of mucosal sheets in increasing concentrations; SLIGRL-NH<sub>2</sub> (■) was only administered contraluminally. Each data point represents the mean  $\pm$  S.E. of responses in 16 tissues from 8 pigs for contraluminal trypsin, 7 tissues from 3 pigs for luminal trypsin, and 14 tissues from 7 pigs for contraluminal SLIGRL-NH<sub>2</sub>. The mean 50% effective concentrations for contraluminal SLIGRL-NH<sub>2</sub> and trypsin were  $184 \pm 67$  and  $769 \pm 272 \text{ nM}$  (*P* = .053, two-tailed unpaired *t* test).

*P* > .05). Relative to its effects after contraluminal addition, luminally applied trypsin was less potent and effective in elevating *I*<sub>sc</sub> (Fig. 2).

Mucosal responses to the contraluminal addition of trypsin at 10  $\mu$ M were reduced in tissues pretreated with 5  $\mu$ g/ml SBTI added to the contraluminal bathing medium (mean  $\Delta I_{sc}$  after trypsin in absence and presence of SBTI =  $33 \pm 5$  and  $10 \pm 6 \mu\text{A} \cdot \text{cm}^{-2}$ , respectively; one tissue from each of three to four pigs, *P* = .01).

**Mechanism of Trypsin and SLIGRL-NH<sub>2</sub> Action.** To elucidate the mechanisms underlying the effects of trypsin and SLIGRL-NH<sub>2</sub> on *I*<sub>sc</sub>, tissues were pretreated with Na<sup>+</sup>/K<sup>+</sup>/Cl<sup>-</sup> cotransport blocker furosemide, the neuronal conduction blocker saxitoxin, or the cyclooxygenase inhibitor indomethacin; these substances were added to the contraluminal aspect of mucosal sheets (Fig. 3). Pretreatment of the tissues with 10  $\mu$ M furosemide before trypsin or SLIGRL-NH<sub>2</sub> addition significantly decreased subsequent mucosal responses to trypsin by 82% and SLIGRL-NH<sub>2</sub> by 51%. Saxitoxin at 0.1  $\mu$ M reduced subsequent mucosal responses to trypsin by 84% and SLIGRL-NH<sub>2</sub> by 80%. Indomethacin at 10  $\mu$ M significantly decreased subsequent mucosal responses to trypsin by 97% and SLIGRL-NH<sub>2</sub> by 49% (Fig. 3).

The effects of trypsin or SLIGRL-NH<sub>2</sub> on *I*<sub>sc</sub> remained unaffected in tissues pretreated with the muscarinic cholinergic antagonist atropine at a contraluminal concentration of 0.1  $\mu$ M. However, secretory responses to 10  $\mu$ M carbachol, a cholinergic agonist, were absent in these tissues (Fig. 4).

The selective  $\delta$ -opioid receptor agonist DPDPE had minimal effects on baseline *I*<sub>sc</sub> after its contraluminal addition at 0.1  $\mu$ M, but it reduced mucosal responses to trypsin by 66%. This inhibitory action of DPDPE was not produced in tissues pretreated with an equimolar concentration of the selective  $\delta$ -opioid receptor antagonist naltrindole (Fig. 5).

**Immunohistochemical Localization of PAR-2 Immunoreactivity.** PAR-2 immunoreactivity was localized in neurons within the myenteric plexus and the external and internal submucosal plexuses. These neurons exhibited a relatively diffuse pattern of immunoreactivity compared with

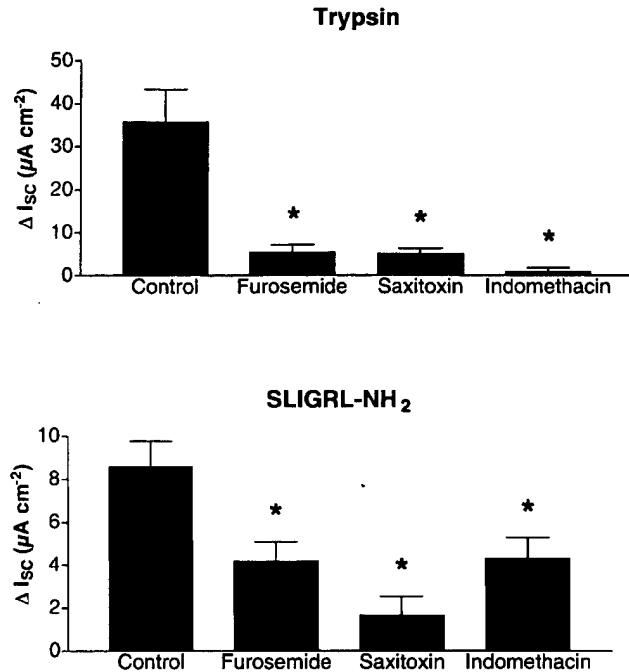


**Fig. 3.** Effects of inhibitors on mucosal responses to contraluminal addition of 1  $\mu M$  trypsin (top) or SLIGRL-NH<sub>2</sub> (bottom). Tissues were contraluminally pretreated with furosemide (10  $\mu M$ ), saxitoxin (0.1  $\mu M$ ), or indomethacin (10  $\mu M$ ) for 5 min before the contraluminal addition of trypsin or SLIGRL-NH<sub>2</sub>. Dimethyl sulfoxide, the vehicle for indomethacin and furosemide, was without effect (data not shown). Each column represents the mean  $\pm$  S.E. of  $I_{sc}$  elevations in 6 to 11 tissues from 5 to 6 pigs. \* $P < .05$  relative to agonist effect in tissue controls untreated with blockers, Tukey's test.

neurons displaying PGP 9.5 immunoreactivity. In all preparations, however, PAR-2-immunoreactive neurons and fibers also expressed PGP 9.5 immunoreactivity. Intense immunoreactivity for PAR-2 was observed in several neurons, although some neurons displayed relatively less intense PAR-2 immunoreactivity. Immunoreactivity for the cholinergic marker ChAT was highly colocalized with PAR-2 immunoreactivity in myenteric and submucosal neurons (Fig. 6). In contrast, fibers immunoreactive for PAR-2 that innervated circular smooth muscle did not express ChAT immunoreactivity. In the ileal epithelium, intense PAR-2 immunoreactive cells were observed scattered in the villus epithelium; these had the appearance of open-type enteroendocrine cells and did not display ChAT immunoreactivity (Fig. 7A). Relatively thin and sometimes varicose PAR-2-immunoreactive nerve fibers were localized at the base of the villous epithelium (Fig. 7B). In comparison, ChAT-immunoreactive fibers were mostly situated in the midregion of villi; some of the thicker fibers also displayed PAR-2 immunoreactivity.

### Discussion

Our results show that application of the PAR-2 agonist SLIGRL-NH<sub>2</sub> and trypsin to the contraluminal side of the porcine ileum produces increases in  $I_{sc}$  that are due to anion secretion because furosemide, an inhibitor of basolateral chloride loading into epithelial cells, inhibited these effects. PAR-2 agonists stimulate active anion transport by a neurogenic mechanism because saxitoxin also inhibited this stim-

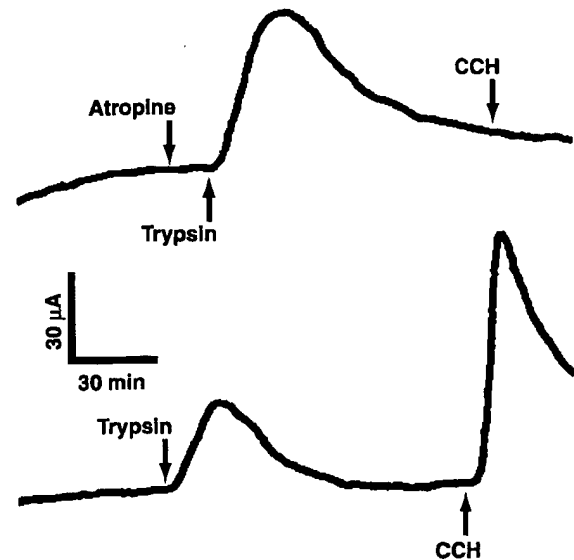


**Fig. 4.** Effect of atropine on trypsin action. Representative chart tracings depict the lack of effect of atropine (0.1  $\mu M$ , contraluminal addition) on mucosal  $I_{sc}$  responses to the contraluminal addition of 1  $\mu M$  trypsin (top). The effect of trypsin in the absence of atropine is shown (bottom) for comparison. Carbachol (CCH, 10  $\mu M$ , contraluminal addition) was included at the end of each experiment to confirm blockade of muscarinic cholinergic receptors. Similar results were obtained with SLIGRL-NH<sub>2</sub>. Mean changes in  $I_{sc}$  for trypsin alone and after atropine were  $15 \pm 2$  and  $15 \pm 4 \mu A \cdot cm^{-2}$ , respectively ( $n = 7-8$  tissues from three pigs). Mucosal responses to 1  $\mu M$  SLIGRL-NH<sub>2</sub> alone and in the presence of atropine were  $9 \pm 1$  and  $8 \pm 2 \mu A \cdot cm^{-2}$ , respectively ( $n = 6-8$  tissues from four pigs).

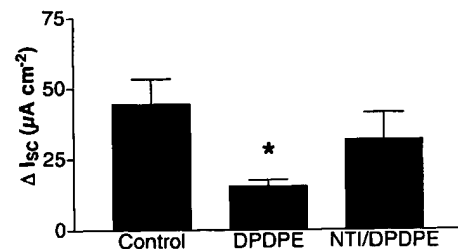


**Fig. 5.** Inhibition of trypsin action by the  $\delta$ -opioid agonist DPDPE and prevention of this effect by the  $\delta$ -opioid antagonist naltrindole (NTI). Tissues were contraluminally pretreated with DPDPE (0.1  $\mu M$ ) 5 min before the contraluminal addition of trypsin. Some tissues were contraluminally pretreated with naltrindole (0.1  $\mu M$ ) 5 min before DPDPE addition (NTI/DPDPE). Each column represents the mean  $\pm$  S.E. of  $I_{sc}$  elevations in 10 to 16 tissues from 9 pigs. \* $P < .05$  relative to trypsin effect in control tissues untreated with DPDPE or naltrindole, Tukey's test.

ulation. Moreover, a large proportion of submucosal neurons and nerve fibers that were situated in proximity to the basolateral membrane of enterocytes expressed immunoreactive PAR-2. Mast cells containing tryptase are closely associated with nerve fibers in the normal and inflamed human intestine (Berin et al., 1999). Thus, our results support the hypothesis that tryptase, which is released from mast cells when they degranulate, cleaves PAR-2 on submucosal neurons to trigger the release of unidentified neurotransmitters that stimulate fluid and electrolyte secretion from enterocytes. This novel mechanism of regulation of anion secretion by proteases and their receptors may serve to protect the intestinal mucosa from pathogen invasion.

Trypsin and the PAR-2-specific-activating peptide SLI-

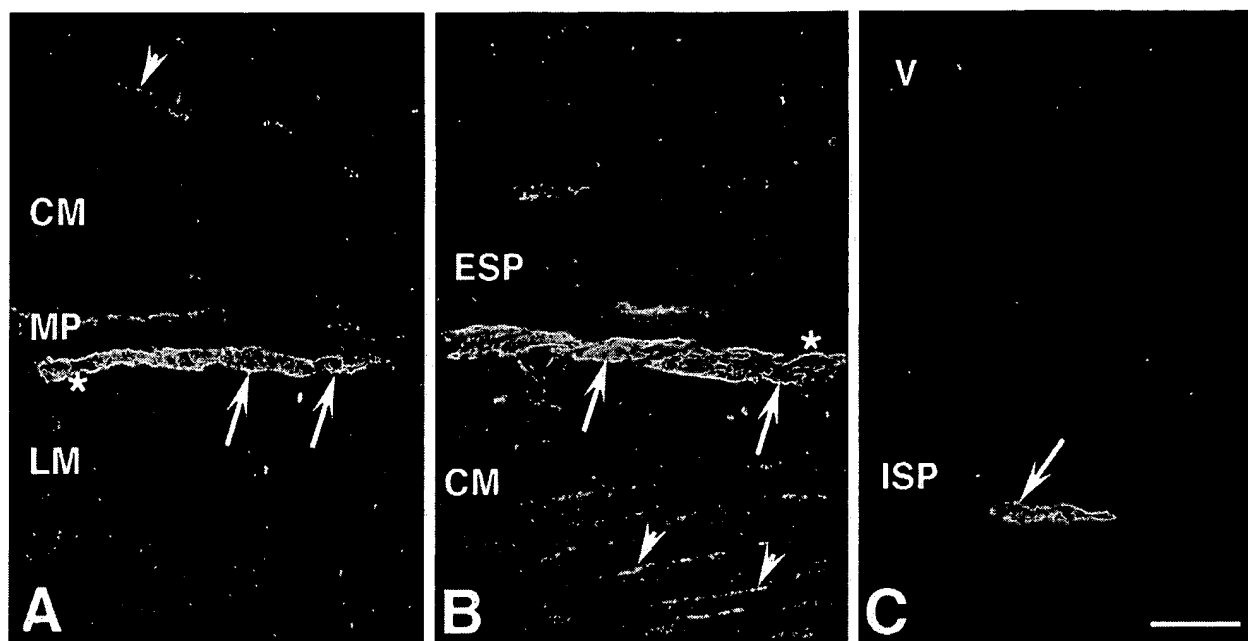


**Fig. 6.** Localization of PAR-2 and ChAT immunoreactivities in porcine ileum. **A**, intense PAR-2 and ChAT immunoreactivities are colocalized in neurons (\*, yellow) of the myenteric plexus. Due to the diffuse nature of the immunoreactivity, relatively weak PAR-2 immunoreactivity is observed in some neurons (arrows). PAR-2-immunoreactive fibers (arrowhead, red) that are not colocalized with ChAT-immunoreactive fibers are seen in the circular muscle. **B**, cluster of large neurons in the ganglionated external submucosal plexus that exhibits colocalization (yellow hue) of PAR-2 (red) and ChAT (green) immunoreactivities. PAR-2 and ChAT immunoreactivities are highly colocalized (\*); however, weak PAR-2 immunoreactivity in the presence of ChAT immunoreactivity is also seen, which imparts a slightly greenish hue in some neurons (arrows). PAR-2-immunoreactive fibers (arrowheads) are seen in the circular muscle. **C**, colocalization of PAR-2 and ChAT immunoreactivities in neurons (arrow) of the external submucosal plexus. CM, circular muscle; ESP, external submucosal plexus; ISP, internal submucosal plexus; LM, longitudinal muscle; MP, myenteric plexus; V, villi. Scale bars in **A** to **C**, 50  $\mu$ m.

GRL-NH<sub>2</sub> increased Isc after their contraluminal addition to ileal mucosa sheets with potencies that were at least an order of magnitude higher than reported for their actions in other intestinal and nonintestinal preparations *in vitro* (Nystedt et al., 1994; Santulli et al., 1995; Bohm et al., 1996a,b; Corvera et al., 1997; Vergnolle et al., 1998). Over the course of the entire investigation, however, mucosal responses to SLIGRL-NH<sub>2</sub> tended to display some interanimal variability (cf. Figs. 2 and 3). Its actions were nevertheless specific because a peptide bearing a reversed amino acid sequence (LRGILS-NH<sub>2</sub>) was inactive. Although trypsin has been found to be more potent than SLIGRL-NH<sub>2</sub> in several previous reports *in vitro* (Nystedt et al., 1994; Santulli et al., 1995; Bohm et al., 1996a,b; Corvera et al., 1997), its potency was not significantly different from that of SLIGRL-NH<sub>2</sub> in the porcine ileal mucosa, a finding that may suggest that the activating sequence or ligand-binding domains of the porcine PAR-2 differ from that characterized in rodents or that a second subtype of SLIGRL-NH<sub>2</sub>-preferring PAR-2 is expressed in the intestine, as previously hypothesized (Vergnolle et al., 1998). Mucosal responses to trypsin or SLIGRL-NH<sub>2</sub> at a fixed concentration did not differ after the contraluminal addition of these agonists at single or increasing cumulative concentrations. Although the effects of SLIGRL-NH<sub>2</sub> were measured in porcine ileal mucosa pretreated with a protease inhibitor cocktail, a recent report suggests that SLIGRL-NH<sub>2</sub> is not susceptible to rapid protease degradation. Its ability to alter ion transport in rat jejunum remained unaltered in the presence or absence of protease inhibitors (Vergnolle et al., 1998).

The Isc elevations occurring in response to the PAR-2 agonist SLIGRL-NH<sub>2</sub> or by trypsin may be attributable to

active anion secretion because the effects of trypsin and, to a lesser extent, SLIGRL-NH<sub>2</sub> were markedly reduced by furosemide, an inhibitor of basolateral chloride loading in enterocytes. This finding is in agreement with that of Vergnolle et al. (1998) who reported that mucosal responses to SLIGRL-NH<sub>2</sub> were attenuated in rat jejunal mucosal sheets bathed in chloride-free buffer. The furosemide-resistant portion of the Isc response to the PAR-2 agonists might be attributable to bicarbonate secretion or furosemide-insensitive chloride transport. In contrast to this previous report, the prosecretory actions of trypsin and SLIGRL-NH<sub>2</sub> in porcine ileum were inhibited by saxitoxin, a neuronal conduction blocker. This result, in combination with our immunohistochemical data, supports the hypothesis that PAR-2 is present on submucosal neurons that release prosecretory neurotransmitter substances. The neural circuits expressing PAR-2 do not appear to contain muscarinic cholinergic synapses because mucosal responses to SLIGRL-NH<sub>2</sub> or trypsin were unaltered by atropine, administered at a contraluminal concentration that was sufficient to antagonize the secretory actions of the cholinergic agonist carbachol (Chandan et al., 1991). It is possible that PAR-2 activation does not result in release of acetylcholine from submucosal neurons or that the neurotransmitter acts on postsynaptic nicotinic, rather than muscarinic, cholinergic receptors. The actions of trypsin were nearly abolished by the cyclooxygenase inhibitor indomethacin; those to SLIGRL-NH<sub>2</sub> were less sensitive to this drug. The different sensitivities of trypsin and SLIGRL-NH<sub>2</sub> to both indomethacin and furosemide may be a manifestation of an additional, prosecretory prostanoid component in trypsin action. Eicosanoids released by cells in the lamina propria

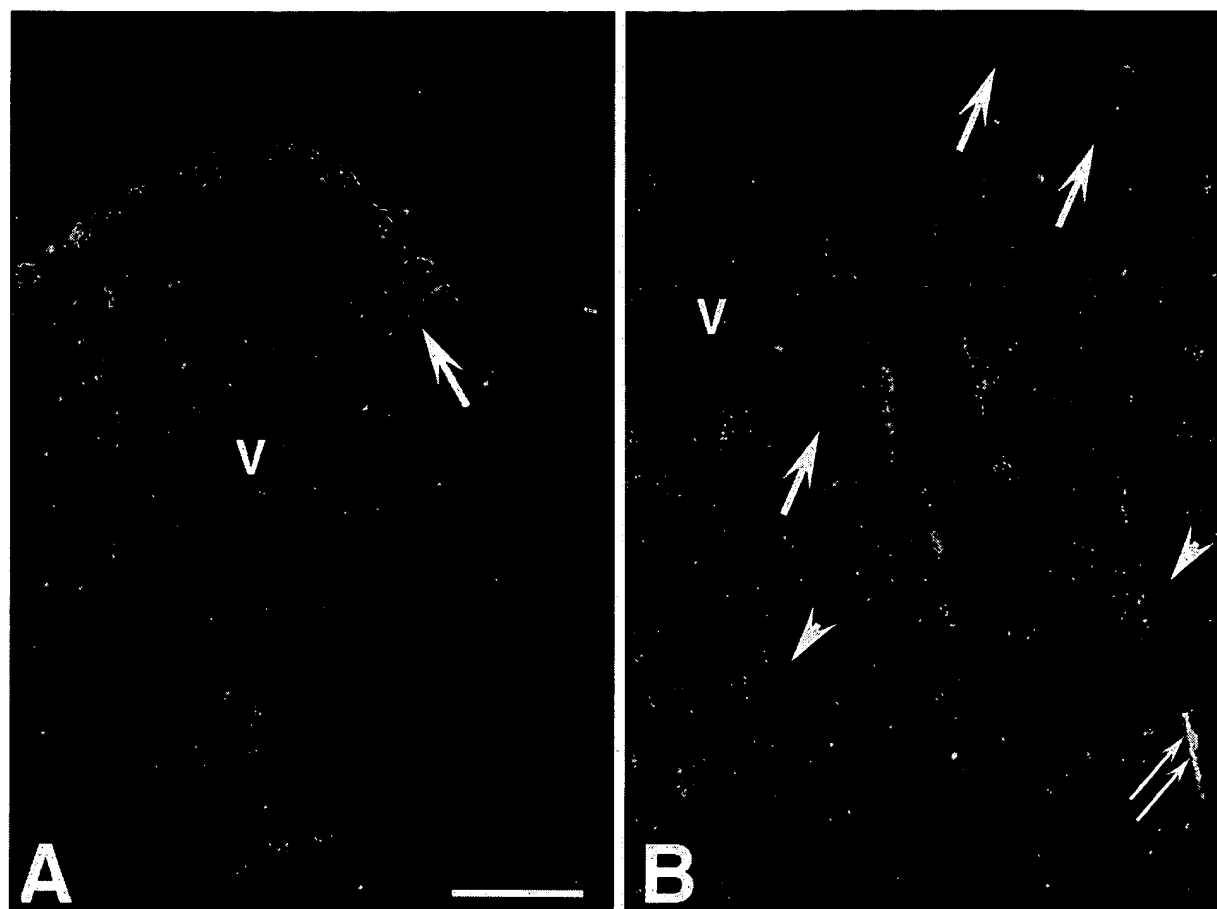


**Fig. 7.** Localization of PAR-2 and ChAT immunoreactivities in the porcine ileal submucosa. **A**, intense PAR-2 immunoreactivity is observed in enteroendocrine-like cells in the epithelium (arrow). ChAT immunoreactivity is not expressed by these cells. **B**, PAR-2-immunoreactive fibers are visualized at the base of the villous epithelium (arrows, red). Note that a separate population of ChAT-immunoreactive (arrowheads, green) fibers is seen in the midregion of the villi. PAR-2 and ChAT immunoreactivities are colocalized in a small population of thicker fibers (double arrow, yellow). V, villus. Scale bars in A and B, 50  $\mu$ m.

play an important role in intestinal inflammation (Eberhart and Dubois, 1995). Some prostanoids may indirectly evoke mucosal secretion through interactions with enteric neurons (Bern et al., 1989). The prostanoid(s) involved in the PAR-2-mediated mucosal responses to trypsin should be identified in future investigations. With respect to the blocking agents used in these experiments, it should be noted that the apparent differences in the magnitude of their inhibitory effects on tissue responses to trypsin and SLIGRL may be the consequence of the use of these PAR-2 agonists at single concentrations. Although it would be desirable to assess the effects of blockers over the entire effective concentration ranges for each agonist, this approach was impractical with the present paradigm.

Opiates such as morphine and loperamide are effective in alleviating secretory diarrheas through their actions on enteric neurons that modulate intestinal motility and transepithelial ion transport (Brown, 1994).  $\delta$ -Opioid receptors predominate in the porcine ileum (Brown et al., 1999). They are expressed on submucosal neurons and mediate the antisecretory effects of opiates (Quito and Brown, 1991; Brown et al., 1998). In this study, we addressed the hypothesis that submucosal opioid receptors inhibit the enteric neural pathways that trigger active anion secretion and are activated by in-

flammatory mediators. DPDPE, an agonist highly selective for  $\delta$ -opioid receptors (Mosberg et al., 1983), significantly attenuated the secretory effect of trypsin. Furthermore, the inhibitory action of DPDPE was reduced by the highly selective  $\delta$ -opioid receptor blocker naltrindole (Portoghese et al., 1988), a result indicating that it was mediated by  $\delta$ -opioid receptors.

In rat jejunum, luminally applied trypsin is effective in stimulating mucosal transport (Kong et al., 1997). In porcine ileum, however, trypsin was more potent and effective in increasing *I*<sub>sc</sub> after its contraluminal addition to porcine mucosal sheets. Moreover, the colocalization of PAR-2 immunoreactivity with the neuronal marker PGP9.5 within the submucosal plexus supports our functional observations that PAR-2 is present on enteric neurons. However, the apparent localization of PAR-2 immunoreactivity in enteroendocrine cells suggests that this receptor may regulate the release of GI hormones under the influence of luminal trypsin. The present results clearly indicate that the cellular expression of PAR-2 in the small intestine may vary according to the species or intestinal segment examined.

Human intestinal mast cells are concentrated in the intestinal submucosa, where they secrete tryptase (Aldenborg and Enerbäck, 1994). Trypsin and tryptase have a similar cata-

lytic activity, and neuronal PAR-2 may be in juxtaposition to mast cells in the ileal submucosa to permit their activation by tryptase (Molino et al., 1997). Indeed, nearly 90% of mast cells in the human intestine are within 2  $\mu$ m of neurons, and recent evidence indicates that there are direct interactions between nerves and mast cells (Suzuki et al., 1999). Neuronal PAR-2 may function in intestinal host defense by mediating active anion secretion that could provide the means to rid the intestinal mucosa of potentially pathogenic microorganisms. Opiates, particularly those interacting with  $\delta$ -opioid receptors, may be clinically beneficial in alleviating diarrheas associated with PAR-2 activation and other intestinal inflammatory states.

#### Acknowledgment

We thank Dr. Morley D. Hollenberg for the generous gift of anti-PAR-2 antiserum.

#### References

- Aldenberg F and Enerbäck L (1994) The immunohistochemical demonstration of chymase and tryptase in human intestinal mast cells. *Histochem J* 267:587–596.
- Berlin MC, McKay DM and Perdue MH (1999) Immune-epithelial interactions in host defense. *Am J Trop Med Hyg* 60 (Suppl 1):16–25.
- Bern MJ, Sturbaum CW, Karayalcin SS, Berschneider H, Wachsmann JT and Powell DW (1989) Immune system control of rat and rabbit colonic electrolyte transport. Role of prostaglandins and enteric nervous system. *J Clin Invest* 83:1810–1820.
- Bohm SK, Khitin LM, Grady EF, Apontes G, Payan DG and Bunnett NW (1996a) Mechanisms of desensitization and resensitization of proteinase-activated receptor-2. *J Biol Chem* 271:22003–22016.
- Bohm SK, Kong W, Bromme D, Smeeckens SP, Anderson DC, Connolly A, Kahn M, Nelken NA, Coughlin SR, Payan DG and Bunnett NW (1996b) Molecular cloning, expression and potential functions of the proteinase-activated receptor-2. *Biochem J* 314:1009–1016.
- Brown DR (1994) Antidiarrheal drugs: Pharmacologic control of intestinal hypersecretion, in *Principles of Pharmacology: Basic Concepts and Clinical Applications* (Munson PL ed) pp 1083–1091, Chapman & Hall, London.
- Brown DR, Poonyachoti S, Osinski MA, Kowalski TR, Pampusch MS, Elde RP and Murtaugh MP (1998) Delta-opioid receptor mRNA expression and immunohistochemical localization in porcine ileum. *Dig Dis Sci* 43:1402–1410.
- Brown DR, Poonyachoti S and Townsend D (1999) *delta*-Opioid receptors in porcine ileum. Proceedings of the 30th Annual Meeting of the International Narcotics Research Conference; 1999 July 10–15; Saratoga Springs, NY: 41 p.
- Chandan R, Hildebrand KR, Seybold VS, Soldani G and Brown DR (1991) Cholinergic neurons and muscarinic receptors regulate anion secretion in pig distal jejunum. *Eur J Pharmacol* 193:265–273.
- Corvera CU, Déry O, McConalogue K, Böhm SK, Khitin LM, Caughey GH, Payan DG and Bunnett NW (1997) Mast cell tryptase regulates rat colonic myocytes through proteinase-activated receptor 2. *J Clin Invest* 100:1–11.
- Corvera CU, Déry O, McConalogue K, Gamp P, Thoma M, Al-Ani B, Caughey GH, Hollenberg MD and Bunnett NW (1999) Thrombin and mast cell tryptase regulate guinea-pig myenteric neurons through proteinase-activated receptors-1 and -2. *J Physiol (Lond)* 517:741–756.
- Déry O, Corvera CU, Steinhoff M and Bunnett NW (1998) Proteinase-activated receptors: Novel mechanisms of signaling by serine proteases. *Am J Physiol* 274:C1429–C1452.
- Eberhart CE and Dubois RN (1995) Eicosanoids and the gastrointestinal tract. *Gastroenterology* 109:285–301.
- Hollenberg MD (1999) Protease-activated receptors: PAR4 and counting—How long is the course? *Trends Pharmacol Sci* 20:271–273.
- Kong W, McConalogue K, Khitin LM, Hollenberg MD, Payan DG, Böhm SK and Bunnett NW (1997) Luminal trypsin may regulate enterocytes through proteinase-activated receptor 2. *Proc Natl Acad Sci USA* 94:8884–8889.
- Marone G, Spadaro G, De Marino V, Alipeta M and Trigianni M (1998) Immunopharmacology of human mast cells and basophils. *Int J Clin Lab Res* 28:12–22.
- Molino M, Barnathan ES, Numerof R, Cark J, Dreyer M, Cumashi A, Hoxie JA, Schechter N, Woolkalis M and Brass LF (1997) Interactions of mast cell tryptase with thrombin receptors and PAR-2. *J Biol Chem* 272:4043–4049.
- Mosberg HI, Hurst R, Hruby VJ, Gee K, Akiyama K, Yamamura HI, Galligan JJ and Burks TF (1983) Cyclic penicillamine containing enkephalin analogs display profound delta receptor selectivities. *Life Sci* 33 (Suppl 1):447–450.
- Nystedt S, Emilsson K, Wahlestedt C and Sundelin J (1994) Molecular cloning of a potential proteinase activated receptor. *Proc Natl Acad Sci USA* 91:9208–9212.
- Perdue MH and McKay DM (1994) Integrative immunophysiology in the intestinal mucosa. *Am J Physiol* 267:G151–G165.
- Portoghese PS, Sultana M and Takemori AE (1988) Naltrindole, a highly selective and potent non-peptide delta opioid receptor antagonist. *Eur J Pharmacol* 146: 185–186.
- Quito FL and Brown DR (1991) Neurohormonal regulation of ion transport in the porcine distal jejunum. Enhancement of sodium and chloride absorption by submucosal opiate receptors. *J Pharmacol Exp Ther* 256:833–840.
- Saifeddine M, Al-Ani B, Cheng C, Wang L and Hollenberg MD (1996) Rat proteinase-activated receptor-2 (PAR-2): cDNA sequence and activity of receptor-derived peptides in gastric and vascular tissue. *Br J Pharmacol* 118:521–530.
- Santulli RJ, Derian CK, Darrow AL, Tomko KA, Eckardt AJ, Seiberg M, Scarborough RM and Andrade-Gordon P (1995) Evidence for the presence of a protease-activated receptor distinct from the thrombin receptor in human keratinocytes. *Proc Natl Acad Sci USA* 92:9151–9155.
- Steinhoff M, Vergnolle N, Young SH, Tognetto M, Ennes EH, Trevisani M, Hollenberg MD, Wallace JL, Caughey GH, Mitchell SE, Williams LM, Geppetti P, Mayer EA and Bunnett NW (2000) Agonists of proteinase-activated receptor 2 induce inflammation by a neurogenic mechanism. *Nat Med* 6:151–158.
- Suzuki R, Furuno T, McKay DM, Wolvers D, Teshima R, Nakanishi M and Bienenstock J (1999) Direct neurite-mast cell communication in vitro occurs via the neuropeptide substance P. *J Immunol* 163:2410–2415.
- Vergnolle N, MacNaughton WK, Al-Ani B, Saifeddine M, Wallace JL and Hollenberg MD (1998) Proteinase-activated receptor 2 (PAR2)-activating peptides: Identification of a receptor distinct from PAR2 that regulates intestinal transport. *Proc Natl Acad Sci USA* 95:7766–7771.

Send reprint requests to: David R. Brown, Ph.D., Department of Veterinary Pathobiology, University of Minnesota, 1988 Fitch Ave., St. Paul, MN55108-6010. E-mail: brown013@tc.umn.edu

## A murine model of pulmonary damage induced by lipopolysaccharide via intranasal instillation

Roderick J. Szarka <sup>a</sup>, Nandi Wang <sup>a</sup>, Lyle Gordon <sup>a</sup>, P.N. Nation <sup>b</sup>,  
Richard H. Smith <sup>a,\*</sup>

<sup>a</sup> Alberta Research Council, Carbohydrate Chemistry, P.O. Box 8330 Stn. F, Edmonton, Alberta, Canada T6H 5X2

<sup>b</sup> Veterinary Pathology Laboratory, Edmonton, Alberta, Canada T5S 1E8

Received 7 October 1996; accepted 14 November 1996

### Abstract

This study examines the intranasal instillation of lipopolysaccharide (LPS) into BALB/c mice causing acute pulmonary damage, due to neutrophil infiltration and sepsis. A dose response with LPS showed that an intranasal instillation of 167 µg/ml (10 µg/mouse) caused acute lung injury within 2–4 h and reached maximal damage at 24–48 h. We found the method of LPS administration for induction of acute pulmonary damage to be crucial. After 24 h post-LPS injection, a comparison showed a substantial increase in pulmonary damage with intranasal instillation of LPS. As for intravenous injection, it showed a baseline effect. This study indicates that LPS administered intranasally causes acute pulmonary damage, whereas with intravenous and intraperitoneal endotoxin administration a tissue-specific or similar degree of pulmonary injury may not develop.

**Keywords:** Lipopolysaccharide; Endotoxin; Intranasal instillation; Pulmonary damage; Bronchoalveolar lavage; Myeloperoxidase

### 1. Introduction

The pathogenesis of sepsis and related pulmonary diseases, such as adult respiratory distress syndrome (ARDS), remains unclear. In order to gain better insight into these diseases, several experimental approaches using animal models have been studied

(Ognibene et al., 1986; Goldblum et al., 1988; Fink and Heard, 1990; Gatti et al., 1993; Denis et al., 1994). Endotoxin (LPS) is an extremely biologically active substance which can be employed in the investigation of septic shock and acute lung injury (Brigham and Meyrick, 1986; Gatti et al., 1993).

LPS is a macromolecular cell wall surface antigen of Gram-negative bacteria (Rietschel et al., 1982; Fink and Heard, 1990), composed of two components: the 'O'-antigen side chain and the core. The variation of the polysaccharides in the O-antigen side chain gives the antigenic specificity among species and strains of Gram-negative bacteria (Fink and Heard, 1990). The lipid A moiety is the polysaccharide core attached to a lipid molecule and retains the

Abbreviations: i.n., intranasal; i.v., intravenous; i.p., intraperitoneal; LPS, lipopolysaccharide; ARDS, adult respiratory distress syndrome; BAS, bronchoalveolar space; BALF, bronchoalveolar lavage fluid; HTAB, hexadecyltrimethylammonium bromide; MPO, myeloperoxidase.

\* Corresponding author. Tel.: (403) 450-5280; Fax: (403) 988-9028.

toxicity of LPS. Lipid A has been demonstrated to increase lung microvascular permeability. This results in an early deterioration of respiratory function and induction of severe pulmonary edema with recruitment of leukocytes from peripheral blood into the interstitial pulmonary tissue (Harlan et al., 1983; Brigham et al., 1979; Kunkel et al., 1991; Rot, 1992; Worthen et al., 1992; Gatti et al., 1993). Even though the mechanisms by which LPS enhances the injury caused by neutrophil infiltration have not been firmly established, animal models utilizing LPS-induced injuries provide important information about the events which cause sepsis and pulmonary damage.

Intraperitoneal (i.p.) and intravenous (i.v.) injections of bacterial endotoxins are the current administration methods used to develop acute lung injury in animal models. In our study, we have examined the method of administration of LPS(s) via intranasal (i.n.) instillation. This method causes pulmonary inflammation as an acute injury which occurs after 2–4 h and maximizes at 24–48 h. The development of an acute lung injury model by way of LPS i.n. instillation is well suited for preliminary pharmacological studies of new drugs or other therapeutic agents.

## 2. Materials and methods

### 2.1. Materials

LPS from *Pseudomonas aeruginosa* F-D type 1 was obtained from List Biological Laboratories, LPS from *Escherichia coli* serotype 055:B5, myeloperoxidase (EC 1.11.1.7) from human leukocytes was obtained from Sigma, and heat killed *E. coli* serotype 014:K7(L):NM was obtained from American Type Culture Collection and scaled up at the Alberta Research Council, Edmonton, AB, Canada. Mayer's hematoxylin solution, dimethyl sulfoxide, and 3-amino-9-ethylcarbazole were purchased from Sigma, St. Louis, MO. The inhalation anesthetic Metofane (2,2-dichloro-1,1-difluoroethyl methyl ether) was obtained from Pitman-Moore, Mississauga, ON. The aqueous/dry mounting medium for enzyme immunocytochemistry, Crystal/Mount, was supplied by Biomedica Corp., Foster City, CA. All other reagents were from Sigma or Fisher Scientific.

### 2.2. Preparation and treatment of murine lung injury

Female Sprague-Dawley BALB/c mice (19–20 g) were fed Purina rodent chow and water ad libitum. Mice were housed for a minimum of 2 weeks in a quarantine room with a 12:12 h light–dark cycle before used in experiments. Mice were anesthetized by placing a small wad of cotton soaked with Metofane into a jar, and then the mice were placed in the vapor-filled chamber. While anesthetized, i.n. instillation was conducted by placing 10 µg/60 µl (167 µg/ml) LPS or 20 µg/60 µl (334 µg/ml) heat-killed *E. coli* on the nares (Rushton, 1978; Smith et al., 1981). Control mice received 60 µl PBS, pH 7.2, containing 140 mM NaCl, 70 mM Na<sub>2</sub>HPO<sub>4</sub>, 3 mM KCl, and 1.5 mM KH<sub>2</sub>PO<sub>4</sub> alone. The 60 µl samples were applied onto the nares with three 20 µl drops, using an Eppendorf repeater pipet. For i.v. injections, LPS was administered by a 200 µl bolus injection into the tail vein. Visualization of the tail vein was improved by placing the mice briefly under a heat lamp.

Procedures involving mice and their care were conducted in compliance with institutional and national laws and policies (Canadian Council on Animal Care, 'Guide to the Care and Use of Experimental Animals', 2 volumes, CCAC, Ottawa, ON, 1980–1984).

### 2.3. Lung wet weight, lung lavage, and total cell quantitation

The mice were killed by cervical dislocation at selected times after LPS administration. Each experimental group consisted of 12 mice. The lungs from eight mice were excised, cleared of all extrapulmonary tissue and lung weight was measured. Pulmonary edema caused by LPS was determined by calculating the percent increase of lung weight using PBS lung weights (negative control) as the reference weight. Four of the eight murine lungs were fixed in 10% neutral buffered formalin immediately and histopathology was examined.

Bronchoalveolar lavages were performed on the remaining four mice from each group. A tracheostomy was performed and a tracheal catheter was clamped into the trachea with a hemostat. The lungs were washed 5 times repeatedly with 500 µl



PBS. Extreme care was taken with injecting and extracting PBS washing solution from the lungs to eliminate any blood contamination. The bronchoalveolar lavage fluid (BALF), obtained as indicated above, was maintained at 4°C. A volume of 300 µl BALF from each sample was centrifuged (4°C, 1000 rpm, 8 min) to pellet cells. The supernatant was stored at –20°C for protein analysis (data not shown). The cell pellet was resuspended in 120 µl PBS. Determination of total cell counts was completed on a Bright-Lite hemacytometer (Reichert, Buffalo, NY).

#### 2.4. Myeloperoxidase stain granulocyte quantitation

A cytospin of lung lavage cells was performed on standard microscope slides using cytobucket carriers (Fisher Scientific). A 60 µl cell sample containing  $4.0 \times 10^5$  cells was diluted with 200 µl PBS containing 10% fetal calf serum and centrifuged (4°C, 1000 rpm, 8 min). Cells were fixed directly and strained as described by Yam et al. (1971) and Kaplow (1975). Cells were counterstained with Mayer's hematoxylin solution, air-dried, and mounted with Crystal/Mount. Differential neutrophil counts were performed on stained cells and determined averaged over a count of at least 200 cells.

#### 2.5. Myeloperoxidase enzyme assay of bronchoalveolar lavage fluid

The quantitation of granulocytes in the BALF was performed by a cytochemical myeloperoxidase (MPO) enzyme assay. A standard curve was established using a serial dilution of commercial MPO starting at 0.8 units/ml (0.04 U/well) (data not shown). The samples were placed in a flat-bottom 96-well ELISA plate (Limbro), in triplicate, and freeze-thawed 3 times. Each well had a final volume of 50 µl in 50 mM sodium phosphate buffer, pH 6.0, supplemented with 0.5% hexadecyltrimethylammonium bromide (HTAB) (Schultz and Kaminker, 1962; Patriarca et al., 1971; Bradley et al., 1982). A volume of 100 µl MPO substrate in 50 mM sodium phosphate buffer, pH 6.0, containing 0.5% HTAB, 0.167 mM *o*-dianisidine, and 0.0005% hydrogen peroxide was added to each well. After 5 min, MPO

enzyme reaction was stopped with the addition of 100 µl 5.0% sodium azide. MPO activity was measured in a spectrophotometer at an excitation wavelength of 450 nm.

#### 2.6. Methods of histopathology

The lungs were fixed in 10% neutral buffered formalin. Following fixation, a 2 mm thick midsagittal section of each of the left lung and the right caudal lung lobes was made and placed into a tissue processing cassette. Sections in cassettes infiltrated with paraffin in a Citadel automatic tissue processor were embedded using a Tissue Tek embedding center, sectioned at 4 µm with a Reichert microtome, and stained with hematoxylin and eosin using standard methods.

Microscopic examination of stained lung sections was conducted blind by a board-certified veterinary pathologist. Scores were assigned to each section of lung based upon the degree of endothelial damage, severity of inflammation, percentage of neutrophils in the reaction, number of inflammatory cells in alveoli, and numbers of neutrophils in bronchioles.

#### 2.7. Other procedures

The protein content in lung lavage supernatant was measured by the Lowry protein assay (Lowry et al., 1951) using bovine serum albumin as a standard.

### 3. Results

#### 3.1. Time course with induction of murine acute lung injury after LPS administration

Experiments were conducted to determine the optimal time to examine mice for maximum pulmonary inflammation after i.n. administration of LPS. After LPS administration at time zero, lungs were analyzed at selected time points up to 72 h (Table 1). After 24 h, LPS caused a 29% increase of wet lung weight, a strong influx of granulocytes ( $970 \times 10^6$  granulocytes/ml) into the BALF which was verified with a high detection of MPO in the BALF. The histopathology results correlate with the trend showing a 36.3% increase of total cell population, mainly

Table 1  
Time course of post-LPS administration on murine acute lung injury <sup>a</sup>

Time of analysis (h)	Lung weight <sup>c</sup> (% increase) <sup>f</sup>	Lung lavage granulocyte quantitation <sup>d</sup> (total granulocytes × 10 <sup>6</sup> /ml)	Lung lavage MPO <sup>d</sup> (450 OD)	Pathology <sup>c</sup>	
				(% neutrophils) <sup>e</sup>	(inflammation reaction) <sup>g</sup>
PBS <sup>b</sup>	0.0	4.3 ± 5.2	0.002 ± 0.006	0.0 ± 0.0	0.0 ± 0.0
2	14.0	4.0 ± 2.3	0.038 ± 0.015	11.3 ± 6.0	1.8 ± 0.5
4	8.0	78.0 ± 5.5	0.156 ± 0.014	12.5 ± 8.3	1.5 ± 0.6
8	12.0	157.3 ± 36.3	0.16 ± 0.009	31.3 ± 11.7	2.6 ± 0.5
24	29.0	970.7 ± 93.4	0.129 ± 0.012	36.3 ± 9.9	3.1 ± 0.3
48	34.0	1481.3 ± 161.2	0.127 ± 0.013	41.3 ± 16.9	3.0 ± 0.4
72	27.0	273.3 ± 70.9	0.149 ± 0.014	38.8 ± 10.5	3.6 ± 0.4

<sup>a</sup> Mice were administered 167 µg LPS/ml i.n. as described in Section 2. At selected time points, lung tissues were analyzed. LPS was from *E. coli* serotype 055:B5.

<sup>b</sup> PBS values were calculated from the average of each time point.

<sup>c</sup> For measurements of lung and pathology; *n* = 8, *n* = 4 respectively.

<sup>d</sup> For measurements of lung lavage granulocyte quantitation and lung lavage MPO, *n* = 4.

<sup>e</sup> Percent neutrophils is the estimated percent of total cell population in alveolar walls made up of neutrophils.

<sup>f</sup> Percent increase of lung weight was calculated from the LPS lung weight increase greater than average PBS lung weight value.

<sup>g</sup> Scores assigned to each group of lungs based on the degree of inflammation. The description of scoring rank is in Table 5.

neutrophils, in the alveolar walls. These results show that acute lung injury peaked at 24–48 h. The MPO assay on BALF maximized to an optical density reading of 0.16 at 4–8 h and histopathology showed a maximum increase of 41.3% neutrophil population in the alveolar wall at 48 h. Quantitation of neutrophils in the BALF correlates with the above results showing maximum infiltration of 1481 × 10<sup>6</sup> granulocytes/ml after 48 h. After 72 h, the mice were able to overcome the lung inflammation and recover. This was observed with the dramatic de-

crease in lung injury from the experimental analysis. From the time-course experiments, i.n. instillation of 167 µg/ml LPS (*E. coli* serotype 055:B5) caused an acute pulmonary inflammation that peaked at 24–48 h and started recovery after 72 h.

### 3.2. Dose response of LPS-induced acute lung inflammation

A dose response was conducted to determine the optimal concentration of LPS (*E. coli* serotype

Table 2  
Dose response of LPS inducing acute pulmonary inflammation at 2 h <sup>a</sup>

Sample injections (per ml)	Lung weight <sup>b</sup> (mg)	Lung lavage granulocyte quantitation <sup>c</sup> (total granulocyte × 10 <sup>6</sup> /ml)	Lung lavage MPO <sup>c</sup> (450 OD)	Pathology <sup>b</sup>	
				(% neutrophils) <sup>d</sup>	(inflammatory reaction) <sup>e</sup>
PBS	0.0	2.0 ± 0.8	0.024 ± 0.004	0	0.0 ± 0.0
33 µg LPS	9.2	9.0 ± 3.1	0.057 ± 0.021	15 ± 13	1.3 ± 1.0
167 µg LPS	15.0	16.3 ± 3.5	0.047 ± 0.019	47 ± 27	2.0 ± 0.0
833 µg LPS	5.0	3.1 ± 1.0	0.029 ± 0.006	40 ± 45	1.0 ± 1.1
1667 µg LPS	15.0	1.3 ± 0.4	0.027 ± 0.016	47 ± 13	2.0 ± 0.0

<sup>a</sup> Mice were administered i.n. with selected quantities of LPS as described in Section 2. Two hours later, lung tissues were analyzed. LPS was from *E. coli* serotype 055:B5.

<sup>b</sup> For measurements of lung weight and pathology, *n* = 8, *n* = 4, *n* = 4 respectively.

<sup>c</sup> For measurements of lung lavage granulocyte quantitation, and lung lavage MPO, *n* = 4.

<sup>d</sup> % neutrophils is the estimated percent of total cell population in alveolar walls made up of neutrophils.

<sup>e</sup> Scores assigned to each group of lungs based on the degree of inflammation. The description of scoring rank is in Table 5.

055:B5) needed to cause an acute pulmonary inflammation in mice. LPS was administered through the nares into the BAS and murine lungs were investigated after 2 h (Table 2) and 24 h (Table 3). Again, the determination of acute lung inflammation was based on lung wet weight, bronchoalveolar lavage analysis, and histopathology. At 2 and 24 h, the administration of 167  $\mu\text{g}/\text{ml}$  (10  $\mu\text{g}/\text{mouse}$ ) LPS resulted in the maximal increase of lung wet weight, whereas the administration of LPS concentrations greater than 167  $\mu\text{g}/\text{ml}$  yielded comparable results of LPS-treated murine lungs. The same LPS concentration gave the most consistent histopathological changes and a plateau appears with the histopathology scores. These scores consist of endothelial inflammation and estimated percent of total cell population in alveolar walls made up of neutrophils. The histopathology revealed maximum percent neutrophils ( $47 \pm 27\%$ ) in the alveolar walls with 167  $\mu\text{g}/\text{ml}$  (10  $\mu\text{g}/\text{mouse}$ ) LPS i.n. post 2 h and maintained these values with greater concentrations. After 24 h, pathology showed maximum percent neutrophils ( $37 \pm 21.5\%$ ) in the alveolar walls with 167  $\mu\text{g}/\text{ml}$  (10  $\mu\text{g}/\text{mouse}$ ) LPS instillation and retained this increase with greater concentrations. The analysis of BALF collected at 2 and 24 h showed an infiltration of neutrophils into the inflamed lung and BAS. In the BALF, 167  $\mu\text{g}/\text{ml}$  (10  $\mu\text{g}/\text{mouse}$ ) LPS caused a peak value of granulocyte migration post 2 and 24 h. At 2 h, a maximum of  $16.3 \times 10^6$  granulocytes/ml was detected in the BALF, with a very strong infiltration of granulocytes ( $1250 \times 10^6$

granulocytes/ml) into the BALF post 24 h. The concentrations of LPS greater than 167  $\mu\text{g}/\text{ml}$  (10  $\mu\text{g}/\text{mouse}$ ) LPS showed a decrease in granulocyte migration. These observations coincide with MPO activity of BALF. Based on the data from wet lung weight, BALF granulocyte quantitation, BALF MPO quantitation, and histopathology, 167  $\mu\text{g}/\text{ml}$  (10  $\mu\text{g}/\text{mouse}$ ) LPS i.n. instillation caused a maximum degree of acute pulmonary inflammation with the least amount of endotoxin.

### 3.3. Comparison of different types or forms of lipopolysaccharide

Injection of nanograms to micrograms of isolated and purified LPS preparations into animals can elicit a variety of distinct biological effects (Rietschel et al., 1982; Berry, 1977; Galanos et al., 1977; Morrison and Ulevitch, 1978; Nowotny, 1969). To examine the effects that different types of LPS preparations would have on the induction of murine lung injury, when administered i.n., we carried out experiments using various types of LPS. We compared the effect of purified LPS from *E. coli* serotype 055:B5 and *P. aeruginosa* F-D type 1. Over a 72 h time period, the analysis of pulmonary damage was performed at selected time points. As shown in Table 4, the two forms of LPS showed similar results, where *E. coli* LPS caused 46.7% and *P. aeruginosa* caused 44.4% increase in wet lung weight over 72 h. In the analysis of BALF, *P. aeruginosa* LPS caused a greater influx of granulocytes into the bronchiole and alveolar passages ( $1351.9 \times 10^6$  granulocytes/ml)

Table 3  
Dose response of LPS inducing acute pulmonary inflammation at 24 h <sup>a</sup>

Sample injections (per ml)	Lung weight <sup>b</sup> (mg)	Lung lavage granulocyte quantitation <sup>c</sup> (total granulocyte $\times 10^6/\text{ml}$ )	Lung lavage MPO <sup>c</sup> (450 OD)	Pathology <sup>b</sup>	
				(% neutrophils) <sup>d</sup>	(inflammatory reaction) <sup>e</sup>
PBS	0.0	$4.8 \pm 1.5$	$0.000 \pm 0.003$	$0 \pm 0$	$0.0 \pm 0.0$
33 $\mu\text{g}$ LPS	43.0	$818 \pm 143$	$0.135 \pm 0.021$	$37 \pm 21.5$	$1.7 \pm 0.9$
167 $\mu\text{g}$ LPS	56.2	$1250 \pm 476$	$0.176 \pm 0.030$	$39 \pm 15.8$	$2.6 \pm 1.0$
833 $\mu\text{g}$ LPS	45.9	$897 \pm 257$	$0.136 \pm 0.022$	$39 \pm 16.2$	$2.2 \pm 0.9$
1667 $\mu\text{g}$ LPS	52.6	$986 \pm 338$	$0.139 \pm 0.018$	$31 \pm 13$	$1.8 \pm 0.6$

<sup>a</sup> Mice were administered i.n. with selected quantities of LPS as described in Section 2. 24 h later, lung tissues were analyzed. LPS was from *E. coli* serotype 055:B5.

<sup>b</sup> For measurements of lung weight and pathology,  $n = 10$ ,  $n = 10$  respectively.

<sup>c</sup> For measurements of lung lavage granulocyte quantitation, and lung lavage MPO,  $n = 6$ .

<sup>d</sup> % neutrophils is the estimated percent of total cell population in alveolar walls made up of neutrophils.

<sup>e</sup> Scores assigned to each group of lungs based on the degree of inflammation. The description of scoring rank is in Table 5.

Table 4  
Comparison of types of LPS <sup>a</sup>

Type of LPS	Lung weight <sup>b</sup> (% increase)	Lung lavage granulocyte quantitation <sup>c</sup> (total granulocyte $\times 10^6$ /ml)	Pathology <sup>b</sup>	
			(% neutrophils <sup>d</sup> )	(inflammation reaction) <sup>e</sup>
PBS				
24 h	0.0	1.7 $\pm$ 0.5	0.0 $\pm$ 0.0	0.0 $\pm$ 0.0
48 h	0.0	1.5 $\pm$ 0.4	0.0 $\pm$ 0.0	0.0 $\pm$ 0.0
72 h	0.0	1.0 $\pm$ 0.3	0.0 $\pm$ 0.0	0.0 $\pm$ 0.0
<i>E. coli</i> serotype 055:B5 LPS				
24 h	21.3	531.2 $\pm$ 63.2	30 $\pm$ 12	2.2 $\pm$ 0.4
48 h	40.0	782.9 $\pm$ 46.4	49 $\pm$ 10	3.2 $\pm$ 0.6
72 h	46.7	128.3 $\pm$ 33.2	21 $\pm$ 21	1.7 $\pm$ 1.5
<i>P. aeruginosa</i> F-D type 1 LPS				
24 h	24.4	989.7 $\pm$ 72.9	N/A	N/A
48 h	39.3	1351.9 $\pm$ 47.6	N/A	N/A
72 h	44.4	466.3 $\pm$ 29.0	N/A	N/A
Heat-killed <i>E. coli</i> serotype 014:K7(L):NM				
24 h	24.0	318.2 $\pm$ 63.0	48 $\pm$ 13	2.4 $\pm$ 0.5
48 h	30.0	566.0 $\pm$ 94.9	44 $\pm$ 9	2.9 $\pm$ 0.9
72 h	31.0	215.7 $\pm$ 48.7	5 $\pm$ 8	2.4 $\pm$ 0.6

<sup>a</sup> Mice were administered i.n. with selected quantities of LPS as described in Section 2. 24, 48, and 72 h later, lung tissues were analyzed.

<sup>b</sup> For measurements of lung weight and pathology,  $n = 10$ ,  $n = 10$  respectively.

<sup>c</sup> For measurements of lung lavage granulocyte quantitation, and lung lavage MPO,  $n = 6$ .

<sup>d</sup> % neutrophils is the estimated percent of total cell population in alveolar walls made up of neutrophils.

<sup>e</sup> Scores assigned to each group of lungs based on the degree of inflammation. The description of scoring rank is in Table 5.

than did *E. coli* LPS ( $782.9 \times 10^6$  granulocytes/ml). The analysis of BALF after injection of both types of LPS showed a peak neutrophilia at 48 h, which decreased at 72 h. After 48 h, the histopathology of *E. coli* LPS revealed a maximum percent neutrophil influx (49%) into the lung tissue. The data for the pathology of lung tissue exposed to *P. aeruginosa* F-D type 1 LPS are not shown.

A comparison of whole *E. coli* bacteria containing LPS and purified *E. coli* LPS was conducted. Purified LPS caused a greater acute lung injury response than did the whole *E. coli* bacteria. As

shown in Table 4, the pure LPS caused a 46.7% increase in wet lung weight over 72 h, whereas the whole bacteria caused a 31.0% increase. The BALF also showed a difference in pulmonary damage with administration of different forms of LPS. Purified LPS caused a greater influx of granulocytes into the alveolar space ( $782.9 \times 10^6$  granulocytes/ml) as compared to whole *E. coli* bacteria ( $566.0 \times 10^6$  granulocytes/ml). Analysis of BALF showed a peak neutrophilia at 48 h, which decreased at 72 h (Table 4). At 48 h, the histopathology of *E. coli* LPS (purified LPS 49% and *E. coli* bacteria 44% neu-

Table 5  
Key for histopathology scoring of inflammation reaction

Score value	Description of degree of inflammation
0	No reaction in alveolar walls.
1	Diffuse reaction in alveolar walls, primarily neutrophilic, no thickening of alveolar walls.
2	Diffuse presence of inflammatory cells (neutrophilic and mononuclear) in alveolar walls with slight thickening.
3	Distinct (2–3 times) thickening of the alveolar walls due to presence of inflammatory cells.
4	Alveolar wall thickening with up to 25% of lung consolidated.
5	Alveolar wall thickening with more than 50% of lung consolidated.

trophil influx into the lung tissue) revealed the same observation as in the BALF analysis. The maximum degree of inflammatory response was reached with i.n. instillation using an isolated form of LPS.

### 3.4. Comparison of intravenous injections and intranasal instillation

The major mode of LPS administration in animal models is by way of i.v. and i.p. injections (Brackett et al., 1985; Natanson et al., 1986; Law and Ferguson, 1988; Gatti et al., 1993). Experiments were conducted to compare the effect that different routes of administration had on the induction of LPS-in-

duced lung injury. The i.n. instillation was tested to determine if this type of application could compare to the known routes of administration. We have found i.n. instillation of LPS to cause a greater degree of lung injury based on the same concentration administered (Fig. 1). At 2 and 24 h, granulocyte migration in the BALF showed a substantial increase ( $700 \times 10^6$  granulocytes/ml) with  $167 \mu\text{g}$  LPS/ml ( $10 \mu\text{g}/\text{mouse}$ ) i.n. as compared with the identical LPS dose response, administered i.v. The results obtained with the i.v. administration of LPS were comparable to PBS control values. We have shown that i.n. instillation of  $167 \mu\text{g}$  LPS/ml ( $10 \mu\text{g}/\text{mouse}$ ) can cause acute lung injury over 48 h.

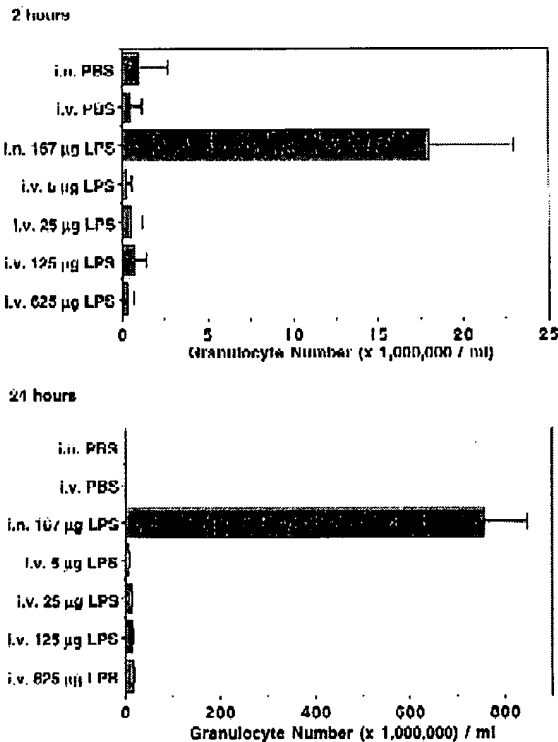


Fig. 1. Comparison of intravenous injections and intranasal administration of LPS. For the i.v. treated mice, LPS was injected into the tail vein and lungs were lavaged after a selected period of time. Intranasal instillation was as described in Section 2. Total granulocytes were quantitated from the bronchoalveolar lavage fluid. 2 and 24 h were the selected time points for lung tissue and lavage fluid analysis. The i.n. installation of LPS was  $10 \mu\text{g}/\text{ml}$  ( $10 \mu\text{g}/\text{mouse}$ ). The i.v. injections were a dose response with the range of  $10 \mu\text{g}$  ( $167 \mu\text{g}/\text{ml}$ ) to  $125 \mu\text{g}$  ( $625 \mu\text{g}/\text{ml}$ ) LPS. The data are expressed as the total granulocytes ( $\times 10^6$ )/ml in the lung lavage. Values represent means  $\pm$  SD from four independent mice.

### 4. Discussion

New information has emerged during the past years regarding the development of pulmonary damage in animal models. A variety of animal models are already available to investigators which may mimic acute clinical situations. Protocols for the induction of an ARDS-like syndrome (Anderson et al., 1990; Simons et al., 1991; Denis et al., 1994), sepsis (Fink and Heard, 1990), septic shock (Fink and Heard, 1990), and LPS-induced pulmonary edema (Gatti et al., 1993) have been established. The majority of pulmonary traumas are induced by i.v. or i.p. injection of an endotoxin. Infusion of LPS results in a strong neutrophilic influx into the lungs of experimental animals, as well as evidence of edema and alveolar septal thickening (Stephens et al., 1988; Denis et al., 1994).

Our present study demonstrates that i.n. instillation of LPS into mice can produce a controlled acute lung injury. In this animal model of lung injury, direct exposure of LPS to lung tissue is crucial. The pulmonary damage resulting from the LPS is predominated by pulmonary edema and recruitment of granulocytes from the vascular lumen into the pulmonary airspace within hours. These results are in agreement with those of Ulich et al. (1991a), who showed neutrophils first appear in BALF 2–4 h after intratracheal injection of endotoxin. The neutrophils migrated to a modest accumulation in the airways within 24 h, peaked at 48 h, and diminished to near-baseline levels after 72 h (Ulich et al., 1991b). Examination of varying the concentrations of LPS

indicates clearly an increase in pulmonary damage. A dose of 167  $\mu\text{g}/\text{ml}$  (10  $\mu\text{g}/\text{mouse}$ ) of LPS instilled into the lungs of mice induces the optimal acute lung injury. Our results are comparable with the literature. Ulich et al. (1991a) caused an induced acute pulmonary inflammation in rats with a dose of 10–100  $\mu\text{g}$  LPS with intratracheal injection. Interestingly, at concentrations above 167  $\mu\text{g}/\text{ml}$  (10  $\mu\text{g}/\text{mouse}$ ), an actual decrease or constant number of granulocytes migrated into the lungs. The higher concentrations may be inducing a sepsis-like response, causing granulocytes to be drawn to other sites away from the lung. Similarly, in rats, large i.v. doses of LPS lead to a decreased cardiac output and an increased systemic vascular resistance (Brackett et al., 1985; Law and Ferguson, 1988; Fink and Heard, 1990). However, very small i.v. doses of LPS elicit a hyperdynamic response characteristic of compensated human sepsis (Natanson et al., 1986; Fink and Heard, 1990).

The results obtained from the experiments examining the optimal time after i.n. administration of LPS required to observe minimal injury clearly showed that acute pulmonary injury can be achieved at 2 h and maximized at 48 h. After 72 h, the granulocytes in the BALF decreased to baseline levels and the mice recovered on their own from the induced lung trauma. These results have shown that i.n. administration of LPS results in an acute self-limiting pulmonary injury.

We have compared purified forms of LPS obtained from *E. coli* and *P. aeruginosa* for inducing lung injury. We also examined the effects of whole heat-killed *E. coli*. LPS from *P. aeruginosa* caused a stronger inflammation over 72 h with the peak granulocyte influx at 48 h. The two purified forms of LPS have different chemical structures which cause different degrees of biological activity (Rietschel et al., 1982). The chemical structures of the 'O'-antigens are specific for each bacterium and serotype which exhibits a range and degree of nonspecific effects (Asonganyi and Meadow, 1980; Rietschel et al., 1982). The purified *E. coli* LPS and heat-killed *E. coli* bacteria showed the same intensity of pulmonary damage, but the isolated LPS was half the concentration of the heat-killed *E. coli* LPS. We have shown that degrees of inflammatory responses can be developed by instilling different forms of

LPS. We assume that in our system, the degree of pulmonary damage could be attributed to the difference in LPS structures. The isolated LPS may have caused an increase of pulmonary damage over the heat-killed bacterium form because purified LPS is readily measured and controlled, whereas the dose of infecting bacteria is typically unknown.

We also compared two different routes of administering LPS, i.n. instillation and i.v. injection. In the literature, i.v. or i.p. injections are the general methods for inducing pulmonary damage (Peristeris et al., 1992; Gatti et al., 1993). These methods use larger amounts of LPS to induce pulmonary damage. A dose of 0.6–1.0 mg LPS was injected i.p. to cause a sublethal acute lung injury (Gatti et al., 1993). In a murine model of adult respiratory distress syndrome (ARDS) injected intraperitoneally with sublethal or lethal doses of LPS, only relatively modest increases in BAL protein levels and edematous reactions were found (Gatti et al., 1993; Denis et al., 1994). In their murine ARDS model, lethal endotoxin shock caused death attributed to failure of organs other than the lungs (Denis et al., 1994). With the direct exposure of LPS intranasally organ failure other than the lungs is eliminated. When comparing i.n. instillation and i.v. injection using the same small concentrations of LPS, i.n. instillation induced a massive recruitment of granulocytes into the BALF compared with the i.v. injection. This observation is consistent with reports showing neutrophils are not present in BALF 4 h after i.v. injection of endotoxin (Ulich et al., 1991a). After 24 h, 10 times the concentration of LPS in the i.v. injection caused very few granulocytes to migrate into the BAS as compared to 10  $\mu\text{g}/\text{mouse}$  i.n. instillation.

The movement of neutrophils from the peripheral blood into inflamed tissue is a fundamental aspect of acute inflammation (Kunkel et al., 1991). A number of investigations have demonstrated this classical, short-lived neutrophil acute inflammation. The LPS-induced lung injury model is a very complex inflammatory cascade which continues to be studied. Pulmonary damage has been experimented in many animal models to understand many different approaches. This LPS i.n. instillation model may help continue the study of pulmonary edema, ARDS, sepsis, and toxic shock, with the understanding of therapeutic development or cytokine effectiveness.

## References

- Anderson, B.O., Brown, J.M., Bensard, D.D., Grosso, M.A., Banerjee, A., Patt, A., Whitman, G.J.R. and Harken, A.H. (1990) Reversible lung neutrophil accumulation can cause lung injury by elastase-mediated mechanisms. *Surgery* 108, 262.
- Asonganyi, T.M. and Meadow, P.M. (1980) Biosynthesis of the core part of the lipopolysaccharide of *Pseudomonas aeruginosa*. *J. Gen. Microbiol.* 117, 1.
- Berry, L.J. (1977) Bacterial toxins. *Crit. Rev. Toxicol.* 5, 239.
- Brackett, D.J., Schaefer, C.F., Tompkins, P., Fagraeus, L., Peters, L.J. and Wilson, M.F. (1985) Evaluation of cardiac output, total peripheral vascular resistance, and plasma concentrations of vasopressin in the conscious, unrestrained rat during endotoxin. *Circ. Shock* 17, 273.
- Bradley, P.P., Priebe, D.A., Christensen, R.D. and Rothstein, G. (1982) Measurement of cutaneous inflammation: estimation of neutrophil content with an enzyme marker. *J. Invest. Dermatol.* 78, 206.
- Brigham, K.L. and Meyrick, B. (1986) Endotoxin and lung injury. *Am. Rev. Respir. Dis.* 133, 913.
- Brigham, K.L., Bowers, R.E. and Haynes, J. (1979) Increased sheep lung vascular permeability caused by *Escherichia coli* endotoxin. *Circ. Res.* 45, 292.
- Denis, M., Guojian, L., Widmer, M. and Cantin, A. (1994) A mouse model of lung injury induced by microbial products: implication of tumor necrosis factor. *Am. J. Respir. Cell. Mol. Biol.* 10, 658.
- Fink, M.P. and Heard, S.O. (1990) Laboratory models of sepsis and septic shock. *J. Surg. Res.* 49, 186.
- Galanos, C., Freudenberg, M., Hase, S., Jay, F. and Ruschmann, E. (1977) Biological activities and immunological properties of lipid A. In: D. Schlessinger (Ed.), *Microbiology 1977*, Am. Soc. Microbiol., Washington, DC, p. 269.
- Gatti, S., Faggioni, R., Echtenacher, B. and Ghezzi, P. (1993) Role of tumor necrosis factor and reactive oxygen intermediates in lipopolysaccharide-induced pulmonary oedema and lethality. *Clin. Exp. Immunol.* 91, 456.
- Goldblum, S.E., Yoneda, K., Cohen, D.A. and McClain, C.J. (1988) Provocation of pulmonary vascular endothelial injury in rabbits by human recombinant interleukin-1 $\beta$ . *Infect. Immun.* 56, 2255.
- Harlan, J.M., Harker, L.A., Reidy, M.A., Gajdusek, C.M., Schwartz, S.M. and Striker, G.E. (1983) Lipopolysaccharide-mediated bovine endothelial cell injury in vitro. *Lab. Invest.* 48, 269.
- Kaplow, L.S. (1975) Substitute for benzidine in myeloperoxidase stains. *Am. J. Clin. Pathol.* 63, 451.
- Kunkel, S.L., Standiford, T., Kasahara, K. and Strieter, R.M. (1991) Interleukin-8 (IL-8): the major neutrophil chemotactic factor in the lung. *Exp. Lung Res.* 17, 17.
- Law, W.R. and Ferguson, J.L. (1988) Naloxone alters organ perfusion during endotoxin shock in conscious rats. *Am. J. Physiol.* 255, H1106.
- Lowry, O.H., Rosebrough, N.J., Farr, A.L. and Randall, R.J. (1951) *J. Biol. Chem.* 193, 265.
- Morrison, D.C. and Ulevitch, R.J. (1978) The effects of bacterial endotoxins on host mediation systems. *Am. J. Pathol.* 93, 526.
- Natanson, C., Fink, M.P., Ballantyne, H.K., MacVittie, T.J., Conklin, J.J. and Parrillo, J.E. (1986) Gram-negative bacteremia produces both systolic and diastolic cardiac dysfunction in a canine model that simulates human septic shock. *J. Clin. Invest.* 78, 259.
- Nowotny, A. (1969) Molecular aspects of endotoxic reactions. *Bacteriol. Rev.* 33, 72.
- Ognibene, F.P., Martin, S.E., Parker, M.M., Schlesinger, T., Roach, P., Burch, C., Shelhamer, J.H. and Parrillo, J.E. (1986) Adult respiratory distress syndrome in patients with severe neutropenia. *N. Engl. J. Med.* 315, 547.
- Patriarca, P., Cramer, R., Marussi, M., Rossi, F. and Romeo, D. (1971) Mode of activation of granule-bound NADPH oxidase in leucocytes during phagocytosis. *Biochim. Biophys. Acta* 237, 335.
- Peristeris, P., Clark, B.D., Gatti, S., Faggioni, R., Mantovani, A., Mengozzi, M., Orencole, S.F., Sironi, M. and Ghezzi, P. (1992) N-Acetylcysteine and glutathione as inhibitors of tumor necrosis factor production. *Cell. Immunol.* 140, 390.
- Rietschel, E.Th., Schade, U., Jensen, M., Wollenweber, H.W., Lüderitz, O. and Greisman, S.G. (1982) Bacterial endotoxins: chemical structure, biological activity and role in septicemia. *Scand. J. Infect. Dis. Suppl.* 31, 8.
- Rot, A. (1992) Endothelial cell binding of NAP-1/IL-8: role in neutrophil emigration. *Immunol. Today* 13, 291.
- Rushton, B. (1978) Induction of pneumonia in mice with *Pasteurella haemolytica*. *J. Comp. Path.* 88, 477.
- Schultz, J. and Kaminker, K. (1962) Myeloperoxidase of the leucocyte of normal human blood. I. Content and localization. *Arch. Biochem. Biophys.* 96, 465.
- Simons, R.K., Maier, R.V. and Chi, E.Y. (1991) Pulmonary effects of continuous endotoxin infusion in the rat. *Circ. Shock* 33, 233.
- Smith, R.H., Babiuk, L.A. and Stockdale, P.H.G. (1981) Intranasal immunization of mice against *Pasteurella multocida*. *Infect. Immun.* 31, 129.
- Stephens, K.E., Ishizaka, A., Wu, Z., Larrick, J.W. and Raffin, T.A. (1988) Granulocyte depletion prevents tumor necrosis factor-mediated acute lung injury in guinea pigs. *Am. Rev. Respir. Dis.* 138, 1300.
- Ulich, T.R., Yin, S., Guo, K., Yi, E.S., Remick, D. and Castillo, J. (1991a) Intratracheal injection of endotoxin and cytokines. *Am. J. Pathol.* 138, 1097.
- Ulich, T.R., Watson, L.R., Yin, S., Guo, K., Wang, P., Thang, H. and Castillo, J. (1991b) The intratracheal administration of endotoxin and cytokines. *Am. J. Pathol.* 138, 1485.
- Worthen, G.S., Avdi, N., Vukajlovich, S. and Tobias, P.S. (1992) Neutrophil adherence induced by lipopolysaccharide in vitro. *J. Clin. Invest.* 90, 2526.
- Yam, L.T., Li, C.Y. and Crosby, W.H. (1971) Cytochemical identification of monocytes and granulocytes. *Am. J. Clin. Pathol.* 55, 283.

**This Page is Inserted by IFW Indexing and Scanning  
Operations and is not part of the Official Record**

**BEST AVAILABLE IMAGES**

Defective images within this document are accurate representations of the original documents submitted by the applicant.

Defects in the images include but are not limited to the items checked:

- ☐ **BLACK BORDERS**
- ☐ **IMAGE CUT OFF AT TOP, BOTTOM OR SIDES**
- ☐ **FADED TEXT OR DRAWING**
- ☐ **BLURRED OR ILLEGIBLE TEXT OR DRAWING**
- ☐ **SKEWED/SLANTED IMAGES**
- ☐ **COLOR OR BLACK AND WHITE PHOTOGRAPHS**
- ☐ **GRAY SCALE DOCUMENTS**
- ☒ **LINES OR MARKS ON ORIGINAL DOCUMENT**
- ☐ **REFERENCE(S) OR EXHIBIT(S) SUBMITTED ARE POOR QUALITY**
- ☐ **OTHER: \_\_\_\_\_**

**IMAGES ARE BEST AVAILABLE COPY.**

**As rescanning these documents will not correct the image problems checked, please do not report these problems to the IFW Image Problem Mailbox.**